

Study of the Vertical Distribution of Ozone in the Lower Atmosphere

Shilpy

Ph.D Thesis
November 2008



**Physical Research Laboratory
Ahmedabad-380 009, India**



Study of the Vertical Distribution of Ozone in the Lower Atmosphere

A THESIS

Submitted to the Gujarat University
for the degree of
Doctor of Philosophy in Physics

by

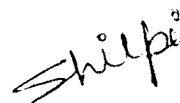
Shilpy



Space and Atmospheric Sciences Division
Physical Research Laboratory
Ahmedabad-380009
India
November 2008

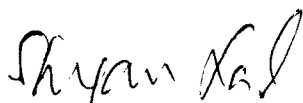
CERTIFICATE

I hereby declare that the work presented in this thesis is original and done by me. It has not formed the basis for the award of any degree or diploma by any University or Institution, except where due acknowledgment has been made in the text.



**Shilpy
(Author)**

Certified by:



**Prof. Shyam Lal
(Thesis Supervisor)**

**Physical Research Laboratory
Navrangpura, Ahmedabad, INDIA**

Dedicated to

*"If you manipulate words, it is a lie
If you play on words, it is a joke
If you rely on words, it is ignorance
If you transcend words, it is wisdom*

*If communication is just on the level of words,
Many questions will come and many answers,
And many questions- it is an endless exercise.
But if the words touch the heart, there is an exclamation- O!"
That is called recognition
When the words spoken do not create a concept in the mind
But bring a recognition.....*

The purpose of words is to create silence"

S_{RI} S_{RI}

Acknowledgements

I am greatly thankful to my thesis supervisor Prof. Shyam Lal for his guidance, encouragement and enthusiasm.

I am indebted to Messers S. Venkataramani, T.A. Rajesh, K. S. Modh and T. K. Sunilkumar for their invaluable help in conducting balloon flights at Ahmedabad and during cruise and field campaigns. Thanks to Mrs. S. Desai for helping in data analysis and her unconditional love and cheerful company throughout my stay at PRL.

My sincere thanks to Drs. Prabir K. Patra, Manish Naja, Duli Chand, Varun Sheel, L.K.Sahu and Y. B. Acharya for their wonderful company, useful comments and discussions. I thank all of these team members for their sincere help and support. I am also thankful to Shuchita, Iman, Rohit, Sumita, Rajesh, Bhavesh, Bhavik, Akhilesh, Ritesh, Subimal, Shashdhar, Suratana, Suruchi, Alok, Manan, Harish bhai, Nagarji, Santosh bhai, Rastogiji, Kuljeet di, Arvinda, Amit and Chinmay for their wonderful company and help during the tenure of this work.

I accord my sincere thanks to Profs. A. Jayaraman, M. M. Sarin, R. Ramesh and Dr. S. Ramachandran for fruitful discussions. I would like to express my sincere thanks to Prof., H. Chandra, H.S.S. Sinha and Drs. S. A. Haider, R. Sekar, K. P. Subramanian, Bhas Bapat, D. Chakrabarty, Som Sharma for their encouragements and helpful comments during my Ph. D. tenure. I am thankful to Mr. P.K. Pillai, Mr. Kaushal Bhatt for helping in my thesis editing work

I also wish to express my gratitude to Drs. Mark Lawreance, Martin Schultz, Andrew Gettelman Laura Pan for their invaluable support, for providing necessary data and guidance. I am also thankful to Drs P. K. Bhartia, S. Chandra, Omar Torres for providing me satellite based tropospheric ozone data. I am thankful to Dr. A. Y. Karpechko for providing the potential vorticity data. I thank NOAA team for providing free access for downloading the back

trajectories from their website. I also wish to thank the TOMS team for making their data available to the scientific community. I am thankful to Prof. Guy Brasseur for useful discussion and giving direction for this work.

My sincere thanks to Prof. J. N. Goswami, Director PRL, Prof A. K. Singhvi Dean PRL, Prof U. Sarkar, Chairman Academic Committee for their all time support and guidance. My special thanks are due to Dr. P. Sharma and to the members of academic committees and experts of all reviews for their comments and suggestions. I also thank all the faculty members who taught me during the course work (2003-04). I thank the personnel of the Computer Center, Library, Canteen, Accounts and all other sections of Administration for their help and support.

I am also grateful to Drs V. Tare, S. N. Tripathi and other members of IIT Kanpur for providing logistic arrangements for the campaign during December 2004. I am also thankful to Drs. R. Sridharan and K. Krishnamoorthy, campaign team members as well as crew members of the ORV. Sagar Kanya for their support in making successful experiments during ICARB 2006.

This work was supported by Indian Space Research Organization (ISRO) as a part of Geosphere-Biosphere Programme (GBP). I am grateful to Drs B. H. Subbaraya, C. B. S. Dutt, V. Jayaraman and for their support and encouragement.

I want to express my sincere thanks to Dr. Sanjay Goyal, University of Purdue and to Dr. Ramya Sunder Raman for their help and for the well-aimed and encouraging review of my thesis and for the most valuable comments.

I have been blessed with an absolutely magnificent family. I owe a great amount of gratitude to my Guruji Sri Sri Ravishankarji for his support, unconditional love and blessings. Whole-hearted thanks to my mother and my father for their support and love. I also wish to thank my brothers, sister, my grandparents, sisters-in-law and my niece and nephews for their unconditional love. I express my heartiest regards to all my teachers, friends and persons for all the help, advice, support, inspiration and encouragement that I received at each and every step to move forward in my life.

TABLE OF CONTENT

CHAPTER 1: Introduction	1
1.1. Ozone chemistry in the stratosphere	2
1.2. Tropospheric ozone	3
<i>1.2.1. Photochemical sources and sinks of tropospheric ozone</i>	5
<i>1.2.2. Dry deposition at earth's surface</i>	7
<i>1.2.3. Transport of O₃ from stratosphere</i>	7
<i>1.2.4 UTLS (Upper Troposphere Lower Stratosphere region)</i>	9
<i>1.2.5 Budget of troposphere ozone</i>	9
1.3. Impact of ozone on the biological system	10
1.4. Role of dynamics	12
<i>1.4.1. Transport</i>	13
<i>1.4.2 Advection (Long Range Transport)</i>	13
<i>1.4.3 Convection</i>	14
1.5. Indian scenario	14
1.6. Objectives and brief outline of thesis	15
 CHAPTER 2: Measurement techniques and instrumentation	 17
2.1. Ozone observations using balloon-borne sensor	19
2.2. Components of a balloon flight	20
2.3. Ozone observations using ECC sonde	20
<i>2.3.1. Operating principle</i>	22
<i>2.3.2. Estimation of ozone</i>	23

2.4.	Meteorological Radiosonde: RS-80	23
2.5.	Global Positioning System (GPS)	25
2.6.	Flight operation	26
	2.6.1 Ozonesonde, Radiosonde and GPS sensor unit	26
	2.6.2. Pre-flight: Preparation and instrumental checks	26
	2.6.3. Post-launch data	27
2.7.	Ground instrument setup for sounding	30
	2.7.1. Post-flight data processing	31
	2.7.2. Pump efficiency	32
	2.7.3. Performance of ECC ozonesonde	33
	2.7.4. Performance of RS-80 Radiosonde	34
	2.7.5. Precision and Accuracy of ECC- RS -80 Sondes	34

CHAPTER 3: Seasonal variation in the vertical distribution of ozone and effect of meteorology over Ahmedabad

		36
3.1.	Description of the site	37
3.2.	Experimental details	37
3.3	Meteorology over Ahmedabad	38
	3.3.1 Wind fields over India	38
	3.3.2 Surface meteorology	43
3.4	Winds observed over Ahmedabad using balloons borne GPS	44
	3.4.1 Annual variation	44
	3.4.2 Seasonal variation	45
3.5	Vertical distributions of temperature and humidity over Ahmedabad	47
3.6	Variation of tropopause over Ahmedabad	49

3.7	Seasonal variations of distribution of ozone	53
3.8	Variation of total ozone content over Ahmedabad	56
3.9	Tropospheric column ozone	59
3.10	Comparison with TOMS derived tropospheric column ozone	62
3.11	Vertical description of tropospheric ozone	63
3.12	Vertical distributions of ozone, temperature and relative humidity during different seasons	64
3.13	Stratospheric-Tropospheric Exchange over Ahmedabad	69
3.14	Day to day variability in tropospheric ozone – A case study	71
	3.14.1 Case 1- Ozone distribution on 9 March, 2005	71
	3.14.2 Case 2- Ozone distribution on 20 April, 2005	74
3.15	Summary	76

Chapter 4: Distribution of ozone and other trace gases over the Indo-Gangetic Plain during a winter month 78

4.1	Significance of the study site	79
4.2	Site description	80
4.3	Experimental details	80
4.4	Metrological conditions, back trajectory and potential vorticity analysis	82
4.5	Result and description	84
	4.5.1 Time and series analysis	84
	4.5.2 Frequencies distribution	85
4.6	Diurnal variations in ozone and its precursors	85
	4.6.1 Foggy days	85
	4.6.2 Clear days	87
4.7	Vertical distributions of ozone	89

4.7.1	<i>Average vertical profiles of ozone and temperature over Kanpur</i>	89
4.7.2	<i>Observed features</i>	90
4.7.3	<i>Case 1: Higher ozone concentration in the lower troposphere</i>	92
4.7.4	<i>Case 2: Ozone intrusion from the stratosphere</i>	94
4.7.5	<i>Case 3: Lower ozone concentration</i>	100
4.8	Comparison with MATCH-MPIC model	101
4.8.1	<i>Surface ozone</i>	101
4.8.2	<i>Vertical distribution of ozone</i>	102
4.9	Summary of the results	103

CHAPTER 5: Distribution of ozone over the marine regions surrounding India **106**

5.1.	Cruise track	109
5.2.	Experimental details	110
5.3.	Meteorology	113
5.3.1.	<i>General wind patterns</i>	113
5.3.2	<i>Variation of meteorological parameters</i>	114
5.4.	Variation of trace gases during ICARB	117
5.5.	Possible loss of ozone due to dust	119
5.6.	Vertical distribution ozone over the Bay of Bengal	120
5.6.1	<i>Variation of integrated total and tropospheric ozone</i>	120
5.6.2	<i>Low ozone in the troposphere on 30 March, 2006</i>	121
5.6.3	<i>Back trajectory analysis</i>	123
5.6.4	<i>Comparison with a photochemical model</i>	124

5.6.5 <i>Distribution of ozone at different pressure levels</i>	125
5.7. Vertical distribution of ozone over the Arabian Sea	126
5.7.1 <i>Variation of integrated total and tropospheric ozone</i>	126
5.8. Latitudinal distribution of ozone	127
5.8.1 <i>Group A: 8-12N</i>	127
5.8.2. <i>Group B: 12-16N</i>	128
5.8.3. <i>Group C: 16-20 N</i>	129
5.9. Day/night change in ozone vertical distribution	130
5.10. Stratosphere-Troposphere Exchange over the Arabian Sea	131
5.9. Summary and Conclusions	133

CHAPTER 6: Summary with general conclusions and outlook 140

6.1 Variations in vertical distribution of ozone over Ahmedabad	141
6.2 Study of ozone distribution over the Indo-Gangetic Plain (IGP) during a winter month	142
6.3 Ship cruise study of ozone distributions over the Bay of Bengal and the Arabian Sea	144
6.4 Future directions and scope	147

CHAPTER- 1

Introduction

The climate of the earth is governed by a delicate balancing system of physical, chemical and biological processes in the atmosphere, the oceans, and land surfaces [Warneck, 1988; Graedel and Crutzen, 1993]. Within the atmosphere, ozone and water vapor play a crucial role in interaction between climate and chemistry of the atmosphere [e.g Ramanathan et al., 1987]. There is mounting evidence that long term changes in trace gases (e.g. ozone, CFCs, carbon dioxide, oxides of nitrogen, methane, carbon monoxide, etc), which have been observed over the last few decades, are linked to human activities and that such changes influence the natural climate system [e.g. World Meteorological Organization - Scientific Assessment of Ozone Depletion, 2007, Intergovernmental Panel on Climate Change (IPCC), 2007].

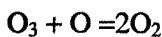
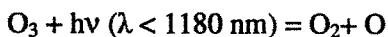
In addition to the serious concerns of significant ozone loss in the stratosphere during past few decades, increasing levels of tropospheric ozone in some parts of the world [Naja and Lal, 1996; WMO, 1998; Logan et al., 1999] have become another issue for concern. Ozone in the stratosphere accounts for 85-90% of the total atmospheric ozone and it is useful as it prevents the harmful solar ultra violet radiation from reaching the earth's surface. In contrast, ozone is also a greenhouse gas and high levels of ozone in the boundary layer lead to the deleterious effects on living beings [e.g. Desqueyroux et al., 2002] as well as significant reduction in the growth of crops and vegetations [e.g. Mauzerall and Wang, 2001; Oksanen and Holopainen, 2001]. It plays a key role in tropospheric chemistry as it is the main source for OH radical, which is an oxidizing agent and which controls the fluxes of many trace gases like CH₄, CO, HCFCs etc. from troposphere to the stratosphere [Thompson et al., 1989]. These issues are of additional concern in the rapidly industrializing countries in the tropics and subtropics, which are

also the regions (particularly Asia) of very limited measurements. Increasing anthropogenic sources [Akimoto, 2003; Naja and Akimoto, 2004] together with the natural factors like higher solar radiation and large amount of water vapor (about 80% of the global budget) are making this region photochemically most active and important to study tropospheric processes.

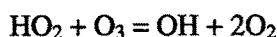
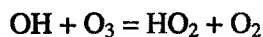
Interestingly, ozone in the troposphere show very large variabilities with very high mixing ratio of up to 500 ppbv over the tropical Atlantic Ocean between 10 and 12 km height [e.g. Suhre et al., 1997] and levels near zero over the equatorial Pacific Ocean between 10 km and tropopause [Kley et al., 1996]. Such large spatial and temporal variations in ozone lead to uncertainty its contribution in radiative forcing and better quantification of its budget.

1.1. Ozone chemistry in the stratosphere

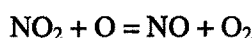
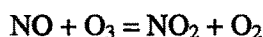
As early as 1930, Chapman had proposed the theory of ozone formation and destruction. Ozone formation begins via photolysis of O_2 at wavelength shorter than 240 nm. Resulting atomic oxygen recombines with O_2 and lead to the ozone formation. Ozone loss occurs by its photolysis and via reaction with atomic oxygen. The entire set of reactions is called 'Chapman Cycle' or the 'Chapman Reactions'.



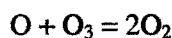
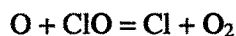
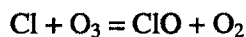
By the mid 1960s it became clear that ozone loss reaction proposed by Chapman are not sufficient to balance its production [Bates and Nicolet, 1950; Benson and Axworthy, 1965]. Hampson [1965] proposed ozone destruction involving OH and HO_2 that was also incorporated in to an atmospheric chemical model [Hunt, 1966].



Crutzen [1970] proposed catalytic ozone loss by NO and NO₂. This role of nitrogen compound has led to realization of the importance of microbiological processes and uses of nitrogen fertilizers and has greatly stimulated interest in bringing biologist and atmospheric scientist together.



Later, Molina and Rowland [1974] proposed additional theory for catalytic ozone loss via halogen



1.2. Tropospheric ozone

Tropospheric ozone concentrations have increased since the pre-industrial era largely due to increase in anthropogenic emissions of the ozone precursors, such as nitrogen oxides (NO_x), carbon monoxide (CO), methane (CH₄) and non-methane hydrocarbons (NMHCs). In future, tropospheric ozone is expected to increase further due to enhanced ozone precursor emissions [e.g. Prather et al., 2003].

Concentration of tropospheric ozone can be affected by various processes as shown in Figure 1.1. The sources of tropospheric ozone are the downward flux from the stratosphere and photochemical production. Downward flux of ozone from the stratosphere was considered to be the main source of tropospheric ozone until few years back. However now photochemical production of ozone has been identified to be at least

as important as downward transport [Logan, 1985; Crutzen, 1995; Lelieveld and Dentener, 2000].

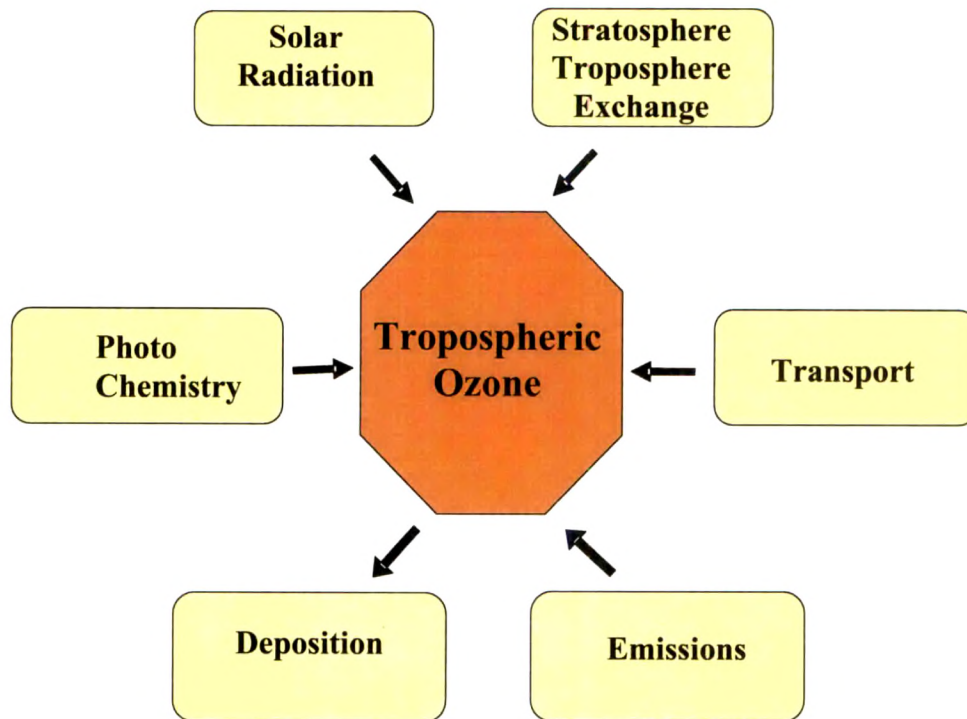


Figure 1.1. Factors affecting budget of tropospheric ozone.

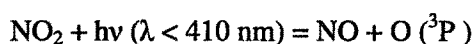
The tropospheric concentrations of ozone are highly variable and the contribution of transport from the stratosphere is poorly known. Measurements of ozone in the upper troposphere and lower stratosphere are very important to understand this exchange between the troposphere and stratosphere. This is one of the main themes of many international programmes e.g. ‘International Solar-Terrestrial Energy Programme (STEP)’, ‘Stratospheric Processes And their Role in Climate (SPARC)’ project of the World Climate Research Programme (WCRP), SHADOZ (Southern Hemisphere Additional Ozone sonde). Estimates of future changes in tropospheric ozone suggest that

the impact of man-made emissions will be largest in the tropics particularly in the South and Southeast Asia [Brasseur et al., 1998; Lelieveld and Dentener, 2000], which are the least studied parts of the world.

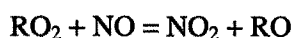
1.2.1. Photochemical sources and sinks of tropospheric ozone

The earlier view assumed that stratospheric ozone is transferred into the troposphere by atmospheric dynamics and destroyed at the surface with no intervening chemistry [Junge, 1962; Fabian, 1973]. Later Chameides and Walker [1973], and Crutzen [1974] proposed the processes of photochemical sources and sinks of ozone in the troposphere. The basics of the photochemical production mechanism were originally identified by Haagen-Smit [1952] as being responsible for the rise of air pollution in Los Angeles in the 1950s. However, still there are substantial differences in different model estimates and observations for accounting the relative importance of these processes controlling ozone levels [e.g. WMO, 1995].

The required atomic oxygen for ozone production is basically supplied by the photodissociation of NO_2 .

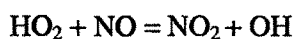
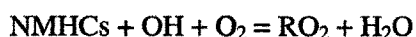


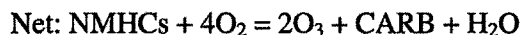
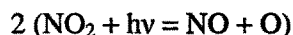
Which is followed by the key NO to NO_2 conversion reaction via hydroperoxy (HO_2) or organic peroxy (CH_3O_2 , $\text{C}_2\text{H}_5\text{O}_2$, or RO_2) radicals.



R is H or an organic radical like CH_3 , C_2H_5 , etc.

RO_2 is the product of the photooxidation of nonmethane hydrocarbons (NMHCs). A simplified form of the photooxidation cycle of NMHCs can be given as:

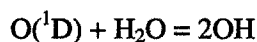
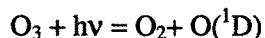




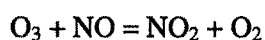
where, CARB is carbonyl compound

In this photochemical process, NO_x ($\text{NO}_2 + \text{NO}$) acts as a catalyst and it continues until it is permanently removed by physical processes (e.g deposition) or transformed to other nitrogen compound. Similar O_3 production cycles take place via CO and CH_4 , but their O_3 yield is much lower than that for NMHCs. On an average the photochemical production of O_3 by each CO, CH_4 , and NMHCs are 1, 3.5, and 10-14 O_3 molecules, respectively [Logan et al., 1981; Singh et al., 1980].

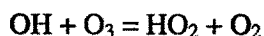
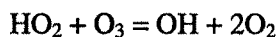
Ozone loss in the troposphere takes place by its photolysis to $\text{O}(^1\text{D})$ followed by the reaction of $\text{O}(^1\text{D})$ with H_2O .



In case of highly polluted region, ozone loss can take place via NO titration reaction as



Additionally, ozone is also consumed by reaction with HO_2 and OH in remote region of the troposphere:



The above two reactions will lead to ultimate ozone loss only in case NO levels are very low and the reaction rate NO_2 formation is small. Here, it should be remembered that NO_2 formation leads to ozone production. Ozone loss also takes place by reaction with organic materials at the Earth's surface (dry deposition).

1.2.2. Dry deposition at earth's surface

Dry deposition refers to the flux into surfaces in the absence of precipitation (but the surface can be wet), whereas wet deposition applies to deposition into fogs, clouds, rain, or snow where the gas is incorporated in the bulk solution. The amount of the species deposited per unit area per second (dry deposition flux) can be calculated by

$$\Phi_i = V_d [C_i]$$

where, V_d is deposition velocity of a species i and C_i is its concentration.

The deposition velocity largely depends on the type of surface (tree, grass, asphalt, etc), atmospheric conditions (temperature, pressure, wind), and the reference height at which the concentration of species is measured [Chameides, 1987]. The deposition on vegetation also depends upon whether the leaf stomata are open or close [e.g. Wesely, 1989]. This also leads to show diurnal and seasonal variations in ozone loss via dry deposition process. There is large variability in ozone loss by surface deposition (500-1500 Tg yr⁻¹) in different model estimates [Derwent, 1994].

1.2.3. Transport of O₃ from stratosphere

As described earlier, the downward transport of ozone rich stratospheric air is another source of tropospheric ozone. It occurs mainly outside the tropics and at extratropical latitude (Figure 1.2), often in connection with tropopause folding events near the jet streams [Danielsen, 1968].

Generally, strong stratification suppresses efficient exchange of this ozone-rich air with the underlying troposphere. An upward transport of tropospheric trace constituents occurs mainly through equatorial deep convective systems.

Therefore, stratosphere troposphere exchange may occur, if layers of constant (potential) temperature cross the tropopause or if there are disturbances and convective transport occurs in the mid-latitudes. In any case the vertical exchange of the troposphere takes hours to days, while the mixing of the stratosphere takes months to years (Figure 1.3).

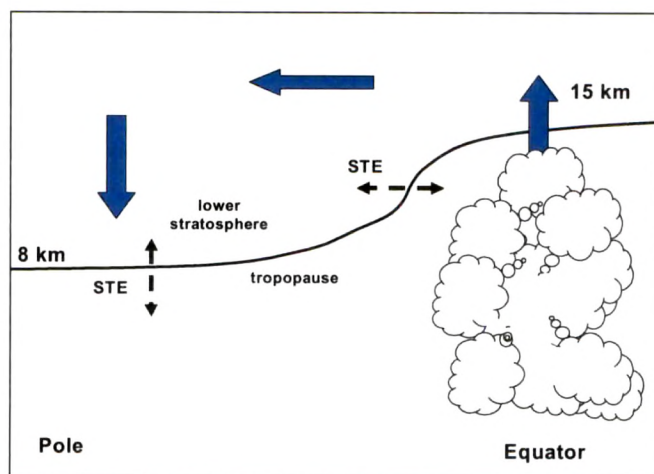


Figure 1.2. Schematic of stratosphere troposphere exchange processes.

In the tropics, maximum outflow from deep convection occurs near ~12-14 km, while the cold point tropopause occurs near 17 km. The intervening region has characteristics intermediate between the troposphere and stratosphere, and is termed the Tropical Tropopause Layer (TTL). Extra tropical stratosphere-troposphere exchange occurs in tropopause folds and intrusions linked with synoptic weather systems; these events transport stratospheric ozone into the troposphere.

Estimates of the amount of O_3 transported from the stratosphere to the troposphere on an annual basis rely on measurements of conserved tracers or on general circulation models. However, these estimates are quite uncertain. In the Northern Hemisphere (NH) O_3 fluxes seem to maximize in spring, being as much as five times the value in the fall. The NH stratosphere -to-troposphere O_3 flux has been estimated to fall in the range of 3 to 8×10^{10} molecules $cm^{-2}s^{-1}$ [Crutzen, 1995]. The Southern Hemispheric (SH) flux may be about half as large. An estimate for the total O_3 production in the stratosphere is about 5×10^{13} molecules $cm^{-2}s^{-1}$, only 0.1% of all O_3 produce in the stratosphere transport down to the troposphere [Crutzen, 1995].

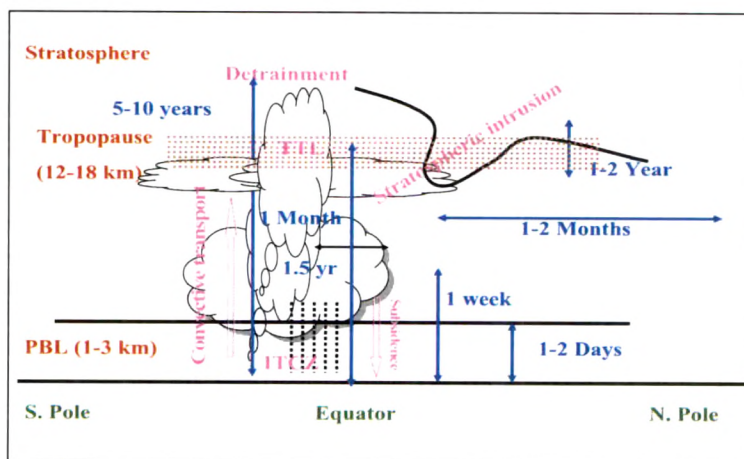


Figure 1.3. Large scale latitudinal circulation patterns in tropics and extra tropics with transport time scales (blue color).

1.2.4. UTLS (Upper Troposphere Lower Stratosphere region)

The UTLS is a highly coupled region where dynamics, chemistry, cloud microphysics and radiation are fundamentally interconnected. Ozone and water vapor, important greenhouse gases in the UTLS, are controlled by stratosphere-troposphere exchange, chemical processes including multi phase chemistry, and cloud micro physics, which in turn are influenced by the temperature and aerosol distributions.

1.2.5. Budget of tropospheric ozone

Ozone abundance in the troposphere typically varies from less than 10 ppbv over remote tropical oceans up to about 100 ppbv in the upper troposphere, and often exceeds 100 ppbv in the downwind of polluted metropolitan regions [e.g. Suhre et al., 1997]. Different global models of tropospheric chemistry have been used to estimate the importance of different sources and sinks in the tropospheric O_3 budget and their estimates are given in Table 1.1. It can be noticed that chemical production and loss process largely control the abundance of tropospheric ozone.

Table 1.1. Budget of tropospheric ozone. [Adapted from Intergovernmental Panel on Climate Change ,1995]

Atmospheric processes	Tg O ₃ yr ⁻¹
Sources	3400-5700
Chemical Production	3000-4600
HO ₂ + NO	70%
CH ₃ O ₂ + NO	20%
RO ₂ + NO	10%
Transport from stratosphere	400-1100
Sinks	3400-5700
Chemical loss	3000-4200
O(1D) + H ₂ O	40%
HO ₂ + O ₃	40%
Others	10%
Dry deposition	500-1500

Considering the large spatial variability in surface ozone observations, the importance of ozone soundings and satellites based sensor were realized in estimated ozone burden from observations. The total column of O₃ from satellites and ozone sounding have been used to infer the tropospheric O₃ column after removing the much larger stratospheric column [Fishman and Brackett, 1997; Hudson and Thompson, 1998]. The current burden of tropospheric O₃ is about 370 Tg, which is equivalent to a globally averaged column density of 34 DU (Dobson unit) or a mean abundance of about 50 ppbv.

1.3. Impact of ozone on the biological system

Ozone effects increase with increasing duration of the exposure period although the exposure-response relationships are rarely linear [Fig 1.3]. Exposure cannot be characterized as the product of concentration and time since the effect of ozone on crop yield depends on the cumulative impact of high concentrations during the growing season. Plant sensitivity is not constant, but varies according to stage of development. Time of increased plant sensitivity is species-specific, but generally occurs at or near the maximum leaf expansion.

Elevated concentrations of ozone at ground-level are known to cause adverse effects on the human health, ecosystems and materials. Due to its deleterious effects, photochemical air pollution is given a high priority in scientific investigations and environmental policies. High ozone concentrations are not confined to the urban environments but is also spreading to the relatively cleaner areas in remote locations. Most of these pollution spreads are observed in the downwind side of the urban/industrial areas [Aneja et al., 1999; Chand et al., 2001, Desqueyroux et al., 2002 Mauzerall and et al 2000 and Lal et al., 2000]. In addition, decline in growth rate in forest vegetation was observed on extreme ozone exposure sites such as mountain tops [Vogelmann, 1982].

Figure 1.4. Effect of seasonal O₃ concentrations on agricultural crop yields [Chameides et al., 1999].

1.4. Role of dynamics

Figure 1.5 shows schematic of influences of dynamical process on tropospheric ozone budget. Net ozone production in the upper troposphere balances net ozone loss in the lower troposphere. Mass exchange between the lower and upper troposphere is represented by the Walker circulation. Deep convective motions over South America, southern Africa and Oceania (rising branches of the walker circulation) inject NO_x from combustion, soil and lightening to the upper troposphere and driving ozone production. Eventually the air subsides over the oceans and net ozone loss takes place in the lower troposphere due to low NO_x concentration and high humidity closing the ozone cycle [Jacob et al., 1996]. This is only about the contribution of ozone photochemistry but how much is the contribution from the STE is not known. [Jacob et al., 1996].

Figure 1.5. Schematic of dynamical fate of tropospheric ozone. (Adopted from Jacob et al., 1996).

This is very pronounced in the equatorial region where the low level trade winds from both the hemispheres converge in the Inter Tropical Convergence Zone (ITCZ). The rising motion in deep convection must be compensated by subsidence in the atmosphere if an overall mass balance is to be maintained. Over certain regions of the tropics, especially the Indonesian Archipelago, deep convective transport can be so vigorous that it even can penetrate into the stratosphere which provides an important mechanism to inject tropospheric trace gases into the stratosphere [Newell and Gould-Stewart, 1981].

1.4.1. Transport

The process whereby air motions carry physical or chemical properties from one region of the atmosphere to another are collectively referred to as transport. Through transport processes human activities have global consequences, changing the chemical balance in remote regions of the atmosphere. Atmospheric gases can be transported through the atmosphere by several processes, such as convection, advection, and frontal circulation.

1.4.2. Advection (Long Range Transport)

Advection or horizontal wind can result in the transport of emissions over great distances even from one continent to other. Several studies have documented the outflow of anthropogenic pollution from USA, Europe, Africa and Asia [e.g. Talbot et al., 1997; Bey et al., 2001; Naja et al., 2003; Naja and Akimoto, 2004]. Intercontinental or Long-range transport of ozone and its precursors are very critical in changing of chemical composition and air-quality standards over a receptor region and these assessments are becoming a challenging task in Asia, particularly in south Asia due to insufficient measurements [e.g. Bey et al., 2001; Naja and Akimoto, 2004].

Among the continental transport, soil dust has been the principal species studied in long range transport from Asia over the North Pacific Ocean in last two decades [Duce et al., 1980; Tsunogai and Kondo, 1982]. Recently, the transport of chemically and radiatively active trace species produced due to increasing population and economic growth has acquired increasing importance in Asia. Many international campaigns have been conducted to study the long range transport of trace species (GAMETAG, RITS, SAGA, PEM, SAFARI, NARE, APARE, INDOEX, BOBEX) in different regions and environments of the globe [Johnson et al., 1990; Smit et al., 1990; Thompson et al., 1993; Singh et al., 1996; Rhoads et al., 1997; Lal et al., 1998]. Among these, the campaigns over the Indian regions were the INdian Ocean EXperiment (INDOEX) and Bay of Bengal Experiment (BOBEX).

1.4.3. Convection

Rapid vertical mixing resulting from heating at the surface that causes air to rise to higher altitudes and for air to subside downward is called atmospheric convection. It is particularly important for the upward motion of air in the tropical regions. Convection vertically redistributes trace gases, and can result in gases with surface sources and/or short lifetimes to be transported to the upper troposphere (UT) [Brasseur et al., 1999]. Once in the UT, gases can be transported over thousands of kilometers. Time taken for mixing of the atmospheric air within the hemispheres, between hemispheres and in vertical direction is shown in Figure 1.2. West to east (zonal) mixing of the air around the globe takes about 2 weeks, inter-hemispheric exchange takes about 1.5 years [Chand et al., 2001] and mixing within a hemisphere takes about 1-2 months. Vertical transport time of trace species in tropics is lowest. It takes few days to months for complete vertical mixing in the tropical troposphere. However, the vertical mixing is very fast at ITCZ (Inter Tropical Convection Zone) and it takes only few hours to transport the trace species from upper troposphere to lower stratosphere under strong convective activity.

1.5. Indian scenario

So far the Indian subcontinent is a data void region for the study of atmospheric trace gases. Only few measurements of ozone and its related gases are available in this region. Measurements of surface ozone were initiated in mid 1950s during pre- International Geophysical Year (IGY) using an Ehmert instrument but regular measurements of surface ozone were started by Indian Meteorological Department (IMD) during 1960-70s at Trivandrum, Kodaikanal, Pune, Nagpur, Delhi and Srinagar. During 1990s, measurements of ozone were started by groups at Jawaharlal Nehru University (JNU) in New Delhi and Indian Institute of Tropical Meteorology (IITM) in Pune [Varshney and Agarawal, 1992; Khemani et al., 1995]. First systematic measurements of ozone together with other trace gases in the Indian subcontinent were started at Physical Research Laboratory (PRL), Ahmedabad in 1992 [Subbaraya and Lal, 1998; Naja and Lal, 1996; Lal et al., 2000] that was followed by observations at other Indian sites [Naja and Lal

2001, Nair et al., 2002; Naja et al., 2003].

There have been different field campaigns to study transport of pollutants over the marine regions surrounding India such as INDOEX, BOBEX, BOBPS etc. [Lal et al., 1998 Lelieveld et al., 2001; Chand et al., 2003 ; Lal et al., 2007; Sahu et al., 2006 ; Lal et al., 2007]. There are some measurements of ozone as a part of MOZAIC (Measurement of OZone by AIrbus in-service airCRAFT) over India. However, they are highly irregular in frequency and limited to height below 300mb [Kunhikrishnan et al., 2006]. Ozone sounding program of Indian Meteorological Department (IMD) in three Indian cities is being continued, however there have been concern about the data quality. This is the first systematic time series distribution of ozone in the lower atmosphere made over Ahmedabad (urban region), Indo-Gangetic Plain (IGP) and over marine regions (Bay of Bengal and the Arabian Sea).

1.6. Objectives and brief outline of the thesis

The scientific objectives of the thesis are:

- i. To determine the spatial and temporal distribution of ozone over land as well as marine regions.
- ii. To estimate the stratosphere-troposphere exchange flux of ozone concentrations and its effect on tropospheric ozone budget.
- iii. To analyze extreme events in ozone distribution in the troposphere.
- iv. To validate these measurements with model results to understand different chemical and dynamical processes.

The thesis comprises of six chapters including this introductory **Chapter 1**.

Chapter 2 discusses experimental techniques applied to the measurement of the vertical distribution of O₃ and meteorological parameters and analyses of surface air samples for measurements of various trace gases (CH₄, and CO).

Chapter 3 deals with the measurements made at Ahmedabad (urban centre). Discussion includes a detailed study of seasonal variations in tropospheric ozone and meteorological parameters for the 2003-2007 period.

Chapter 4 is focused mainly to discuss the distribution of ozone and other trace gases over a site in the Indo-Gangetic Plain (IGP) during a winter month and the effect of both horizontal and vertical transport to study the transport of various trace gases (O_3 , CO, and CH_4) from highly populated urban and industrialized areas of IGP to this oceanic region and study their impact.

Chapter 5 presents results obtained from a ship cruise experiment conducted over the Bay of Bengal (BOB) and Arabian Sea (AS) during March to May 2006. Case studies of some selected measurements (O_3 , RH and temperature) are also made to investigate the underlying atmospheric processes in observed distributions. In addition to vertical distribution of ozone, surface measurements of CO and CH_4 have also been discussed supplementing ozone results. Supporting PV, wind field and back trajectory data also support discussions in all the chapters.

Chapter 6 presents the summary of important results obtained in this work. It also describes the basis provided by this work for future study.

CHAPTER – 2

Measurement techniques and instrumentation

Measurement techniques of ozone have evolved significantly during last century. Historically, observations of surface ozone were made in 19th century by chemical test paper. Chemiluminescence and electrochemical methods were developed in last century [e.g. Regener, 1960; Komhyr, 1969] and finally UV absorption technique was found to be well suited for surface ozone observations [Fonrobert, 1916]. In addition to surface ozone observations, a method was developed for observations of total ozone by Gordon Dobson in the 1930s [Dobson, 1931]. Later, this method was also deployed for deriving vertical ozone distribution and was called Umkehr method [Hahn et al., 1995]. Two decades later, in the 1950s, extensive observations of surface, total and vertical distribution (using rockets and balloons) of ozone were initiated globally during the IGY (International Geophysical Year) period. In addition to the ground based, rocket-borne and balloon-borne measurements, observations of total columnar ozone from space-borne platforms were initiated in the 1970's. Now, light detection and ranging (Lidar) is also used for observations of vertical ozone distribution [Hahn et al., 1995].

Each of above mentioned methods have different advantages and disadvantages depending on the place of observation, required resolution, and accuracy. Additionally, single ozone profiling instrument or technique is not capable of measurements at all altitudes, with adequate global and temporal coverage. Total Ozone Mapping Spectrometer (TOMS) was the first space-borne sensor that provided the total columnar ozone observations from 1978 onwards. Other satellite sensors, like SAGE (Stratospheric Aerosol and Gas Experiment), SBUV (Solar Back Scattered Ultraviolet) (only daytime observation), provided observations from 1979, that too only of the stratosphere [Cebula et al., 1998]. Later on, other satellite sensors like HALOE (Halogen Occultation Experiment) [Russell et al., 1993], MLS (Microwave

Limb Sounder), ILAS (Improved Limb Atmospheric Spectrometer) [Yamamori et al., 2006], OMI (Ozone Monitoring Instrument) [Veefkind et al., 2006] were also launched. All these sensors were capable of total tropospheric columnar ozone observations or observations up to only the lower stratosphere with very poor vertical resolution (about 5 km) with the exception of occultation instruments (SAGE and HALOE), which could provide a resolution a little better than just 2 km. About one decade earlier, with a specific interest on tropospheric ozone observations, satellite-sensors like TES (Tropospheric Emission Spectrometer) [Zhang et al., 2006], and GOME (Global Ozone Monitoring Experiment) [Liu et al., 2006] were launched. Recently, it was realized that the existing space-borne sensors have poor height coverage, vertical resolution, and extensive calibration as needed for long-term observations. Additionally validations are still major issues for satellite-based observations [e.g. Liu et al., 2006; Yamamori et al., 2007; Jiang et al., 2007; Terao and Logan, 2007; Nassar et al., 2008].

Considering the importance of tropospheric ozone observations with height coverage down to the lower troposphere, higher vertical resolution, better accuracy, and sustainability of similar types of instruments for long-term observations, it is understood that balloon-borne sensors are most suited for observations of vertical ozone distributions in troposphere. Interestingly, differences in long-term trends were reported between ozonesonde and satellite based observations [World Meteorological Organization, 1994] and their inter-comparisons. Further, ozone sounding provides longest records (about 50 years) of ozone distribution from surface to 30-35 km compared to any other method.

In this chapter, details of balloon borne sensors for observations of vertical distributions of ozone and weather parameters (temperature, relative humidity, winds and pressure) are presented. Brief descriptions of the electronic interface for different sensors are also outlined. The operational aspects like pre and post flight operation and evaluation of the instrumental performance are also described in the next sections.

2.1. Ozone observations using balloon-borne ozonesonde

The two main chemical techniques employed for the measurement of vertical ozone distribution are chemiluminescence and electrochemical method. In chemiluminescence method, luminescent reaction of ozone with an organic dye, Rhodamine-B (Rh-B), gives a chemiluminescence the light intensity is proportional to the ozone concentration [Regener, 1960]. Its main advantage is fast response and high sensitivity. However, the major drawbacks of this method are higher minimum detection limit, and poor sensitivity of the sensor. The sensitivity varies due to ageing and variations in operating conditions like temperature and humidity [Ulanovsky et al., 2001]. The electrochemical method has been used globally over a network of sites and also at individual sites since the 1950's [e.g. Komhyr, 1969]. The electrochemical method makes use of the reaction of ozone with potassium iodide (KI) solution yielding iodine (I_2). Finally, I_2 makes contact with a cathode and gets reduced to iodide ions by the uptake of 2 electrons per molecule of iodine. Thus, each ozone molecule passes through the solution giving rise to the flow of two electrons in the circuit.

There are two types of electrochemical cells, Brewer-Mast cell (BM) and Electrochemical Concentration Cell (ECC). Both methods are similar, however they largely differ in the types of chambers used for chemical reactions. BM sonde evolved from the Oxford-Kew ozonesonde developed by Brewer and Milford, [1960] and consists of a single cell with a silver anode and platinum cathode immersed in an alkaline KI solution. A polarising potential of 0.42V is applied between the electrodes such that no current flows unless free iodine is present. The ECC sonde was developed by Komhyr [1969, 1971] and it consists of two half cells, made of Teflon, which serve as cathode and anode chambers. Both half cells contain platinum meshes, which are serving as electrodes. They are immersed in KI solution of different concentrations. The ECC sonde does not require an external electrical potential, in contrast to the BM sonde. The ECC sonde obtains its driving emf from the difference in the concentrations of the KI solution. There are other modified versions of BM sonde and ECC sonde like the Indian version of BM sonde and the Japanese version of ECC sonde. These different BM sondes and ECC sondes are in use for long-term

observations of vertical ozone distribution over Europe, USA, Canada, Japan, and India since the 1950s.

2.2. Components of a balloon flight

Apart from ozone sensor, other components those are used in a balloon flight can be divided in two units (i) air segment unit and (ii) ground segment unit.

(i) Air segment unit

The balloon flight package consists of the following components:

1. Ozonesonde of type ECC (U.S.A.).
2. Standard meteorological radiosonde for measuring pressure, temperature and relative humidity of the RS80- type (Vaisala, Finland).
3. GPS sonde for determining wind and tracking the balloon.
4. Microcomputer controlled sonde data interface board for in flight coupling and digital processing of all measured parameters as temperature (C), humidity (%), pressure (hPa) and ozone (nb).
5. Digital coded data stream of two signals modulated on the UHF transmitter (400-406 MHz) of the RS 80 radiosonde.
6. A 1200 gram balloon (Japan) filled with helium.
7. A small parachute to slow the descent rate after burst of the balloon.

(ii) Ground segment unit

1. UHF Antenna
2. Receiver
3. Modem for converting the two tone data stream into a hexadecimal coded data frame of ASCII- characters.

2.3. Ozone observations using ECC sonde

Table 2.1 gives the brief summary of models of ECC sondes and their manufacturers. It is to be noted that model 6A from Science Pump is being used since 1995. Different models of ECC sondes, other types of ozonesonde and different procedures have been tested in organized intercomparison campaigns. Twelve such major ozonesonde intercomparisons have been documented in SPARC report [SPARC, 1998]. WMO international ozonesonde intercomparison [Kerr et al., 1994], Mauna Loa Ozone

intercomparison (MLO3) [McPeters et al. 1996], and Julich Ozonesonde Intercomparison Experiment (JOSIE) [Smit et al., 1998] showed good precision in the ECC ozonesondes.

Table 2.1. Development of different ECC ozonesondes from 1968 to present.

Manufacturer	Model	Period
Science Pump	1A	1968
Science Pump	3A	1968-1981
Science Pump	4A	1978-1995
Science Pump	5A	1986-1997
Science Pump	6A	1995 to present
EN-SCI	1Z	1993-1998
EN-SCI	2Z	1997 to present

In the present work, the ECC ozonesonde from Science Pump Corporation, USA (Model 6A) is used. The basic design of the ECC sensor is similar to that described by Komhyr [1969]. It contained two bright platinum electrodes those are immersed in two separate cells. Both the cells are made of polytetrafluoroethylene (Teflon TFE resin) and contain KI solution of different concentrations (Figure 2.1).

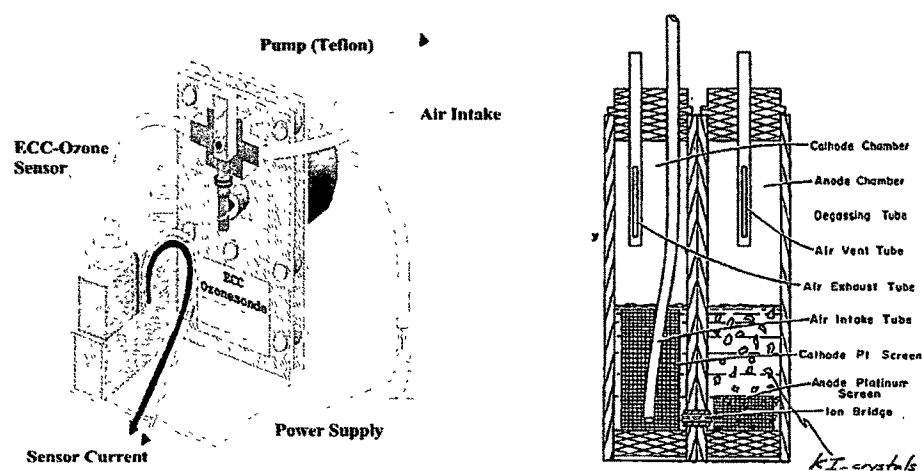


Figure 2.1. Scheme of the electrochemical concentration cell (ECC) ozonesonde (left) and sensing cell with showing of electrodes and ion bridge (right) (adapted from

Komhyr et al., 1971).

Both these chambers are linked together by an ion bridge that serve as an ion pathway and retards mixing of the cathode and anode electrolytes, thereby preserving their initial concentrations.

2.3.1. Operating principle

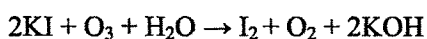
As mentioned earlier, the ECC gets its driving emf from the difference in the concentration of the KI solution in the cathode (0.06 Mol/l, i.e. 1% KI) and anode (8.0 Mol/l, saturated KI) chamber. Driving emf for the cell is approximately 0.13 V at 25°C and is defined by Nernst equation as:

$$E \approx - (0.0591/2) \times \log K$$

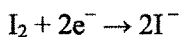
$$\text{where } K = (a_1)_{I_3^-} \times (a_3)_{I^-}^2 / (a_4)_{I_2} (a_2)_{I^-}^3$$

where a_1 , a_2 are the activities of the tri-iodide (I_3^-) and iodide (I^-) respectively within the anode chamber; and a_3 , a_4 are the activities of the iodide and iodine within the cathode chamber respectively.

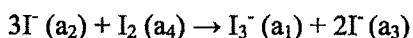
Chemical reactions begin in the cell when ambient air, containing ozone is forced through the cathode cell having KI solution of lower concentration. I_2 is formed following the redox reaction:



At the surface of the Pt cathode, I_2 is reduced to iodide ions (I^-) by uptake of 2 electrons per molecule of iodine.



While at the anode surface, iodide ion is converted into Iodine releasing two electrons. Finally, the cell converts the iodine to iodide in accordance with the overall reaction



In this manner, each ozone molecule bubbled through the solution gives rise to the flow of two electrons in the circuit. A pictorial view of suction pump, data processing card and electro chemical cell is shown in Figure 2.2.

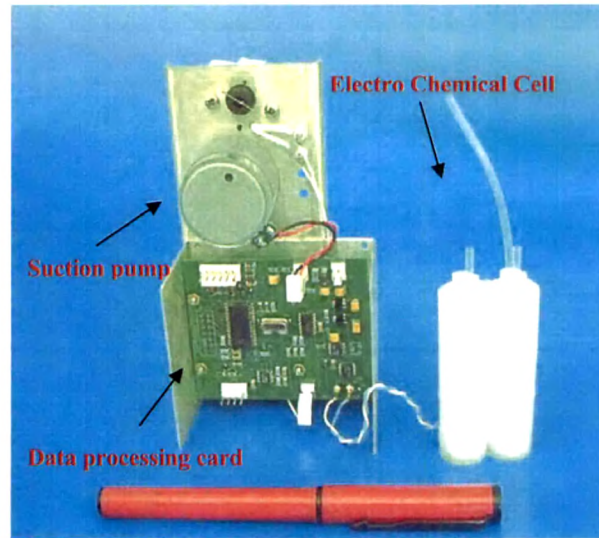


Figure 2.2. Suction pump, data processing card (left) and the electrochemical concentration cell (ECC) (right)

2.3.2. Estimation of ozone

Ozone partial pressure in nanobars (nb) is derived using the following relation

$$\text{Ozone partial pressure (P}_3\text{)} = 4.307 \times 10^{-3} (I - I_{BG}) \times T_p \times t \times C_{ef} \text{ (nb)}$$

Where

The constant 4.307×10^{-3} is determined by the half ratio of gas constant and Faraday constant [Komhyr, 1969]

I = sensor current due to ozone (in μA)

I_{BG} = current produced by oxidants other than ozone (mainly O_2) (in μA)

T_p = measured air flow temperature in K from pump base

t = pumping time for 100 ml of air in seconds

C_{ef} = correction due to reduced ambient pressure for pump

2.4. Meteorological Radiosonde: RS-80

The radiosonde is of the type RS-80 of Vaisala, Finland (Figure 2.3). The RS-80 is a small sized (55 x 147 x 90 mm) and light weighted (200g) package. It has sensors for

pressure (P), temperature (T) and relative humidity (U) which are all capacitive devices.

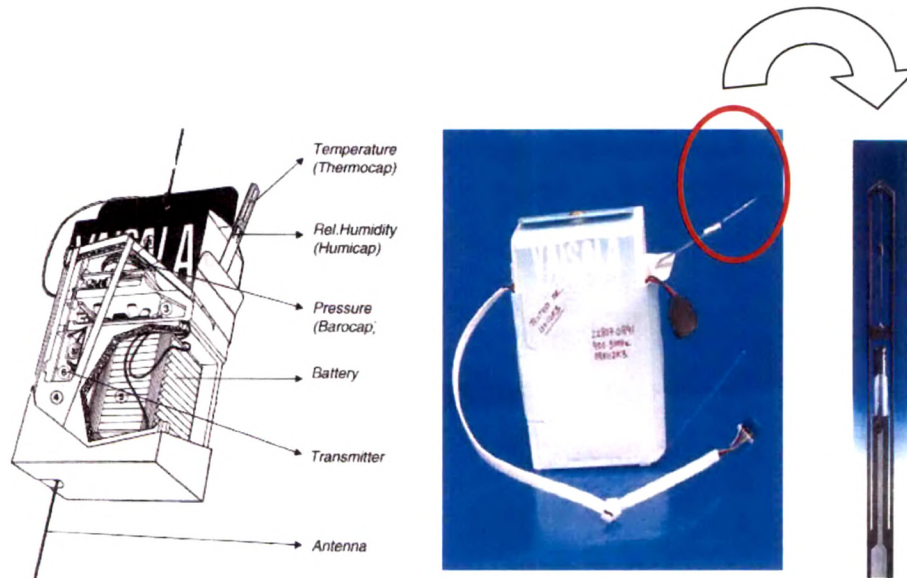


Figure 2.3. RS-80 Radiosonde of Vaisala (left) with sensing boom (right).

The pressure sensor (Barocap) is a small aneroid capsule with capacitive transducer plate inside. The external diameter of the capsule is 35.5 mm and the weight of the complete assembly is only 5 g. The sensor is mounted inside the radiosonde package. To correct for temperature influences, an additional temperature sensor is mounted inside the sensor housing of the Barocap. The resolution of the pressure sensor is 0.1 hPa. The temperature sensor (Thermocap) is based on temperature dependent dielectric ceramic material. The sensor (2.5×1.5 mm) is coated with an electrically grounded thin film of aluminum to minimize radiation errors. The resolution of the sensor is 0.1K. The humidity sensor (Humicap type A) is a thin film capacitor on a glass substrate. A hydro active polymer whose capacitance depends on the amount of water vapor adsorbed is used as dielectric between two electrodes. The sensor is small (4×4×0.2 mm) and the polymer film is only 1 micron thick. The surface electrode is porous to air humidity. An aluminum cap protects the sensor from direct rain and

radiation effects. The sensor gives relative humidity with respect to liquid water with a resolution of 0.2%.

The PTU (pressure, temperature, relative humidity) transducer signals are converted within an electronic multiplexed oscillator circuit into frequencies varying between 7 and 10 kHz (Fig. 2.9). At normal operation the six analogue signal frequencies are modulated on the UHF transmitter (403MHz) of the radiosonde and transmitted to the ground station for further data processing.

2.5. Global Positioning System (GPS)

The GPS system uses a constellation of between 24 to 32 medium earth orbit satellites that broadcast microwave signal that enables GPS receiver to determine their current location, time and velocity. The onboard GPS uses ultra accurate atomic clock and the GPS receiver contains a quartz regulated clock. A pictorial view of GPS sensor is shown in Figure 2.4.

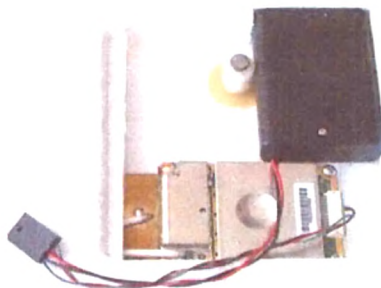


Figure 2.4. GPS-25-LVC (GARMIN) attach to the top of the ozonesonde unit.

The GPS receiver process signals from at least 4 satellites to determine its position. The GPS sensor module GPS-25-LVC from GARMIN is used with the present setup. It can track upto 12 satellites with an update rate of 1 - 2 sec. It is a light weight module with horizontal measurement precision of $\pm 2\text{m}$ and vertical measurement precision of $\pm 10\text{m}$.

2.6. Flight operation

2.6.1 Ozonesonde, Radiosonde and GPS sensor unit

The ozone sensor is packed in a styrofoam box with an inlet tube (2mm dia) coming out through it. A GPS sensor is also fitted at inner top side of the styrofoam box. The radiosonde is attached with this box as shown in Figure 2.5.



Figure 2.5. Ozonesensor in side the styrofoam box, (middle) a packed ozonesonde along with attached radiosonde (left). A combined unit of ozonesonde and radiosonde is ready for flight is shown on the right side (right).

2.6.2. Pre-flight: Preparation and instrumental checks

a) Advance preparation 3-7 days prior to release

Performance of ECC sonde (pump, flow and sensor) was checked before 3-7 days of balloon flight. Pump voltage (12-13 V), pump current (<100 mA), pressure (1600 - 1800 mb) and vacuum (180 -200 mb) were checked with a limiting value. Charging of sensor cathode and anode sensors with 3 ml and 1.5 ml respectively were done. Sensor response to low O₃ (5 μ A) was checked and was stored in a dark clean-air environment at a temperature of 20-25°C until launch. The flow chart (Fig. 2.6) depicts the procedure followed for conducting the balloon flight.

b) Preparations on the day of release

Pump performance was checked and conditioning of the pump only with high O₃ for 10-20 min. Cathode solution and anode solution in the sonde were changed.

Measurement of sensor's background currents ($<0.5\mu\text{A}$), sensor air flow rate were measured. Room temperature, pressure and relative humidity were also measured.

c) Preparations before (0-2 h) release

Ozone destruction filter is attached to pump inlet tube and the background current is measured for 10 minutes. Details of sonde parameters, flow rate and measured background current values are fed in a computer for sounding program (initialization). Ozone sensor was connected to interface card and overall system operation was checked.

Activation of radiosonde battery 20 min. prior to release was done. Surface data was collected for 20 minutes prior to launch. The balloon is launched after verifying payload operation and weather condition. These balloon flights were conducted in co-ordination with Air Traffic Control (ATC) for the time of launch.

2.6.3. Post-launch data

Launch time, surface wind speed, wind direction, sky condition, sounding data storage file and other information are recorded. Generally, balloon flight is conducted fortnightly at about 1000 hrs from the top of the building (about 40 m). Figure 2.7 shows a schematic of ascending payload, when balloon is inflated and a descending payload after the burst of balloon and parachute is operational. Generally sonde reaches up to 30-33 km after that balloon burst takes place and descent motion of sonde begins. Each sounding is made with a set of new instruments. Therefore, proper characterization prior to flight and consistency of the instruments with regard to their quality and characteristics with uniform operating procedures is carried out for every flight following the guidelines as described in Komhyr [1986], Science Pump Corporation [1996], and Vaisala [1988].

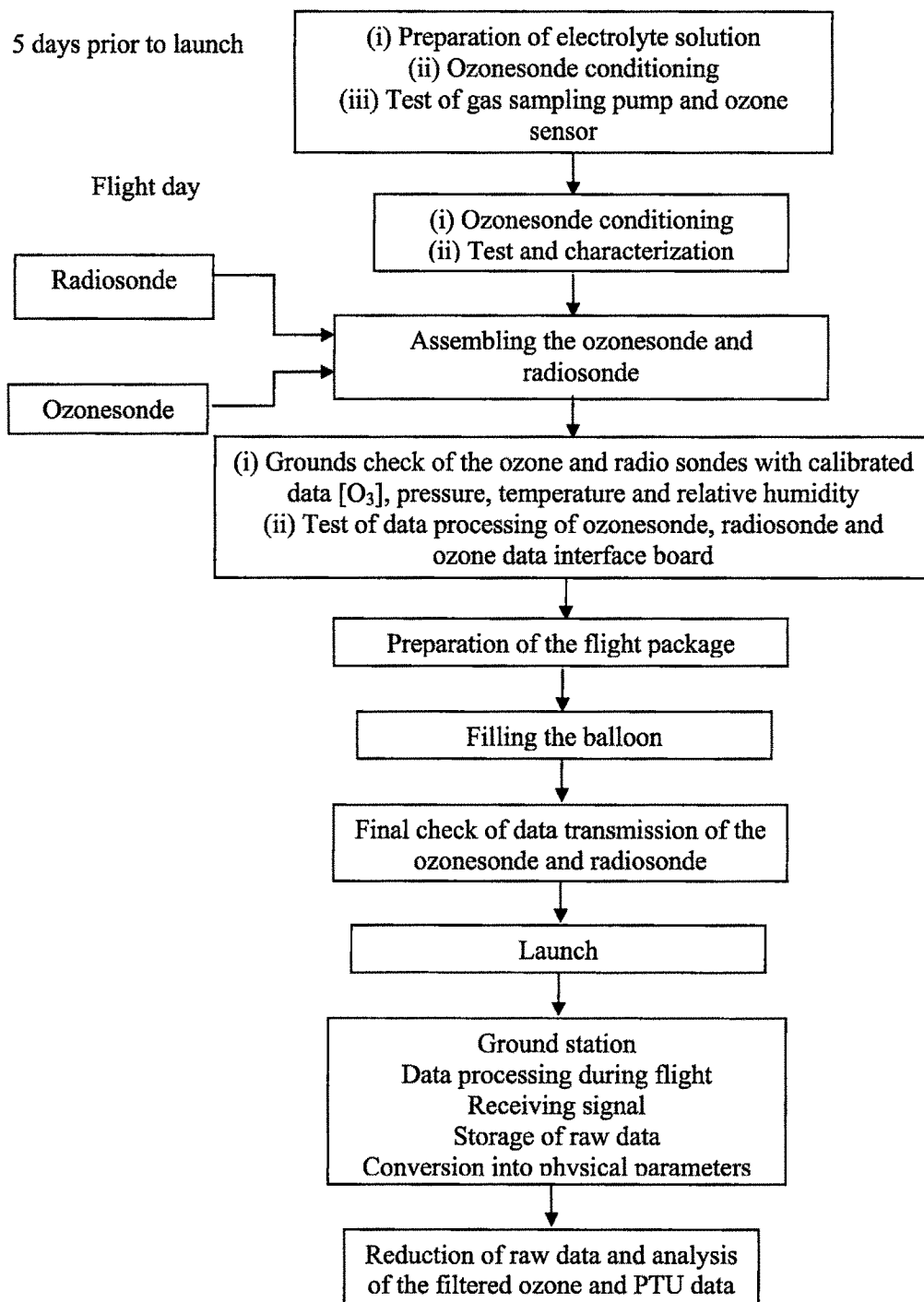


Figure 2.6. Flow-diagram showing the sequence of operation for balloon sensor testing and flight

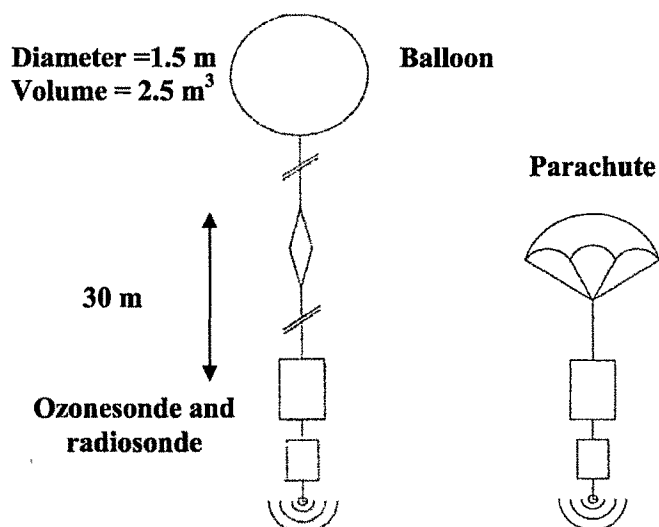


Figure 2.7. Ascending ozone and radio sensors, when balloon is inflated with gas (left) Descending sensors after the burst of balloon when parachute is operation (right)

In brief, preparation of electrolyte solution for ozone sensor begins about 5 days prior. Functioning of the pump, sensor back ground current, sensor response current and flow rate are tested. Table 2.2 shows average values of these parameters measured at Ahmedabad.

Table 2.2. Average values of back ground current, flow rate and sensor response observed during the balloon flight preparations.

Back ground current (μA)	0.03 - 0.05
Flow rate (ml sec ⁻¹)	27 – 29
Sensor Response (%)	80 – 90

2.7. Ground instrument setup for sounding

Major Components of ground instrument setup e.g antenna, wide band receiver, Modem and data acquisition system are shown in Figure 2.8. The composite setup deployed for the sounding is shown in Figure 2.9.



Figure 2.8. Component of the ground instrument setup (Antenna, wide band receiver and Modem).

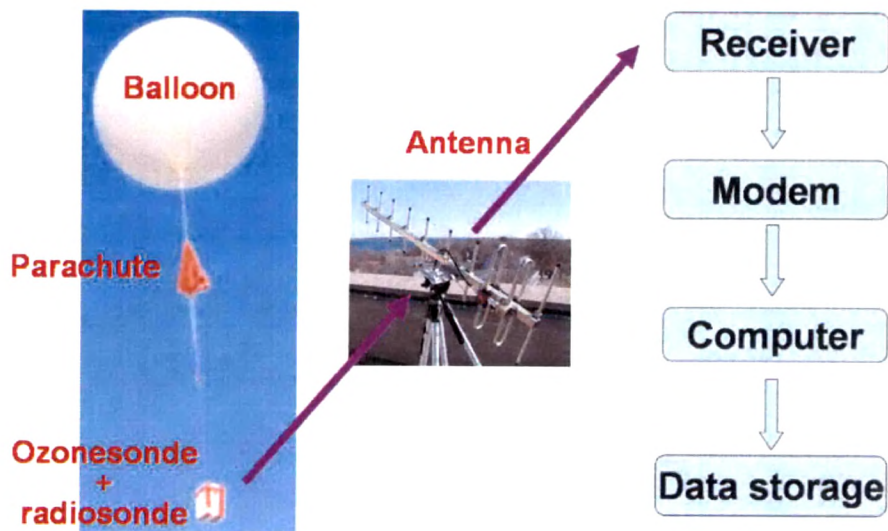


Figure 2.9. Setup deployed for sounding together with data transmission system.

The Vaisala radiosonde (RS-80) consists of a suite of sophisticated meteorological sensors (PTU) signal processing electronics and a radio transmission to relay the measurements back to receiver at the ground. The ozonesonde data and the GPS

sensor module data are interfaced to the radiosonde unit. The base band data are frequency shift keyed (FSK) before frequency modulation for transmission. At the ground the radio frequency signal is received through yaggi antenna, where it is pre amplified and fed to a wide band radio receiver. The frequency modulated carrier signal is demodulated at this receiver and the base band FSK signal is demodulated by an external modem. The data acquisition software running on a PC is interfaced to the modem for the proper data reception. During the balloon flight ground based receiver receive signal from GPS, signal of ozonesonde and radiosonde. After data processing, the real time values of the sounding height, temperature, RH, pressure, wind speed, direction and ozone is determined and stored. Moreover, vertical profiles of these parameters are plotted in time.

2.7.1. Post-flight data processing

After each flight, the recorded raw sounding data were processed by incorporating the corrections resulting from the ground check procedures described in section 2.4.2. The ozone partial pressure was derived from the measured ECC current (I) using equation 2.5. A new method of background correction was applied, which is based on laboratory studies made in environmental simulations chamber [Smit et al., 1998]. Simulations of vertical ozone soundings made in chamber under realistic atmospheric conditions of pressure, temperature and ozone concentrations have shown that the most accurate results are achieved with full subtraction of the background current at each pressure [Smit et al., 1994/1998].

Conventionally, it is assumed that the background current is dependent on oxygen pressure, with very small contribution to the overall signal in the middle/upper troposphere and above [Komhyr, 1986]. In contrast, laboratory studies showed that background current is independent of the oxygen pressure [Thornton et al., 1982;1983; Smit 1998]. Therefore, at each pressure the measured ozone sensor current (I) is corrected by subtraction of the background current I_{BG} , which was determined during the pre-flight checks before exposure to ozone.

Experimental evidences have shown that total ozone normalization should not be used

for ECC sonde tropospheric ozone profiles measurements [SPARC 1998]. Therefore, the ozonesonde data presented in this thesis have not been normalized to any spectroscopic measurement of the total ozone column density.

2.7.2. Pump efficiency

During the flight, the pump flow rate reduces at lesser air pressure mainly due to pump leakage dead volume in the piston of the pump, and the back pressure exerted on the pump by the sensing cathode solution through which gas is forced [Komhyr, 1967]. This decrease in pump efficiency is corrected by multiplying the Pump Correction Factor (PCF) as a function of atmospheric pressure. The loss of efficiency is smaller than 1% below 20 km altitude, while it is smaller than 2-3 % up to an altitude of 30 km [Komhyr et al., 1986, 1995, Torres, 1981]. However, the loss becomes significantly larger than 3-5 percent only in the upper stratosphere, above 30 km.

The ozone sounding carried out during both the campaigns (land as well as cruise campaign) did not exceed altitudes above 32 km, such that the corrections for losses of pump efficiency are marginally small while during regular observations over Ahmedabad some soundings have exceeded 30 km. In the final processing of the ozonesonde data, pump correction factors were included by using the curve as reported by Komhyr [1986] and given in Table 2.3.

Table 2.3. Pump Correction Factor (PCF) at different pressure levels.

P(hPa)	1000	200	150	100	70	50	30	20	15	10	7	5	3
P.C.F	1	1	1.01	1.01	1.01	1.02	1.03	1.04	1.05	1.07	1.08	1.13	1.24

Effective volumetric flow rate is also corrected accordingly as given by –

$$\Phi_{V,ECC} = \Phi_{V,ECC,GROUND} \times \eta_{pump}$$

where $\Phi_{V,ECC,GROUND}$ = Volumetric flow rate of pump as determined during ground checks

η_{pump} = Efficiency of pump which is pressure dependent

2.7.3. Performance of ECC ozonesonde

The volumetric flow rate of the gas sampling pump was determined with a burette tube by measuring the displacement time needed for a soap bubble to pass through a well defined volume of the burette. The performance of the ECC ozone sensor is checked for response time and conversion efficiency by comparison with an ozone reference, background current at ozone free air.

Uptake rate of ozone in the cathode chamber is determined by the equation:

$$P_{O_3, ECC} = C_{ECC} \cdot I_{O_3, ECC}$$

where

$P_{O_3, ECC}$ = Partial pressure of ozone [mb]

$I_{O_3, ECC}$ = Electrical current due to sampled ozone [μA]

C_{ECC} = Conversion efficiency of the ECC sensor

$$= 0.04307 \eta_{ECC} T_{ECC} / \Phi_{V, ECC} \quad (\text{as determined by [Komhyr, 1969]})$$

η_{ECC} = Efficiency of pump

T_{ECC} = Temperature of the air sampling pump

$\Phi_{V, ECC}$ = Volumetric flow rate of air sampling pump [mls^{-1}]

The overall electrical current, measured by the ECC sonde is a superposition of the ozone current $I_{O_3, ECC}$, and the background current $I_{B, ECC}$. Therefore, ozone current is determined as given below:

$$I_{O_3, ECC} = I_{M, ECC} - I_{B, ECC}$$

where

$I_{M, ECC}$ = Overall current measured by ECC sensor

$I_{O_3, ECC}$ = Electrical Current measured by ECC sensor due to ozone

$I_{B, ECC}$ = Electrical Current measured by ECC sensor due to background.

The background Current ($I_{B, ECC}$) varies for individual ozone sensors and it is determined just prior to launch of sounding.

2.7.4. Performance of RS-80 Radiosonde

Prior to launch, the RS-80 radiosonde was also checked in the laboratory following the guidelines of the manufacturer [Vaisala, 1985]. The PTU signals of the radiosonde were checked at ambient pressure and temperature measured by a reference barometer (accuracy = ± 0.2 hPa) and a thermometer (accuracy = ± 0.2 C) at ground respectively. The measured signals of the RS-80 radiosonde are processed according to the standard procedure described by the manufacturer [Vaisala, 1988] with one exception for the thermal behavior of the Humicap-A humidity sensor at low temperatures. Relative humidity measurements made with the Humicap-A sensor are known to be unreliable at temperatures below 250K. The reliability of the calibration curve provided by the manufacturer (Vaisala) for every Humicap-A sensor is limited because it is only based on calibrations made between 20°C and 0°C [Vaisala].

2.7.5. Precision and Accuracy of ECC and RS -80 Sondes

Different studies addressing the performance of different sensors of the ECC and RS-80 sondes have been conducted in the field. Sonde validation experiments were conducted under controlled laboratory conditions at the environmental simulation facility established at Forschungszentrum Julich (FZJ) (Germany). A temperature and pressure controlled vacuum chamber enabled to investigate the performance of different types of airborne ozone, humidity, temperature and pressure sensors under realistic atmospheric conditions with proper reference instrument [Smit et. al, 1998]. A summary of these investigations about the performance of the ECC ozonesonde and RS-80 radiosonde in terms of precision and accuracy of the different sensors are presented in Table 2.4.

Table 2.4. Precision and accuracy of ozonesonde in different height ranges [Komhyr et al., 1989]

Measurement Errors	(775-200) mbar (2.3–12.4 km)	(200-100) mbar (12.4–16.7 km)	(100-10) mbar (16.7 – 31.8 km)
Precision (%)	± 4 to ± 12	± 12 to ± 3	± 3
Background current (μA)	-1 to 5	+5 to +2	+2
Solution evaporation	± 0	± 0 to +1	+1 to +2
Sensor response time (sec)	± 0	± 0 to -4	-4 to ± 0
Pump temperature (C)	± 0	± 0 to +1	+1 to ± 0
Accuracy (%)	-1 \pm 5 to (+5 \pm 12)	+5 \pm 12 to -1 \pm 4	-1 \pm 4 to +1 \pm 4

CHAPTER – 3

Seasonal variation in the vertical distribution of ozone and effect of meteorology over Ahmedabad

Tropical region plays a key role in controlling the chemistry and climate of the tropical troposphere. Higher levels of solar flux coupled with higher amount of water vapour make it a chemical laboratory, where significant photochemical activities continue to occur almost throughout the year. This is also the region of strong convective activity which transports efficiently emitted gases into the free troposphere all over the globe. Atmospheric ozone is mainly produced in the tropical atmosphere. It then gets transported over the higher latitudes in both the hemispheres. Measurements of ozone have been made in the tropical region but mostly confined to total ozone or vertical distribution in the stratosphere using ground based, balloon, rocket and satellite techniques [Subbaraya et al., 1994; Mandal et al., 1999; Fishman et al., 2003; Saraf and Beig, 2004]. Since ozone also plays a significant role in the greenhouse effect in the troposphere and thereby in climate change, its measurements in the troposphere are very important. However, measurements of tropospheric ozone in the tropical region are very limited. A network of stations for balloon soundings was established as a part of Southern Hemisphere Additional Ozonesondes (SHADOZ) in the southern tropical region [Thomson et al., 2003], however, there is no such network in the northern tropical region. The India Meteorological Department (IMD) makes balloon sounding measurements from three sites in India regularly but these results are not published in detail especially for the tropospheric region [Peshin et al., 2001]. In view of this lack of measurements, a project was initiated to study the distribution of tropospheric ozone over Ahmedabad as a part of a major Geosphere Biosphere Program of Indian Space Research

Organization (ISRO). The Asian region, comprising of China, India and other East-Asian countries is a rapidly developing region with increasing levels of pollution caused by industries, vehicles, and other anthropogenic activities [Akimoto, 2003]. Thus, this study is motivated by the need to understand the effect of rising levels of anthropogenic activities on an increase in O₃ concentrations in the troposphere [Crutzen, 1979, 1988; Logan et al., 1981] and its potential impact on the chemistry and climate of this region [IPCC, 2001].

3.1. Description of the site

The observational site, Physical Research Laboratory (PRL), is situated on the western edge of the Ahmedabad (23.03N, 72.54 E, 49 m asl) city. Ahmedabad is a fast growing urban city in India having numerous industries and a thermal power station. The population of Ahmedabad is in excess of 5 million and currently the total number of vehicles is over 5.5 million. There is also a rapid increase in the number of vehicles (about 10% per year) in the city which includes buses, cars, two-wheelers (motorbikes, scooters) and three-wheelers (Indian auto-rickshaws) all of which contribute significantly to the emission of various kinds of pollutants.

3.2. Experimental details

Balloon soundings carrying ozone and radio sondes have been made fortnightly from Ahmedabad from May, 2003 to September, 2007. The details of these sondes and sensors were discussed in Chapter 2. The first ozone sounding was made on 7 May 2003 on a trial basis. A total of about 85 balloon flights were made from this site. These soundings were made in the morning between 0930 hrs and 1000 hrs (0400 – 0430 hrs GMT). Most of these balloons reached a ceiling height of about 32 km. However, there were breaks in the field campaigns during 2004 and 2006 due to technical difficulties. Total number of ozone soundings during each month is shown in Figure 3.1. The number of soundings was at a minimum (5-6) during the winter months and at a maximum (9-11) during the monsoon months.

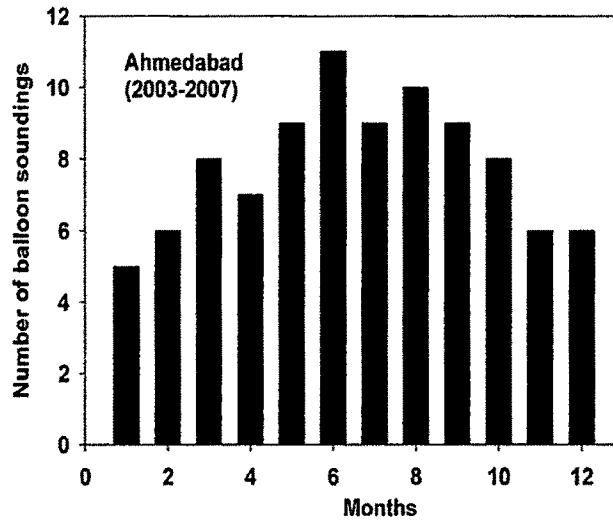


Figure 3.1. Monthly distribution of total number of soundings performed over Ahmedabad from 2003 to 2007.

3.3. Meteorology over Ahmedabad

3.3.1. Wind fields over India

The observed seasonal changes in wind flow over the sub-continental region of India and SE Asia are associated with the onset and withdrawal of monsoon. A monsoon seasonal change is characterized by a variety of physical mechanisms, which produce strong seasonal winds, a wet summer and a dry winter. Surface heating during summer favors enhanced convection over land, which is fueled by moist inflow at low levels. NCEP (National Center for Environmental Prediction) wind data were utilized to derive the wind streamline flow over India and surrounding marine regions.

There are four main seasons viz winter (December, January, and February - DJF), pre-monsoon (March, April, and May - MAM), monsoon (June, July, August, and September - JJAS) and post monsoon (October and November - ON) over this site. Figures 3.2a, 3.2b, 3.2c, and 3.2d show the general mean wind streamline plots during DJF, MAM, JJAS, and ON months respectively at four different pressure levels of 925 mb (1km), 700mb (~3 km), 400 mb (~7.5 km), and 250 mb (~11km).

During the winter season (DJF) wind flow at 950 mb and 700 mb is from north-west over Ahmedabad, but in the middle and upper troposphere, the winds are stronger and are from the west. The pattern changes during pre-monsoon months. The direction of wind at 925mb is now from west over Ahmedabad. Also the winds at 400 and 250mb are slower than during winter months. The winds during monsoon months are south-westerly over the entire Indian region at lower heights (925 and 700 mb). Apart from speed, wind direction can also play a role in determining the concentration of ozone present over a location as it helps bring in either ozone or its precursors from different neighboring regions to the measurement site due to ozone's longer life time in free troposphere. The seasonal wind patterns for the year 2003 can be considered representative for all the four years.

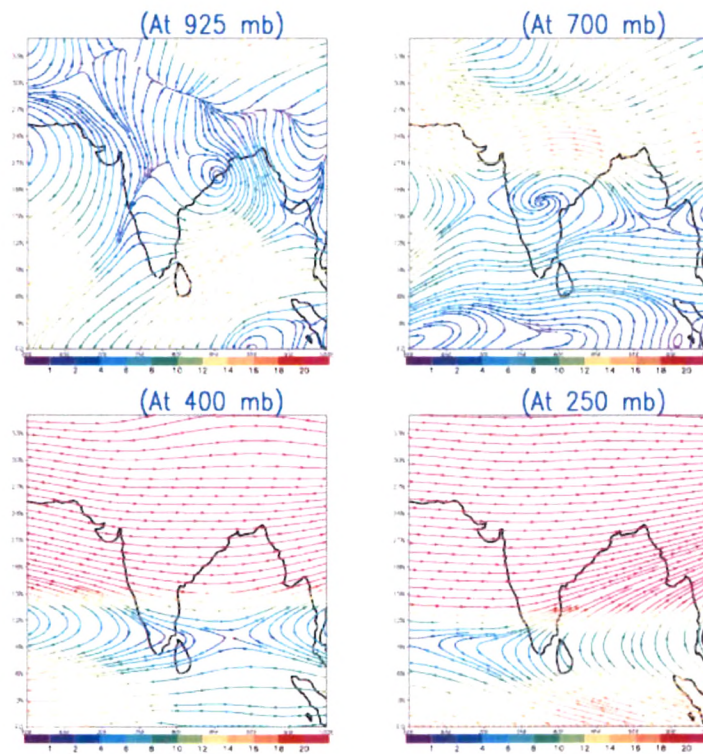


Figure 3.2a. Mean wind fields at four different pressure levels during winter (DJF) for the year 2003 over the Indian sub-continent. Color bars represent the magnitude of wind speed (m/s). Data adapted from NCEP.

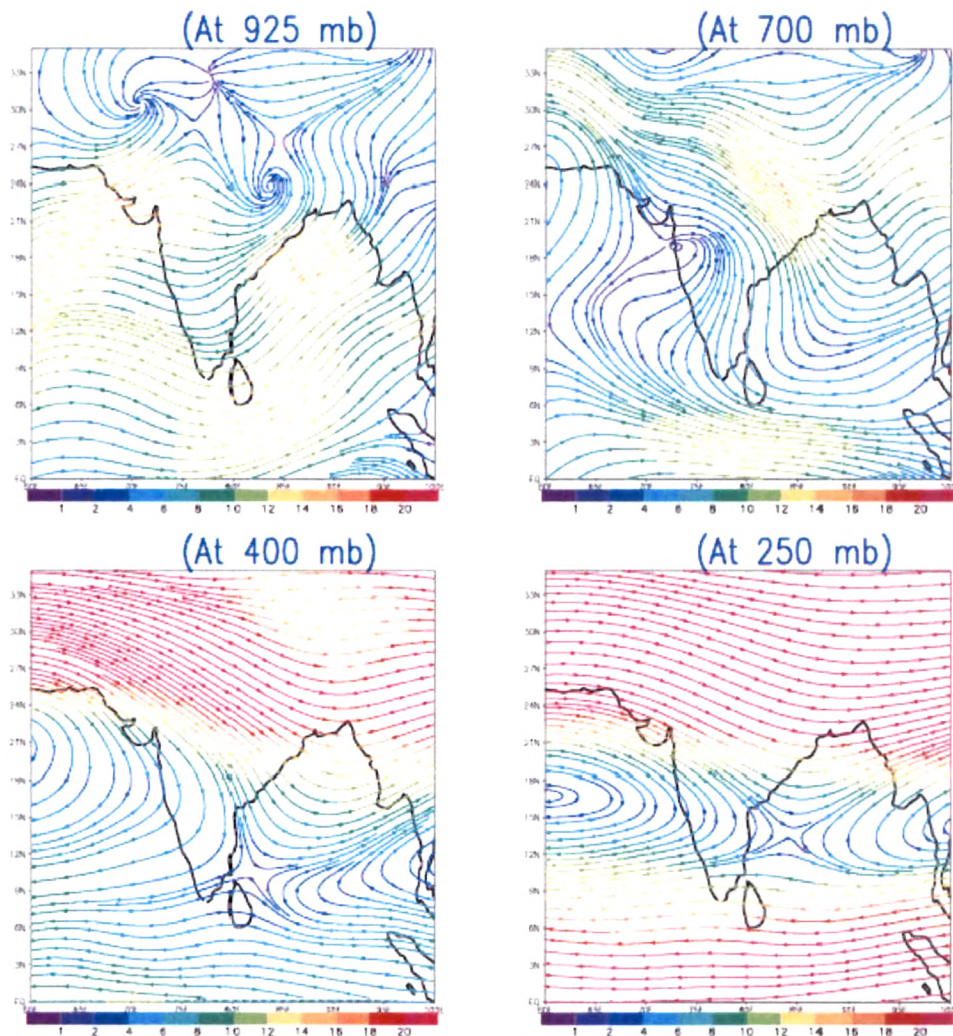


Fig. 3.2b. Mean wind fields at four different pressure levels during the pre-monsoon (MAM) season for the year 2003 over the Indian sub-continent. Color bars represent the magnitude of wind speed (m/s). Data adapted from NCEP.

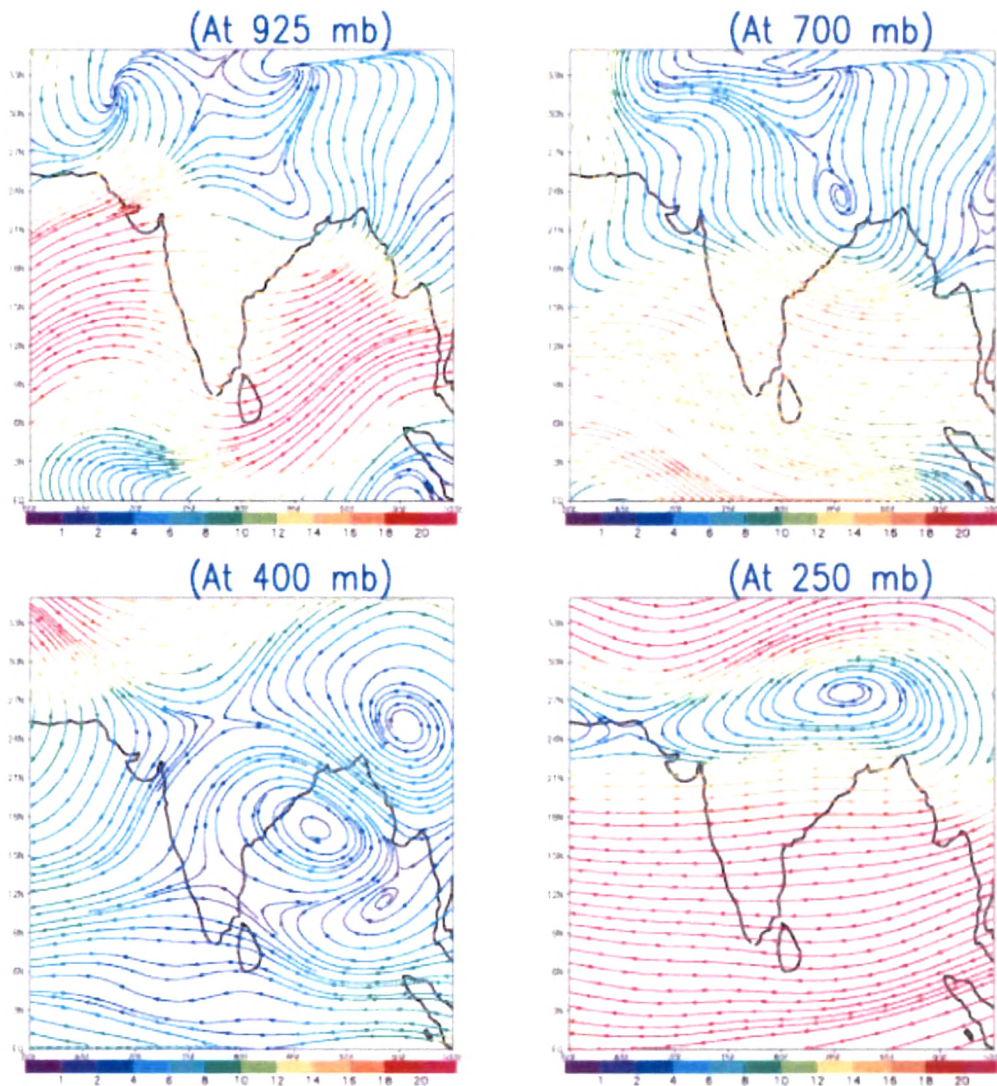


Figure 3.2c. Mean wind fields at four different pressure levels during the rainy season (JJAS) for the year 2003 over the Indian sub-continent. Color bar represents the magnitude of wind speed (m/s). Data adapted from NCEP.

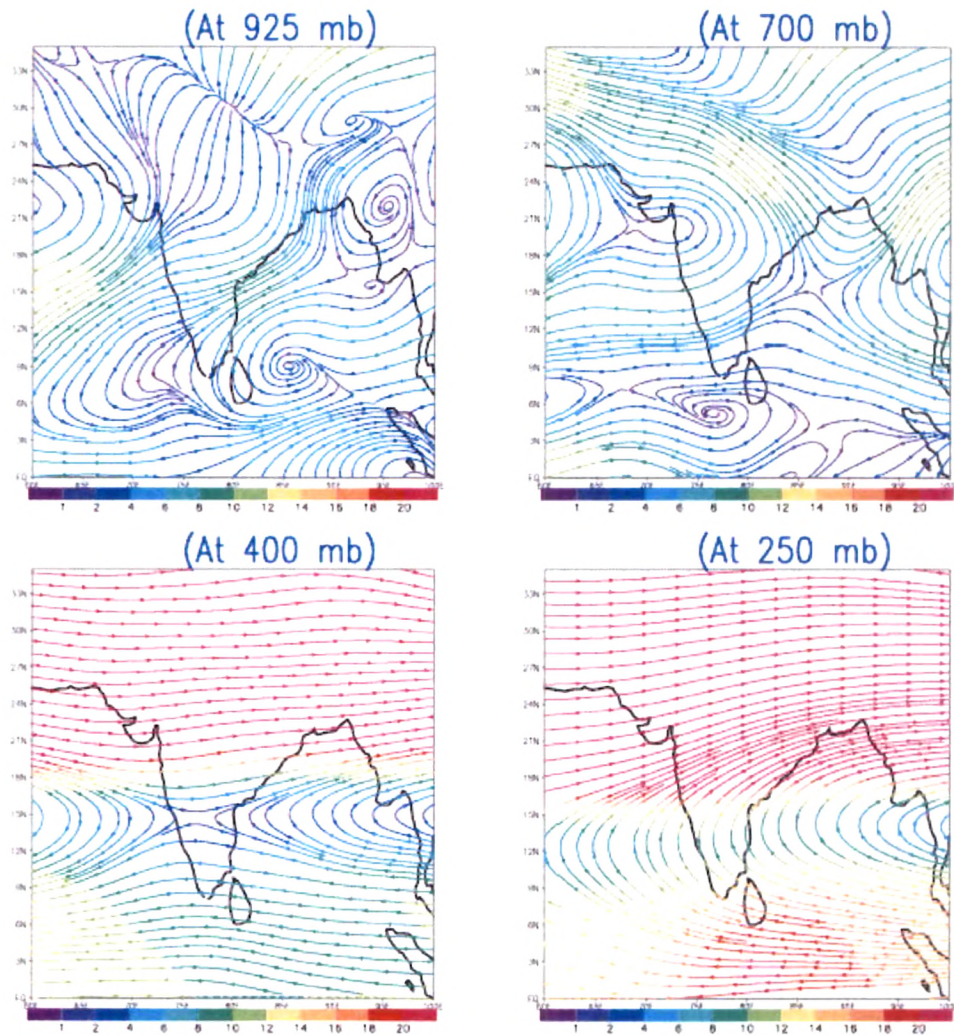


Fig. 3.2d. Mean wind fields at four different pressure levels during the post-monsoon (ON) season for the year 2003 over the Indian sub-continent. Color bar represents the magnitude of wind speed (m/s). Data adapted from NCEP.

3.3.2. Surface meteorology

Daily average values of surface air temperature, relative humidity, and wind speed are shown in Figure 3.3 for Ahmedabad between 2003 and 2007 (data downloaded from <http://www.wunderground.com>). The average temperature values range from 18 °C to 35 °C with a minimum during the winter (January) and maximum during the summer (May - June). There was a slight decrease in July-August due to the rainy period. Relative humidity (RH) was found to be less than 30% during the winter season while it ranged between 30 and 40 % during both pre-monsoon and post-monsoon seasons. The season which markedly differs from all other seasons in a year is the monsoon season, when average relative humidity over this site was more than 70 % and surpassed 90 % mark quite a few times within this season.

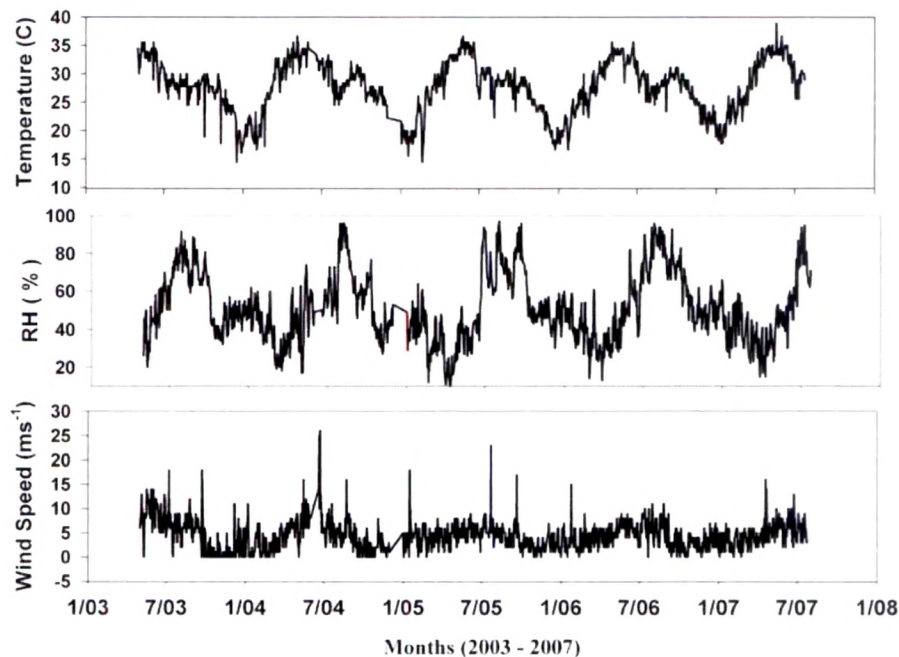


Figure 3.3. Seasonal variations in three important surface meteorological parameters measured over Ahmedabad during the four year period from 2003 to 2007.

The Indian summer monsoon is part of a large scale circulation pattern, which develops in response to the thermal gradient between the warm Asian continent in the north and cooler Indian Ocean in the south. A strong south-westerly flow in the lower troposphere brings a substantial supply of moisture into the continental region, which is released as precipitation. Surface wind speed over Ahmedabad was highest during the pre-monsoon season ($\sim 5 \text{ ms}^{-1}$), whereas it was usually calm during the post-monsoon and winter seasons ($\sim 3 \text{ ms}^{-1}$).

3.4. Winds observed over Ahmedabad using balloon borne GPS

3.4.1. Annual variation

Global Positioning Systems (GPS) were launched along with ozone and radiosondes on most of the balloon soundings from Ahmedabad. Total wind speed and wind direction as well as its zonal (U) and meridian (V) components were calculated from the position data of the GPS during the balloon flights. Monthly variation of average wind speed, U-wind and V- wind from surface to 10 km are shown in Figure 3.4. Total wind speed and zonal (U) wind reached up to 40 ms^{-1} during the winter months while these were low about 10 ms^{-1} during summer and rainy seasons. On the contrary V-wind component remained high ($4\text{-}8 \text{ ms}^{-1}$) during the months of March, April, May as well as in October. There was little variation in the direction of V-wind during different months over Ahmedabad.

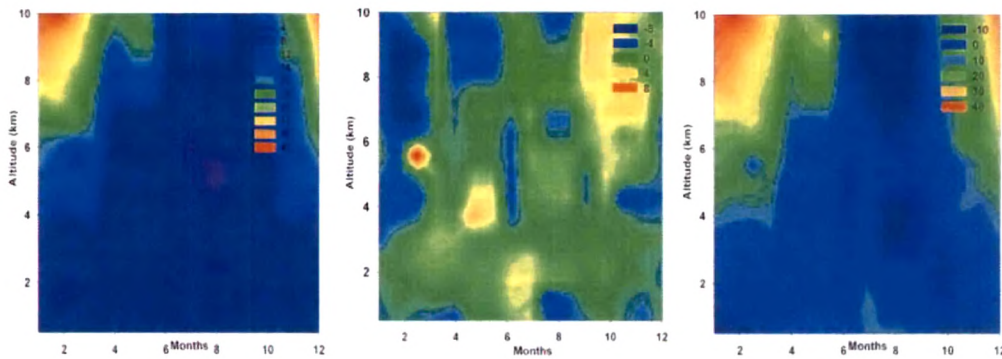


Figure 3.4. Average wind speed, ms^{-1} (left), zonal wind component, U-Wind (middle), meridional component, V-Wind (right) over Ahmedabad from 2003 to 2007.

3.4.2. Seasonal variation

Vertical profiles of wind speed, U-wind and V-wind for different seasons pre-monsoon, monsoon, post-monsoon, and winter are shown in Figure 3.5. Except for the monsoon season, wind speed and U-wind showed peak wind speeds at around 12 km height. This peak value was at its highest ($\sim 40 \text{ ms}^{-1}$) during winter and its lowest ($\sim 25 \text{ ms}^{-1}$) during the pre-monsoon period. However, during the monsoon season this peak was not pronounced. Comparison of vertical profiles of wind speed, U-wind, V-wind with those from NCEP data show excellent matching. Figure 3.6 a and b show a typical comparison of the wind speed based on GPS data with that from NCEP on November 12, 2003 and on 30 June, 2004.

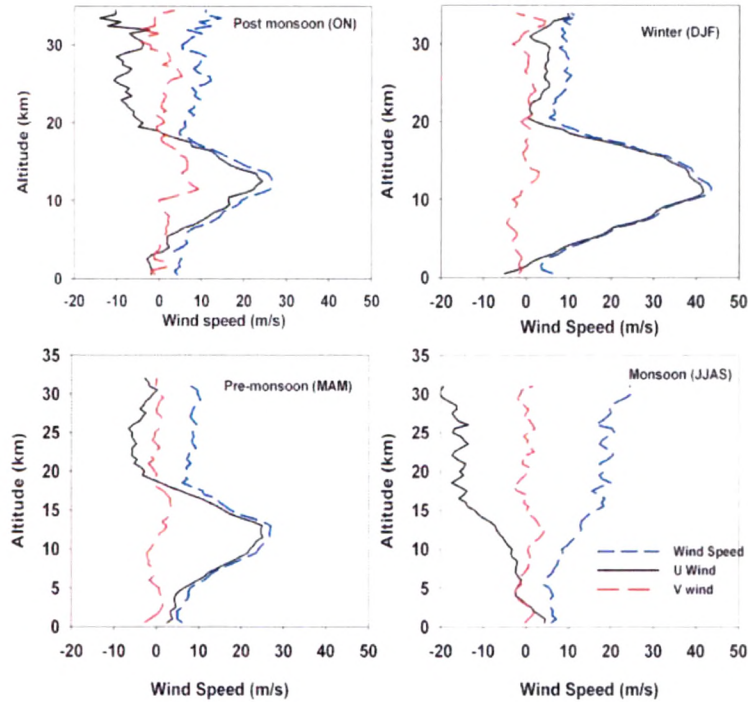


Figure 3.5. Vertical distribution of average wind components measured over Ahmedabad for the period 2003-2007 using a GPS (Global Positioning System) during the post-monsoon (top left), winter (top right), pre-monsoon (bottom left), and monsoon (bottom right) seasons.

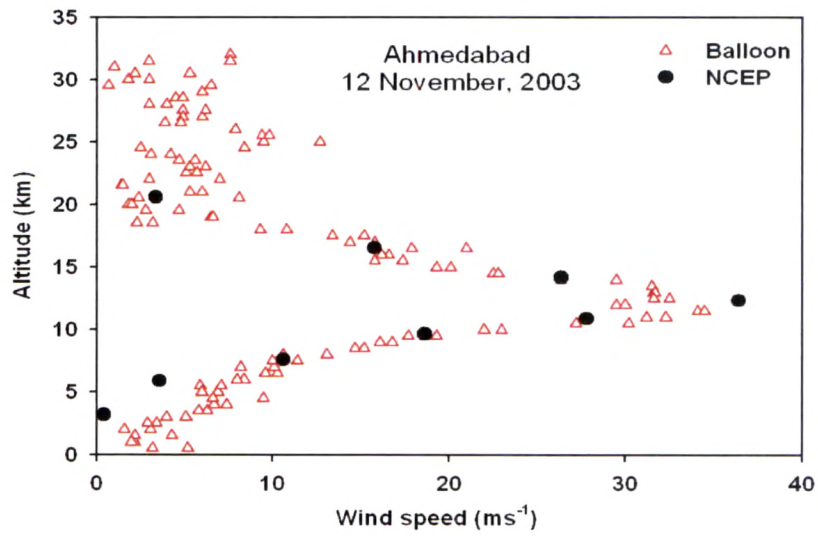


Figure 3.6a. Comparison of wind speed measured using radiosonde-GPS over Ahmedabad and NCEP data on 12 November, 2003.

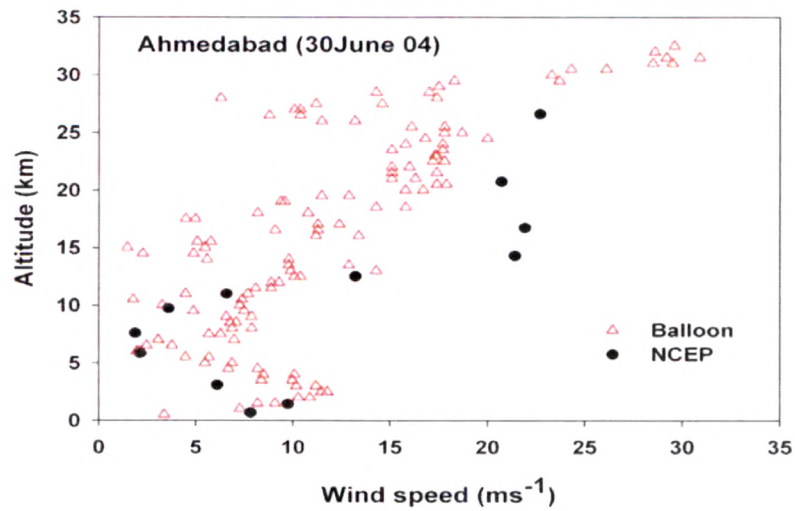


Figure 3.6b. Comparison of wind speed measured using radiosonde-GPS over Ahmedabad and NCEP data on 30 June, 2004.

3.5. Vertical distributions of temperature and humidity observed over Ahmedabad

As mentioned earlier in Chapter 2, each balloon had a radiosonde along with an ozonesonde and a GPS. The average monthly temperatures observed for the height range of 0-10 km during 2003-2007 are shown in Fig. 3.7 a and b. Contour plot of monthly variation of temperature from 0 to 5 km and 5 to 10 km are shown in Figures 3.7 a and b. In the lower troposphere temperature was at a maximum during the rainy season.

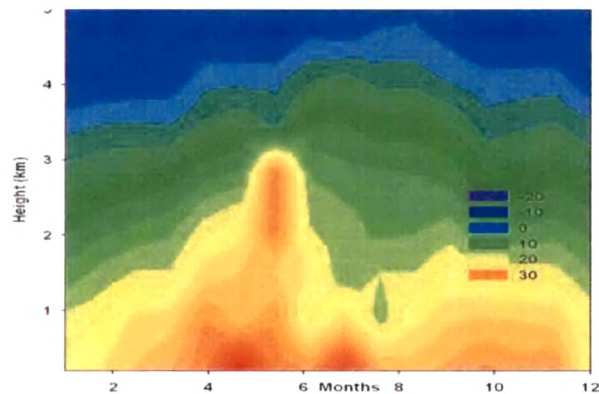


Figure 3.7a. Contour plot of monthly average temperature from 2003 to 2007 over Ahmedabad for 0-5 km.

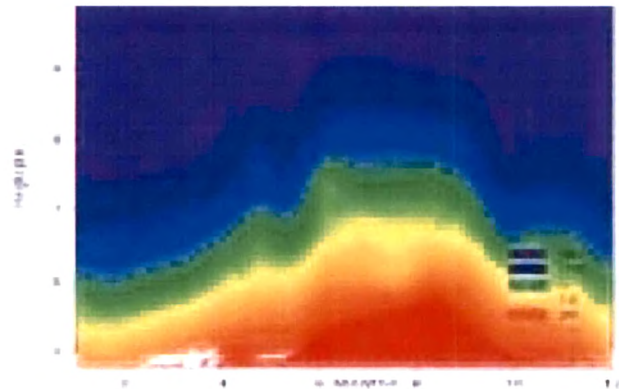


Figure 3.7b. Contour plot of monthly average temperature from 2003 to 2007 over Ahmedabad for 5-10 km.

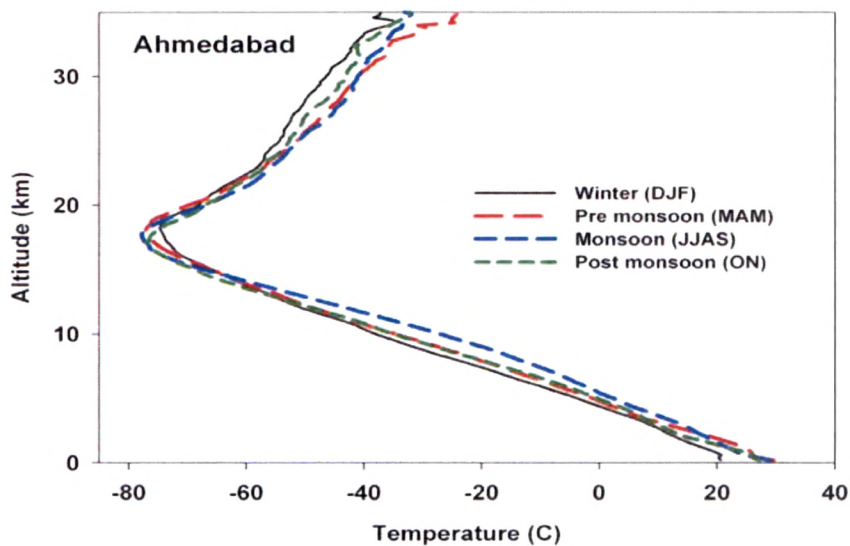


Figure 3.8. Seasonally averaged vertical profiles of temperature over Ahmedabad.

In the boundary layer, the minimum temperature was observed during the winter while the maximum was observed during the monsoon. Near tropopause, temperature was minimum in winter. In the stratosphere, winter was very cold compared to the monsoon season (Fig. 3.8).

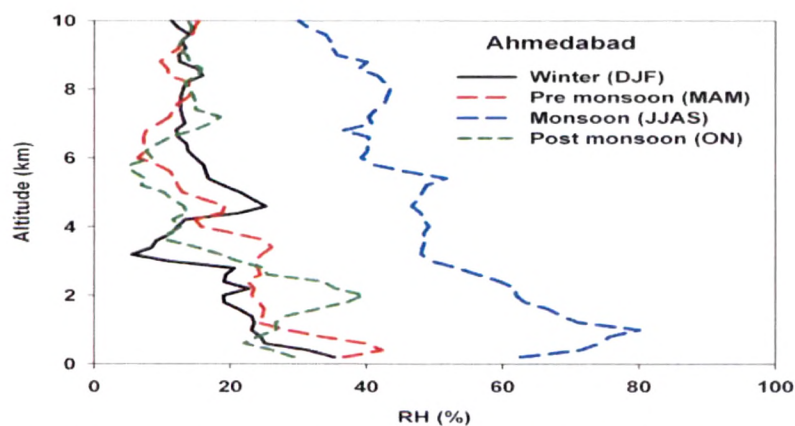


Figure 3.9. Seasonally averaged vertical profiles of relative humidity RH (%) over Ahmedabad.

/3040

From Figure 3.9, it can be seen that near the surface, relative humidity was exceptionally high at about 70% during the rainy season while during other seasons it showed an average of 30%.

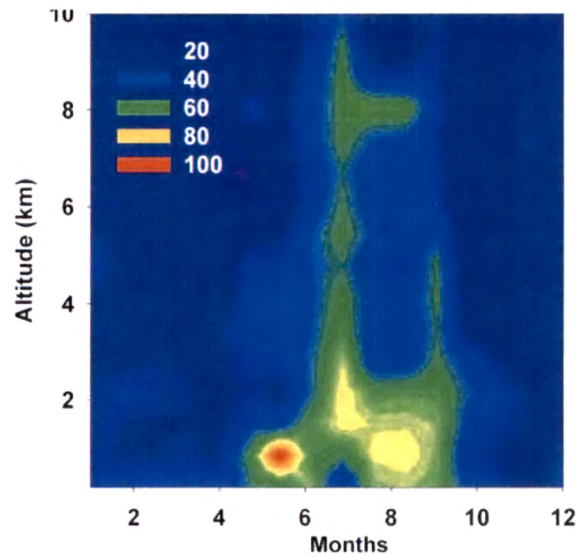


Figure 3.10. Contour plot of relative humidity RH (%) between 1-10 km at Ahmedabad during 2003-2007.

Relative humidity, RH (%) was measured by the radiosonde up to 10 km of altitude. RH (%) showed high values between May and September. It remained high even in the free troposphere up to 10 km of altitude during the month of July (Fig. 3.10).

3.6. Variation of tropopause height over Ahmedabad

Tropopause height was obtained from the radiosonde temperature data collected during each balloon flight. There are many methods for determining the tropopause. The cold point tropopause method was used in this study. Variation of monthly average tropopause height is shown in Figure 3.11. Tropopause height was at its lowest (~ 17.2 km) during October and at its highest (18.2 km) in March. These two months also show minimum and maximum variability, respectively. The average tropopause height based

on the entire data over Ahmedabad was 17.6 ± 0.4 km and the tropopause temperature was 78.5 ± 1.1 C.

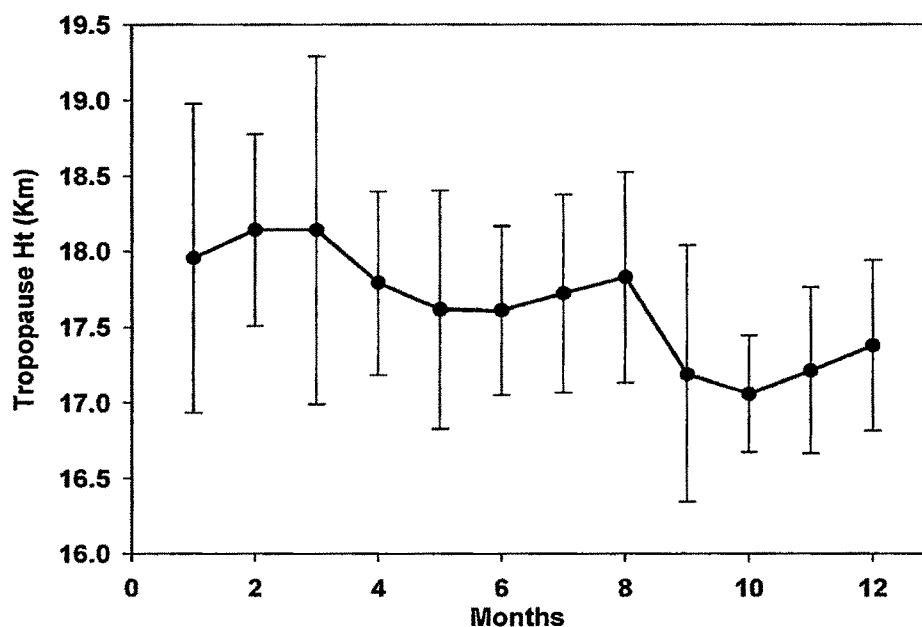


Figure 3.11. Variation of monthly average tropopause height over Ahmedabad from 2003 to 2007.

Monthly average change in Tropical Tropopause Layer (TTL) is depicted in Figure 3.12. It is observed that tropopause weakens in the months of March, April, May, August and September, but Stratosphere-Troposphere-Exchange (STE) was observed only during the months of March and April. STE depends on two factors, tropospheric structure and presence of jet streams (Figure 3.13). In August and September, jet streams are not present.

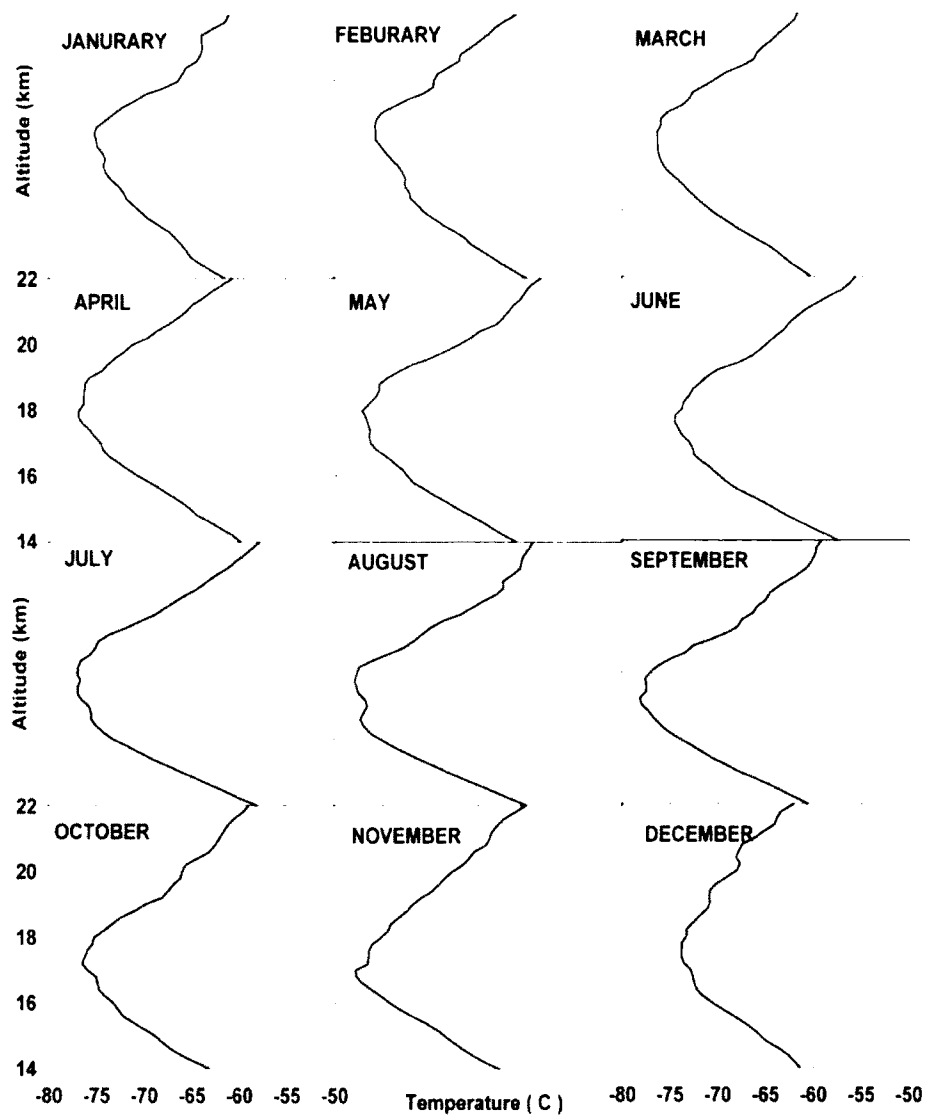


Figure 3.12. Monthly average temperature in TTL region over Ahmedabad during 2003-2007.



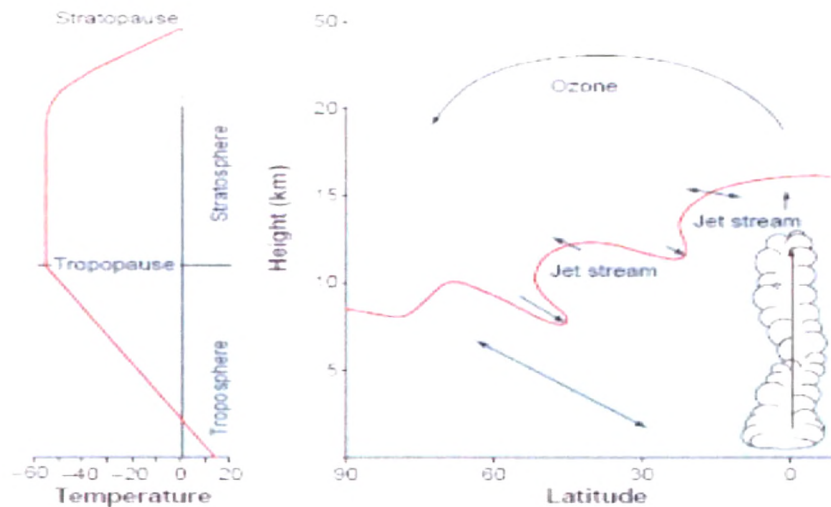


Figure 3.13. Typical vertical profile of atmospheric temperature (left). Schematic vertical section from equator to pole on a particular day, showing the tropopause with westerly jet streams, tropical convection, and transport and exchange (right). Tropospheric structure and jet streams adapted from Hoskins et al. [2003].

The tropopause is important on a daily basis because it puts a lid on tropospheric convection. The tropospheric air that eventually moves high into the stratosphere crosses the tropopause in the equatorial region. However, the winds are such that while the air crosses the tropopause it must also move a considerable horizontal distance. In the subtropics, there is a two-way exchange, whereas at higher latitudes, streamers and cut-off pools of stratospheric air are produced by weather systems and later absorbed into the troposphere [Hoskins et al., 2003].

Movement of the tropopause determines the extent of Stratosphere-Troposphere Exchange (STE) events. It was found that the stratospheric signature can be observed at pressures as low as 190 hPa during the northern hemisphere spring season. The major implication for such a pronounced vertical movement is that the downward penetrated air from the stratosphere is likely to deposit elevated levels of ozone in the upper troposphere. Though the analysis at 250 hPa revealed that the values of the stratosphere-troposphere index are consistent with other studies, it was also found that the stratosphere to troposphere penetration is more likely to occur during the winter to spring period than other seasons. Monthly variation in the structure of tropopause over Ahmedabad is shown in Figure 3.12. This figure indicates the weakening of tropopause in the months of March, April, July, August, and September but STE was observed only during the months of March and April. This observation may be because of the presence of a 'jet stream' during these months near the tropopause which brings ozone rich air from the stratosphere.

3.7. Seasonal variations in distribution of ozone

Vertical distribution of ozone was obtained up to about 32-35 km height. These data are grouped to study the seasonal variation in its distribution based on all the balloon flights made during 2003 to 2007. Figure 3.14 depicts average ozone profiles during the four seasons viz winter, pre monsoon, monsoon, and post monsoon. Ozone partial pressure decreased with height in the free troposphere and reached a minimum (around 10 nb) near the tropopause. There was a large variability (10 nb to 65 nb) in the boundary layer with a minimum in the monsoon and highs during the post-monsoon and winter seasons. The peak ozone concentration shows a maximum during the monsoon season (140 nb) and a minimum during the winter season (120 nb). After this peak, ozone decreased again. This is the general pattern observed at other places in the tropical region [Subbaraya et al., 1994; Chan et al., 2004]. Ozone chemistry and its production and loss reactions are well known and are given in the standard books of atmospheric science [Brasseur and Solomon, 1985]. The peak ozone concentration during monsoon is due to

intense solar radiation and photochemical production of ozone at stratospheric heights.

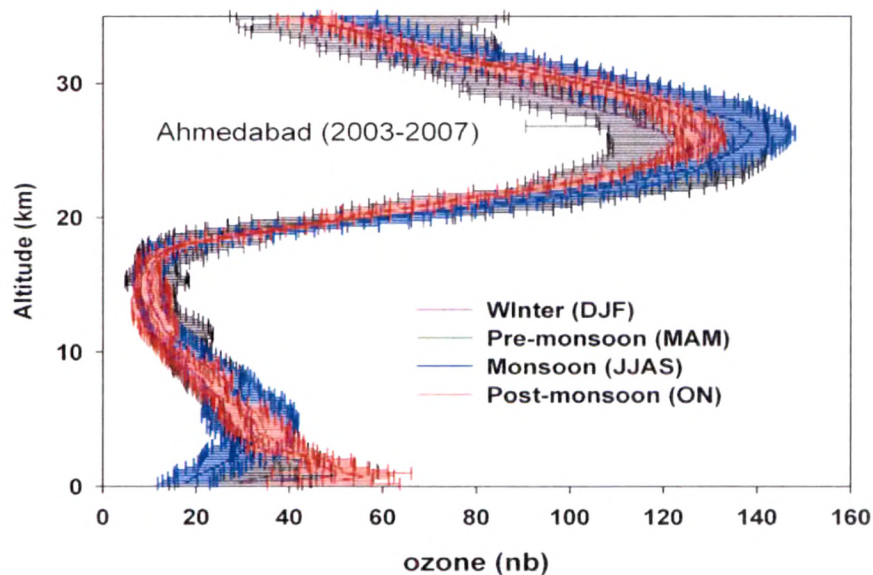


Figure 3.14. Average seasonal profiles with one sigma spread in vertical distribution of ozone observed over Ahmedabad during 2003-2007.

Table 3.1. Annual average ozone (nb) from 1 to 35 km with a spread of $\pm 1 \sigma$

Height (km)	Ozone (nb)	Standard deviation
1	41.8	9.8
2	45.2	3.6
3	36.0	2.4
4	30.4	1.0
5	28.0	0.5
6	26.5	0.8
7	24.7	0.8

8	22.1	0.7
9	19.1	0.9
10	17.6	0.4
11	16.2	0.9
12	13.6	0.8
13	12.1	0.4
14	10.6	0.4
15	10.1	0.5
16	10.7	0.1
17	12.9	1.6
18	18.0	2.3
19	26.3	3.3
20	46.4	10.1
21	70.3	5.5
22	87.9	7.1
23	107.6	4.1
24	114.8	1.3
25	118.6	1.2
26	121.1	0.7
27	117.5	2.8
28	111.0	3.7
29	101.0	3.3
30	90.8	1.9
31	83.0	2.4
32	72.4	3.6
33	65.7	1.6
34	58.7	4.0
35	56.6	2.7

3.8. Variation of total ozone content over Ahmedabad

The observed ozone profiles are used to compute total columnar ozone over Ahmedabad. However, these data are limited to a maximum height of about 35 km and a significant amount of ozone is present above this height. These profiles are extrapolated using the method described by McPeters et al. [1997]. Monthly average total columnar ozone is shown in Figure 3.15 based on all the balloon flights made from Ahmedabad. The maximum ozone (285 DU) was observed in June and minimum (240 DU) was observed in December (Fig 3.15). High variability was observed during February, March and April while low variability was observed during the months of July and October. A comparison of the total ozone from ozonesonde data with those from total ozone mapping spectrometer (TOMS) shows good correlation in all seasons except rainy season. Average integrated ozone was 261 DU and average integrated ozone in the troposphere was 39.4 DU.

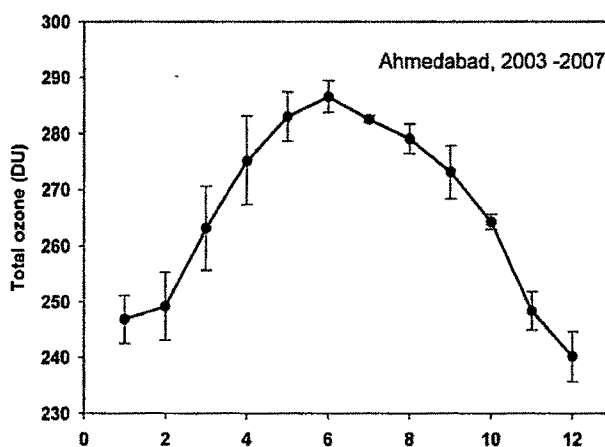


Figure 3.15. Average seasonal profiles with one sigma spread in vertical distribution of ozone observed over Ahmedabad during 2003-2007.

Stratospheric ozone has decreased over the last several decades, while tropospheric ozone has increased over the Northern Hemisphere mid-latitudes [Logan et al., 1999]. About 40% of the global ozone is located in the tropics between 25N and 25S, and a strong decadal variation of total ozone in the tropics with maxima approximately in phase with the 11 year solar cycle has been documented [World Meteorological Organization, 2003].

Statistically significant negative trends in total ozone were found at all latitudes except possibly in the tropics, where ground-based measurements show no long term trends [Madronich et al., 1994]. From total column ozone data (Dobson spectrophotometer) for the period 1957–1994, Chakrabarty et al. [1998] have found no long-term trend over the Indian tropical station, Pune. However, the Dobson ozone data of the same station for the period 1981–1998 showed a decreasing trend [Londhe et al., 2003]. The impact of changing air quality is largely felt through photochemical smog, in which tropospheric ozone plays a key role, through the increasing concentration of aerosol particles and the potential impacts of increasing UV-B radiation caused by the loss of stratospheric ozone. The changes in the earth's ozone layer due to anthropogenic activities and geological events significantly impact our biosphere. The seasonal variation of total ozone over India almost resembled the typical feature for low latitude stations characterized by a winter minimum and a summer maximum. Moreover, seasonal variation of surface ozone compared with that for total ozone may not show any correlation implying the role of vertical transport of ozone over the concerned location. Several measurements made during NASA's Global Tropospheric Experiment program over the Pacific and Atlantic Oceans have reported distinct pollution plumes of tropospheric ozone and its precursors in the middle and upper troposphere [e.g., Chameides et al., 1989; Davis et al., 1996; Fishman et al., 1996; Singh et al., 1996, 2000; Schultz et al., 1999].

Two ways to measure ozone in the atmosphere are measurement of total column ozone and measurement of the vertical distribution of ozone. Regular measurements of total column ozone are available from a network of surface stations, mostly in the mid-latitude Northern Hemisphere, with reasonable temporal coverage extending back to the 1960s.

Near-global, continuous total ozone data are available from satellite measurements since 1979. The ratio of the intensity of direct sunlight at two wavelengths in the 300–320nm range is a measure of the total abundance of ozone in a column through the atmosphere. This forms the basic operating principle for a variety of optical instruments that monitor atmospheric ozone. The ground-based ozone monitoring instruments Dobson and Brewer spectrophotometers are universally accepted for measuring column ozone but are expensive, heavy, and large in dimension.

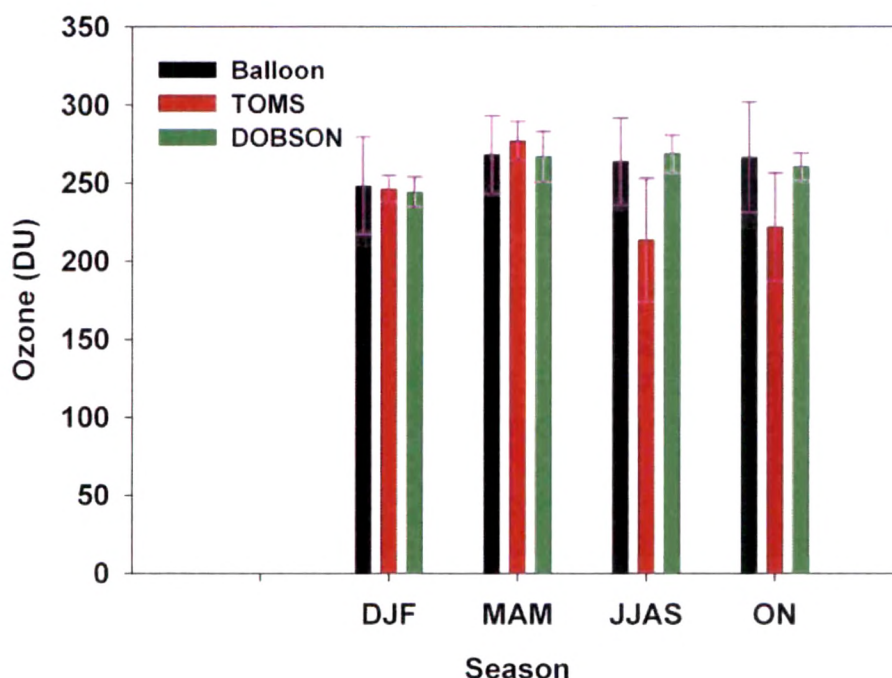


Figure 3.16. Seasonal variation of total ozone measured using ozonesonde, TOMS, and DOBSON from 2003-2007.

As discussed earlier, integrated total ozone was calculated by extrapolating the ozone concentration from 35 km to 60 km by a method prescribed by McPeters et al. [1997]. Total ozone was also calculated using the measurements obtained from the Dobson

instrument over Ahmedabad from 2003-2006. Comparison of the total ozone measured using ozonesonde, TOMS and DOBSON is shown in Figure 3.16. It is clear from the figure that for the winter season all the three instruments give almost similar values within the limits of error. For the pre-monsoon season TOMS ozone was slightly higher compared to the ozonesonde and DOBSON, while during the rainy season the reverse was true. Lower TOMS ozone during the rainy season may be due to the presence of cloud during rainy season over the tropical region. During the post monsoon season also TOMS total ozone amount was lower than the ozonesonde and DOBSON ozone concentrations.

3.9. Tropospheric column ozone

Focus of this study is on the tropospheric ozone distribution. The integrated columnar ozone up to the tropopause was calculated for each profile. The monthly average values are shown in Figure 3.17 based on all the soundings. Tropospheric column ozone increased from January (~ 36 DU) to a maximum value in April (43 DU) and later started decreasing. The lowest column content was observed during the monsoon period, with a minimum during September (34 DU). In fact this is the end of the monsoon season. After September, columnar ozone started increasing again and reached a value of about 42 DU in December. Variation of tropospheric column ozone differed much from the total integrated values as discussed in the previous section. The maximum in April seems to be related to transport from stratosphere to the upper troposphere.

Monthly average total tropospheric ozone (TTO) over Indonesia shows a double peak, one in the month of May and another in October. Maximum TTO was observed over Africa and South America during the month of October (Fig 3.18). However, over Ahmedabad trends similar to Indonesia were observed. An increasing trend was observed until April and then it started decreasing reaching a minimum in September (Fig. 3.17). Beyond September, again an increasing trend was observed peaking during the month of October (Fig. 3.17).

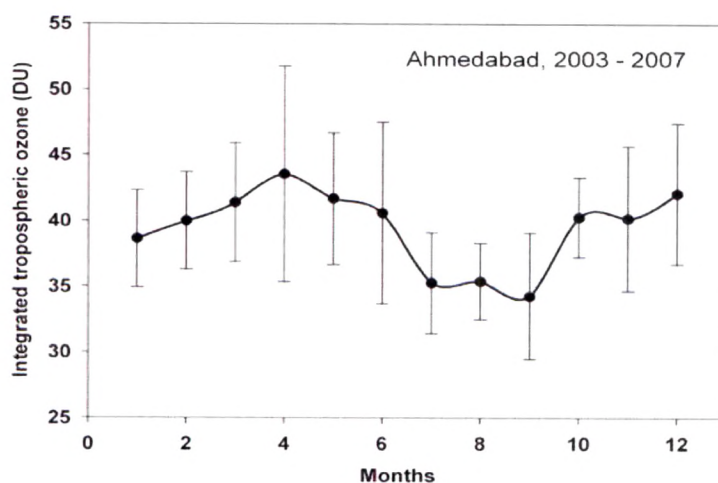


Figure 3.17. Monthly average Integrated tropospheric ozone (DU) up to the tropopause height over Ahmedabad.

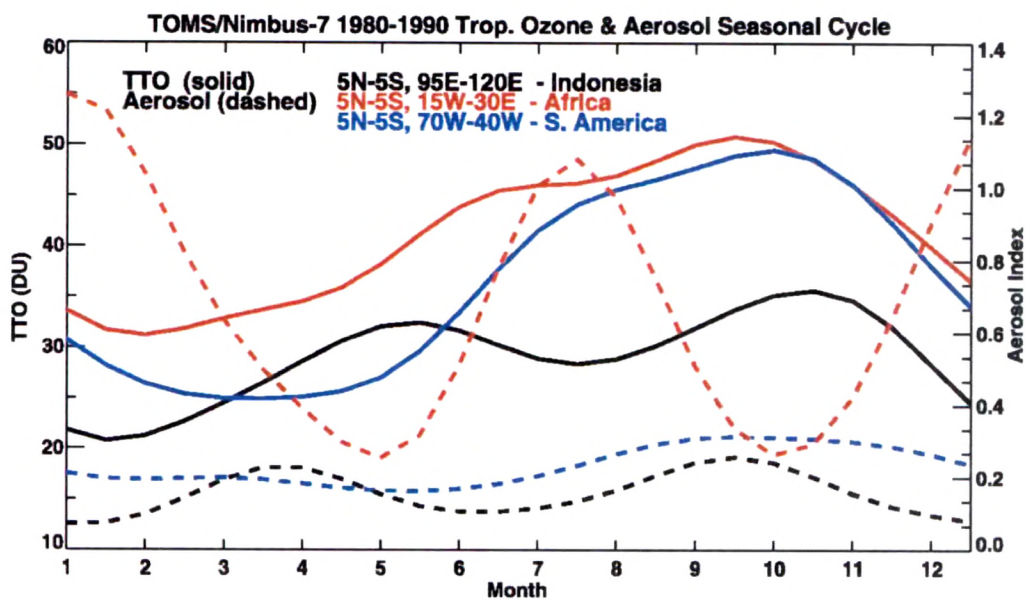


Figure 3.18. Integrated total tropospheric ozone TTO over different regions [adapted from Thompson et al., 2003].

Table 3.2. Monthly variation of average integrated tropospheric ozone (DU) measured using ozonesonde with spread of $\pm 1 \sigma$

Month	Total Tropospheric ozone (DU)	Standard deviation
January	38.6	3.7
February	40.0	3.7
March	41.4	4.5
April	43.5	8.2
May	41.7	5.0
June	40.6	6.9
July	35.3	3.8
August	35.4	2.9
September	34.3	4.8
October	40.3	3.1
November	40.2	5.5
December	42.1	5.4

The decreasing trend after April also coincided with the change in the wind pattern from north-west to west and south-west directions in the troposphere. The south-west winds bring cleaner air from the Indian Ocean to the sampling site. The seasonal variability in TTO is shown in Figure 3.19. A maximum was observed during the pre-monsoon season and a minimum was observed during the rainy season. Winter concentrations were intermediate.

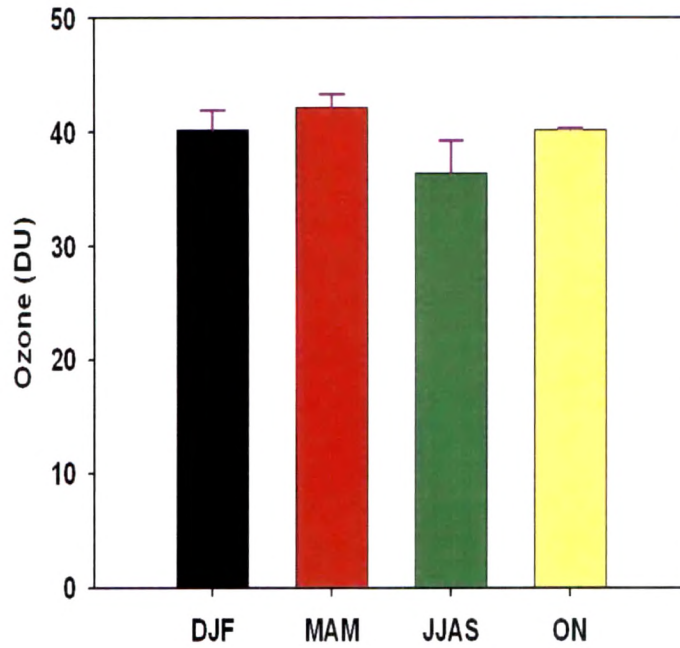


Figure 3.19. Seasonal variations in total tropospheric ozone concentration (DU) over Ahmedabad with $\pm 1\sigma$ standard deviation.

3.10. Comparison with TOMS derived tropospheric ozone column (TOC)

Using stratospheric content from SBUV or other mode of measurements and TOMS data, it is possible to estimate tropospheric ozone column (TOC) also referred as TTO [Chandra et al., 2003]. Figure 3.20 shows a comparison between balloon derived TOC and satellite derived TOC. It is interesting to note that the seasonal patterns of the two data sets match very well. However, there are minor differences. The satellite values are mostly within the spread of the balloon data and the difference is mostly within 5 DU. However, the monthly average TOC values from satellite are higher during monsoon months.

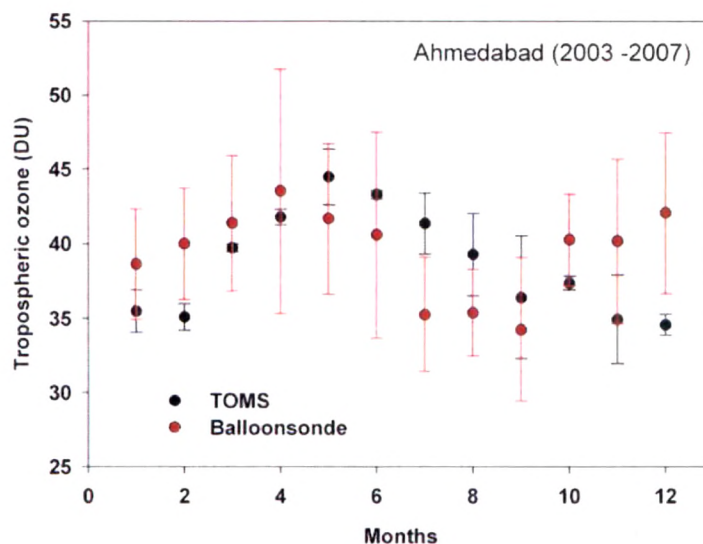


Figure 3.20. Monthly tropospheric ozone (DU) using ozonesonde and TOMS over Ahmedabad.

3.11. Vertical distribution of tropospheric ozone

Ozone mixing ratio (ppbv) for of the troposphere (0-15 km) and the tropopause region (15-18 km) are shown in Figure 3.21(a and b). These contour plots are based on monthly average values from all the balloon soundings at an interval of 200m. Ozone mixing ratio in the lower troposphere was observed to be low from April to September up to about 3 km height. Winter months show higher ozone values in the same height region. Highest ozone was observed from April to June between 5 and 10 km height. In the upper troposphere highest ozone values are observed during the period between April and June. Figure 3.21b, shows ozone variation near the tropopause which is especially known as the Tropical Tropopause Layer (TTL). It is the most important region for the exchange of gases between the stratosphere and the troposphere, also known as STE. In this region

the ozone mixing ratio showed a large variability where ozone varied from 40 ppb to 140 ppb. High ozone values are observed in winter and pre-monsoon months. Vertical profile of tropospheric ozone for the spring season (MAM) was similar to the ozone profile observed at Hong Kong [Chan et al., 2004] which lies on the same latitude as Ahmedabad.

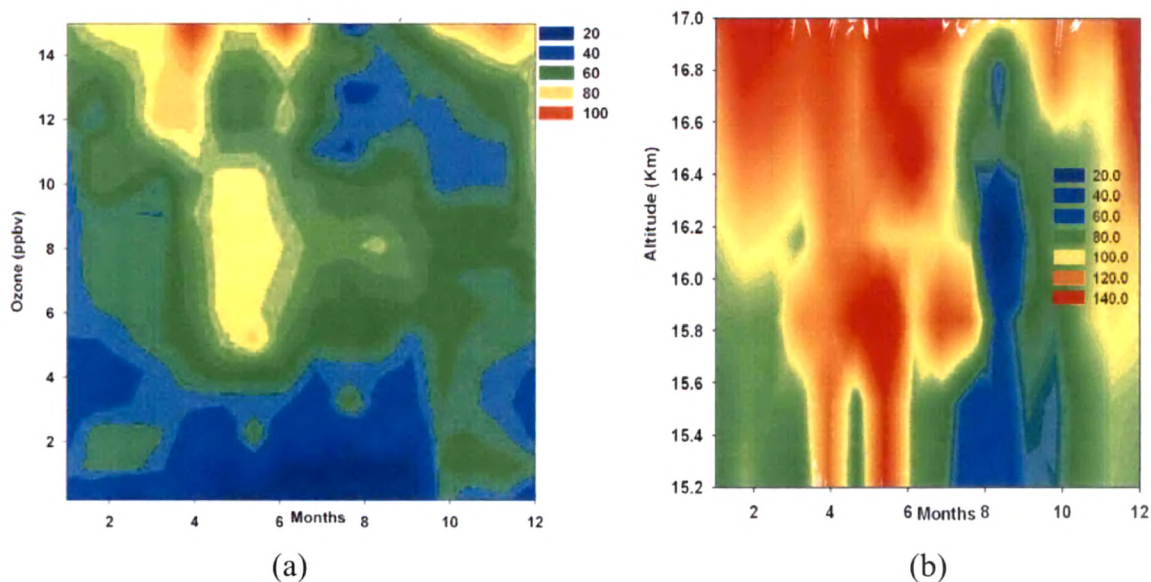


Figure 3.21. Monthly average distribution of ozone measured over Ahmedabad during 2003-2007 from surface to 15 km (a) and from 15 to 18 km (b) Observed over Ahmedabad during 2003-2007

3.12. Vertical distributions of ozone, temperature, and relative humidity during different seasons

In Figure 3.22, seasonally averaged ozone (ppbv), temperature ($^{\circ}\text{C}$) and relative humidity (%) with spread of ± 1 sigma for different seasons are shown. Boundary layer ozone was maximum during the winter and minimum during monsoon. This observation could be due to shallow boundary layer height during winter and wash out of pollutants during monsoon. The summer monsoon ozone minimum in the lower troposphere is attributed

to the onset of summer monsoon when air flow from the Asian continent is replaced by air from the tropical Indian Ocean. The middle tropospheric ozone is maximum during rainy season and minimum during post monsoon season. Near tropopause, large variability was observed during pre- monsoon and winter due to the intrusion of ozone from the stratosphere. A frequently observed feature during the pre-monsoon and winter seasons was high ozone mixing ratio (80-170 ppbv) in the upper troposphere (from about 9 to 16 km). Ozone increase due to STE for the month of March was 5 DU and for April it was 15 DU. This phenomenon is generally observed at higher latitudes but over the tropical region it has been observed mainly in the months of March and April. This is the first experimental study to estimate the flux due to STE process over Ahmedabad.

Increase in ozone lifetime in the free troposphere increases the importance of transport pathways during different seasons over Ahmedabad. It was observed that the trajectories of transported air masses pass through the free troposphere over continental India. Therefore, such transports can also have impacts in the vertical distributions of various trace gases over this region. The main aim of this work is to study how transport processes affect the vertical distributions in the troposphere over the Indian subcontinent.

In the lower and mid-troposphere, high concentrations of O_3 in the spring season could be due to the long-range transport of pollutants by northwesterly winds associated with the winter monsoon circulation. This circulation transports the ozone-rich polluted air masses from the Asian continent. Conversely, summer minima with mean concentration as low as 15 ppbv during July to September period was observed over Ahmedabad. This is related to summer monsoon circulation, advecting clean and moist air from the Indian Ocean.

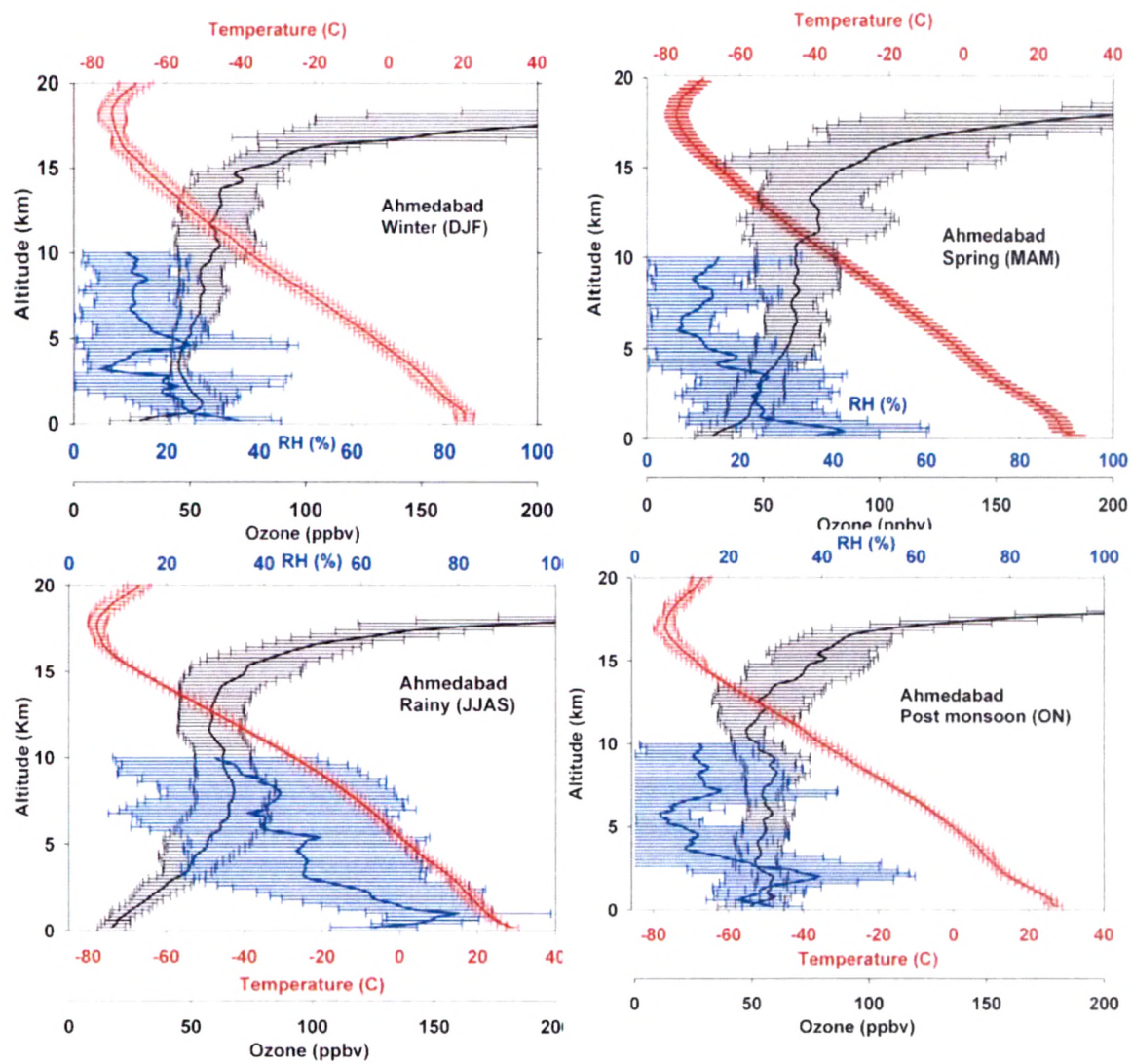


Figure 3.22. Seasonally averaged ozone (ppbv), temperature ($^{\circ}\text{C}$) and relative humidity (%) with spread of ± 1 sigma for different seasons.

Elevated O_3 values of around 100-450 ppbv were observed in the middle and upper troposphere (10-14 km) during the spring season over Ahmedabad. Ozone mixing ratios were around 40-60 ppbv in the lower and middle troposphere while in the upper troposphere values were around 60-80 ppbv during August, September and October months. Occurrences of high O_3 tongues in the spring season follow the propagation of dry air with low relative humidity, suggesting that O_3 is from higher heights, probably of stratospheric origin. The summertime low values over Ahmedabad are attributed to summer monsoon circulation, advecting ozone-poor air mass from the Arabian Sea and the Indian Ocean over the continent during these periods. The convective processes lift the advected ozone-poor air masses from the planetary boundary layer (PBL) to the upper heights. In general, O_3 and water vapor show just opposite seasonal variations, though water vapor distribution is very much localized compared to O_3 . Similar annual patterns in O_3 and water vapor are repeated during different years except some small-scale differences.

Vertical profile of tropospheric ozone for the rainy season over Ahmedabad is shaped like “S” with a minima at the surface and maxima at ~6-7 km with another minima at around 12-13 km and subsequent increase towards the tropopause. Mid tropospheric maxima during the rainy season in the ozone profile over Ahmedabad is similar to those observed in the southern tropical region as shown in Figure 3.23. The mid-tropospheric maxima during rainy season in the O_3 profiles over Ahmedabad are result of convective activity. The lifetime of O_3 is short in the MBL. Convection vents ozone-poor air from MBL to upper troposphere [Lelieveld and Crutzen, 1994]. This ozone-poor air can develop in upper troposphere and in the MBL while the middle troposphere remains relatively unaffected. This resulted as increased O_3 values in the middle troposphere [Folkins et al., 2002].

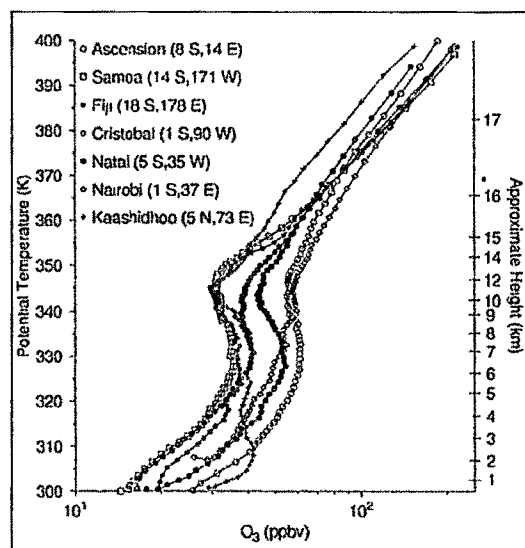


Figure 3.23. The mean annual dependence of ozone mixing ratio on potential temperature measured at different sites in the tropics. Figure adapted from Folkins et al. [2002].

This is due to STE. For spring season, trend of tropospheric ozone profile is like what we see generally over the mid-latitudes while for rainy season, tropospheric profile is like typical profile over the tropical region. This “S-shape” profiles as reported by Folkins et al. [2002] over southern tropical region are shown in Figure 3.23.

Vertical distributions over Ahmedabad show higher background O_3 values than in the troposphere [Folkins et al., 2002]. Dynamics play major role in the seasonal distribution over Ahmedabad. In the lower and middle regions of the troposphere, low O_3 values with high water vapor concentrations in the summer monsoon season are pronounced, whereas in the upper regions of the troposphere, high O_3 values with very low amount of water vapor in the spring season is pronounced [Newell et al., 1998]. Back trajectory analysis suggests that this enhancement resulted from the transport. Air masses arriving at the altitudes where O_3 peaks in the middle troposphere appear to have passed over the regions of biomass burning which occurs at this time of year (October and November months).

3.13. Stratospheric–Tropospheric Exchange over Ahmedabad

It is clear from the tropospheric ozone distribution over Ahmedabad that upper tropospheric ozone increases in the month of March and April. It is also seen that tropospheric column ozone shows higher values as well as higher variability during these months.

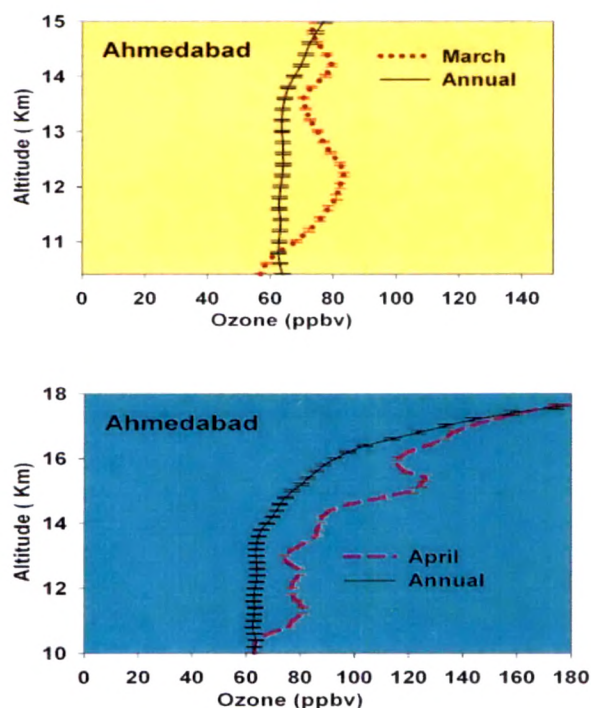


Figure 3.24. Monthly average ozone profiles for the months of March (Red) (top) and April (Pink) (bottom). Average annual ozone (Black) profile is also shown for a comparison.

Consequently, these two months are chosen to compute the increase in tropospheric ozone as compared to the average annual values. The increase in ozone is computed by integrating the excess area as compared to the annual average values as shown in Fig. 3.24.

The increase in tropospheric ozone for the month of March and April 5.3 DU and 14.2 DU (mixing ratios in ppbv are converted to DU) in the height range of 10 to 15 km computed using the Trapezoidal rule as shown in Figure 3.25a and b. This increase in tropospheric ozone can occur due to weakening of the tropopause. Double tropopause was observed for the month of March and April.

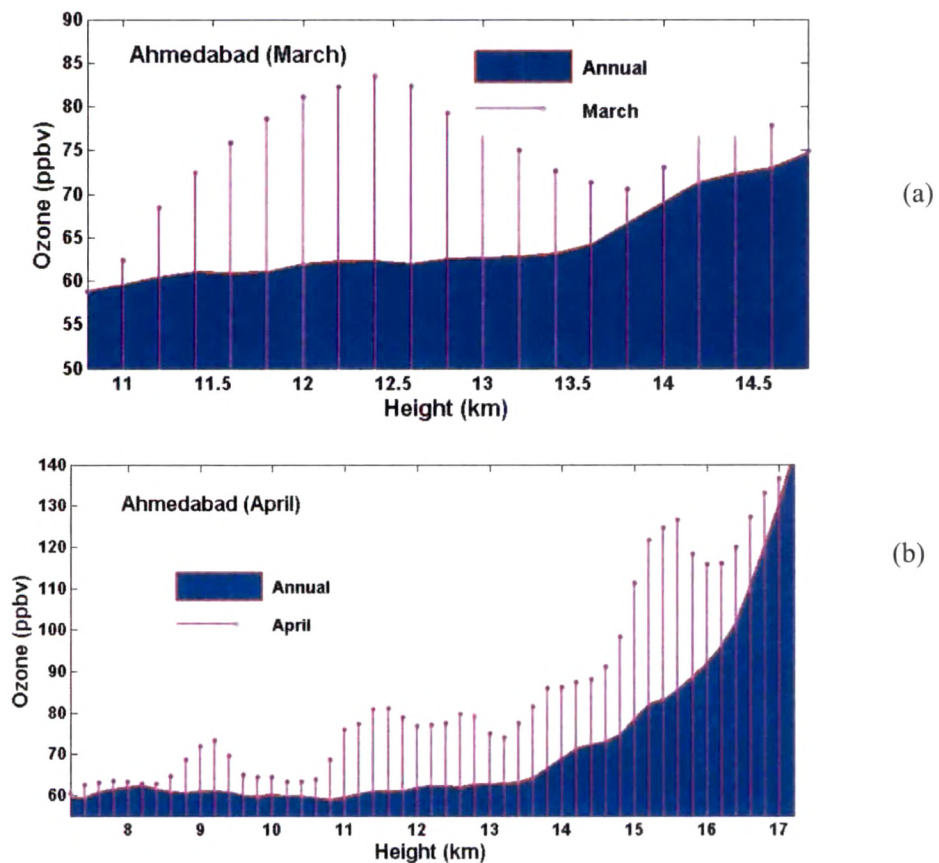


Figure 3.25. a) Annual average ozone vertical profile (Black) and mean vertical profile for the month of March (Red). b) Vertical profile of ozone for April (Pink) and annual average (Black) from 10 to 18 km

3.14. Day-to-day variability in tropospheric ozone: A case study

Each O₃ profile is a unique response to photochemical and dynamic process operating in the atmosphere. There can be large day-to-day variability in the vertical structure of O₃ at any location. Sometimes the vertical structure appears very irregular exhibiting marked stratification, with a single or multiple peaks in the ozone distribution sometimes the absence of structure, exhibits uniform profile. Earlier, mean profiles averaged for a season or a year have been analyzed to understand the long term variation in the vertical distribution of ozone [Logan, 1999; Thompson et al., 2003]. Case study analyses were used to understand the atmospheric processes [Folkins et al., 1999; Zachariasse et al., 2000; Kim et al., 2002]. Long term measurements provides the information about the back ground concentration along with the contribution to our knowledge of O₃ budget, on the other hand, case study analysis enhances our understanding of the processes and frequency of occurrence of such events. In the earlier section, average profiles of ozone were used to study ST exchange. This section describes some special cases.

3.14.1. Case -1: Ozone distribution on 9 March, 2005

Vertical profiles of ozone mixing ratio, temperature and relative humidity on 9 March, 2005 over Ahmedabad are shown in Figure 3.26. In the lower troposphere (from surface up to 5 km) ozone is almost constant and fluctuates between 20-30 ppbv while corresponding humidity profile shows decreasing trend with sharp fluctuations. Ozone value increases to 200 ppbv at 12 km of altitude and then there is another shoot up in the ozone concentration at around 16 km of altitude goes up to 500 ppbv and then again at 17 km goes up to 800 ppbv just below the tropopause. Double tropopause has also been observed on this day i.e. first temperature inversion at 19 km and another at 20 km. This indicated weakening of tropopause structure while allow this stratospheric air to come down to troposphere. Since 90% of the ozone lies in the stratosphere so this double tropopause allows stratospheric ozone to descend to troposphere. This increase in tropospheric ozone just below the tropopause is due to the intrusion of stratospheric ozone in the troposphere.

Ozone value at the surface is around 10 ppbv and shows linear increasing trend in the lower troposphere (from 10 km altitude) while relative humidity varies between 40 -60% in lower 5 km of altitude with some small scale fluctuation. There is sharp increase in O_3 when the values of around 200 ppbv at 10 km altitude and there is a sharp temperature inversion at this altitude which indicate that this temperature inversion is due to sudden increase of tropospheric ozone. Figure 3.27 shows back trajectory plots at altitude 10 km over Ahmedabad for pre-monsoon season. The trajectory arriving on 9 March 05 (Green color) passed over high latitude region.

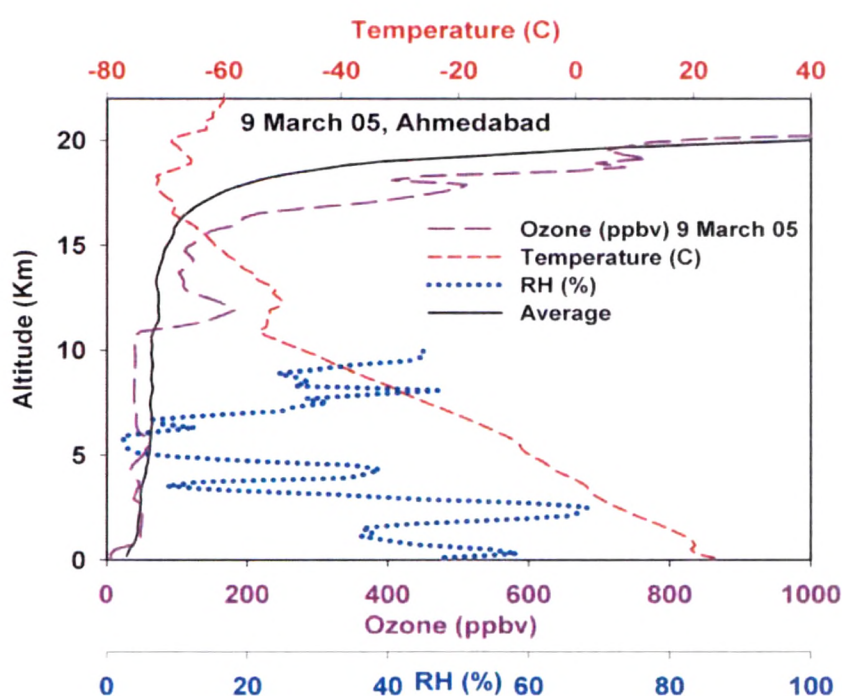


Figure 3.26. Vertical profile of ozone (ppbv), temperature and RH (%) observed on 9 March, 2005 over Ahmedabad. Average corresponds to average ozone concentration during March for the entire study period.

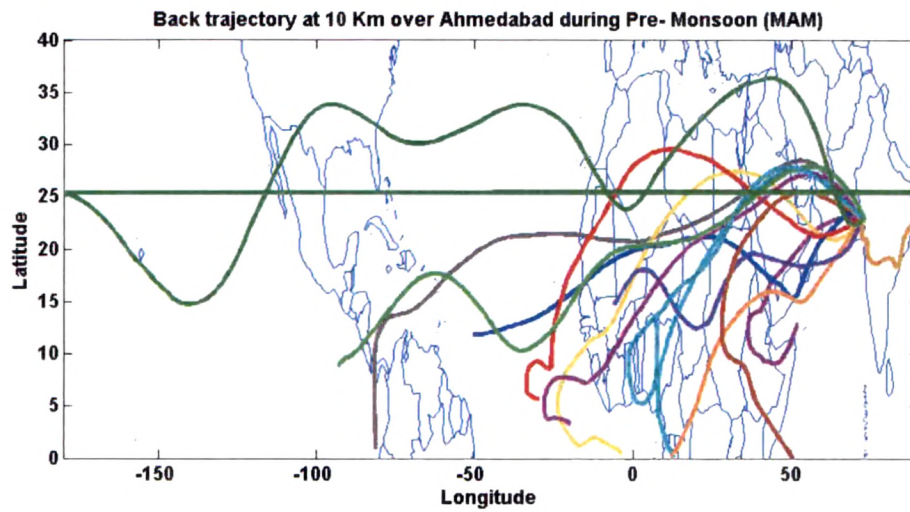


Figure 3.27. Back trajectories over Ahmedabad at 10 km during pre-monsoon months.

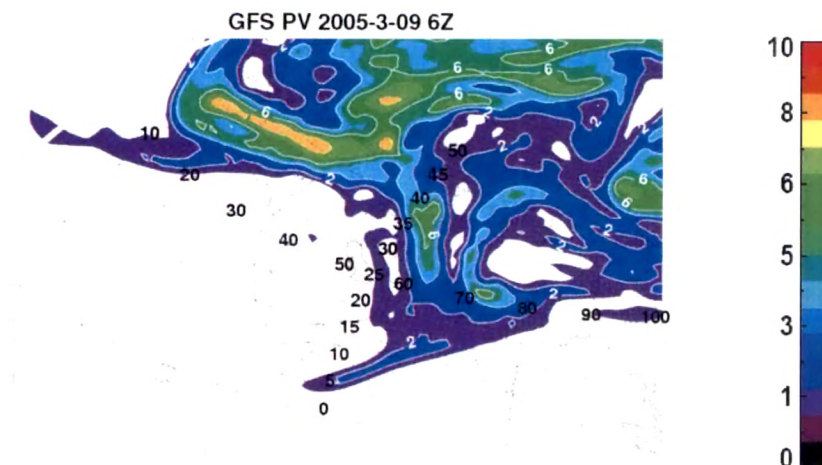


Figure 3.28. Potential vorticity for 9 March, 2005 at 0600 UTC (Data obtained from Global Forecast System (GFS) of NCEP).

In addition to this, potential vorticity (PV) calculated at 350K (14 km) potential temperature surface indicate the intrusion of stratospheric ozone in to the troposphere (Fig. 3.28).

3.14.2. Case -2: Ozone distribution on 20 April, 2005

Vertical profiles of ozone mixing ratio, temperature and relative humidity on 20 April, 2005 over Ahmedabad are shown in Figure 3.29.

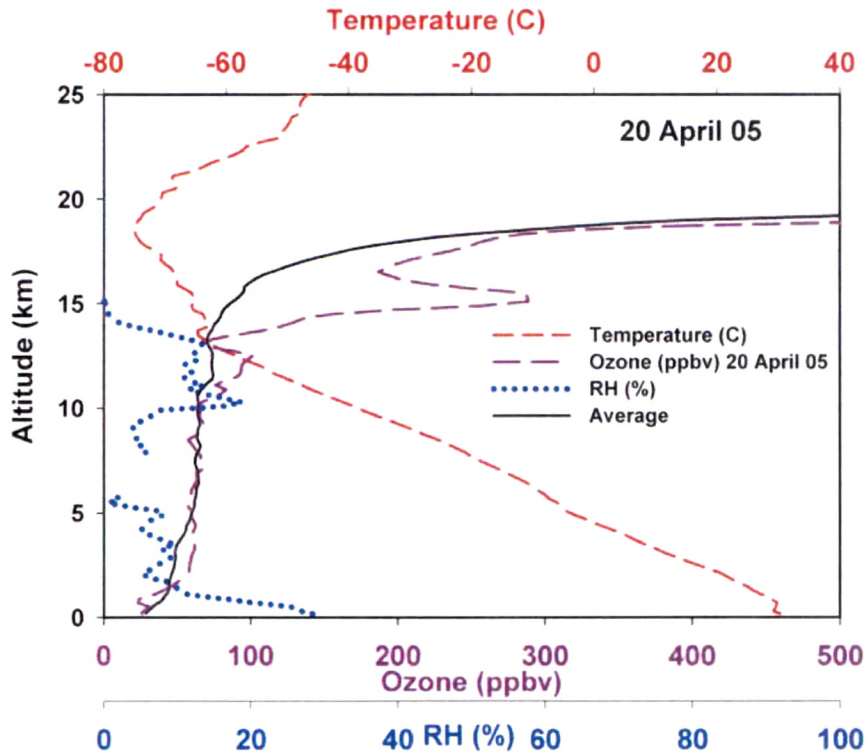


Figure 3.29. Vertical profile of ozone (ppbv), temperature and RH (%) observed on 20 April, 2005 over Ahmedabad. Average corresponds to average ozone concentration during April for the entire study period.

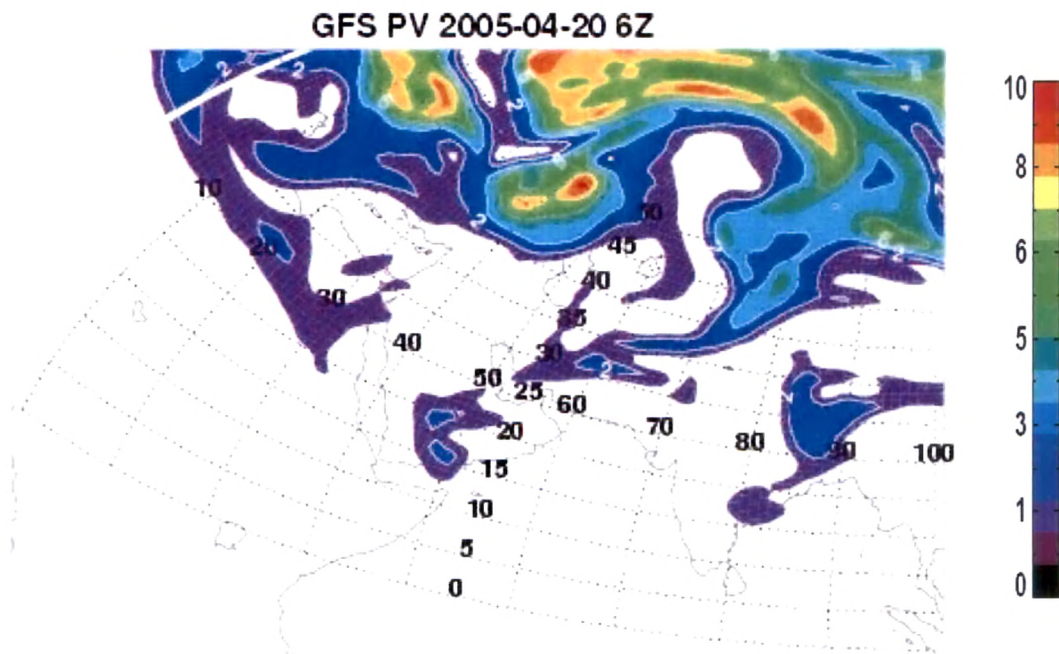


Figure 3.30. Potential vorticity for 20 April, 2005 at 0600 UTC (Data obtained from Global Forecast System, GFS of NCEP).

In the lower troposphere (from surface up to 5 km) ozone is almost constant and fluctuates between 20-30 ppbv while corresponding humidity profile shows decreasing trend with sharp fluctuations. Ozone value increases to 200 ppbv at 15 km of altitude just below the tropopause. Weakening of the tropopause has also been observed on this day. This indicated weakening of tropopause structure while allow this stratospheric air to come down to troposphere. Since 90% of the ozone lies in the stratosphere so this double tropopause allows stratospheric ozone to descend to troposphere. This increase in tropospheric ozone just below the tropopause is due to the intrusion of stratospheric ozone in the troposphere as shown in the Figure 3.30.

3.15. Summary

A total of about 85 balloon flights were made from Ahmedabad. Four years of data obtained over Ahmedabad were classified into four major seasons viz winter (DJF), pre-monsoon (MAM), monsoon (JJAS) and post-monsoon (ON). Boundary layer ozone was at a maximum during the winter and at a minimum during the monsoon. These observations could be due to shallow boundary layer heights during the winter and wash out of pollutants during the monsoon, respectively. The monsoon ozone minimum in the lower troposphere is attributed to the onset of summer monsoon when air flow from the Asian continent is replaced by air from the tropical Indian Ocean.

Monthly mean data were used to study the annual distributions of O_3 , water vapor and temperature during 2003 to 2007 over Ahmedabad. Large seasonal variability was observed in O_3 . In general, vertical distributions over Ahmedabad showed higher background O_3 values compared to other sites in the troposphere. Dynamics played a major role in the seasonal distribution over Ahmedabad.

The middle troposphere ozone was highest during the rainy season and minimum during the post monsoon season. Near the tropopause, large variability was observed during pre-monsoon and winter due to the intrusion of ozone from the stratosphere. A frequently observed feature during pre-monsoon and winter seasons was high ozone mixing ratios (80-170 ppbv) in the upper troposphere (from about 9 to 16 km). Ozone increased due to STE, and for the month of March it was 5 DU (Dobson unit) while during April it was 15 DU. This is the first experimental study to estimate the flux due to STE process over Ahmedabad. In the stratosphere highest peak ozone concentration was observed during the rainy season and the minimum was observed during winter. Elevated ozone concentrations were observed (~200 ppbv) in the upper troposphere (12-14 km) and the TTL region during the spring season. Influence of stratospheric air was identified using potential vorticity over Ahmedabad. Occurrence of high ozone tongue in the spring, with dry air of low relative humidity and potential vorticity indicates the origin of stratospheric air mass.

A comparison of the total ozone from ozonesonde data with those from total ozone mapping spectrometer (TOMS) shows good correlation during all seasons except the rainy season. Average total integrated ozone was 261 DU and average integrated ozone in the troposphere was 39.4 DU. Increased ozone lifetime in the free troposphere increases the importance of transport pathways during different season over Ahmedabad. Seasonal patterns of the two data sets (TOMS and ozonesonde) match very well. However, there were minor differences. The satellite values were mostly within the spread of the balloon data and the difference was mostly within 5 DU. However, the monthly average TTO values from satellite were statistically higher than the TTO measured using an ozonesonde during the monsoon months. TTO over Ahmedabad exhibited trends similar to those observed over Indonesia.

Case study of vertical profiles over Ahmedabad revealed significant day-to-day variability in the vertical structure of O_3 . These studies also revealed influences of the transport of various air masses. In some cases influence of stratospheric origin air masses in the spring season, especially over Ahmedabad were identified using back trajectory analyses.

Vertical profile of tropospheric ozone for the rainy season is shaped like “S” with minima at the surface, maxima at ~6-7 km, and another minimum at around 12-13 km with a subsequent increase towards the tropopause. Mid tropospheric maxima during the rainy season in the ozone profile over Ahmedabad was similar to those observed in the southern tropical region. Case study of vertical distribution of ozone over Ahmedabad revealed day-to-day variability in the vertical structure of ozone. It also revealed the effect of transport (e.g., STE, advection, convection).

CHAPTER - 4

Distributions of ozone and other trace gases over the Indo-Gangetic Plain during a winter month

In December 2004, a land campaign with a multi-institutional scientific effort was carried out in the Indo-Gangetic Plain (IGP) in North India to understand the distribution and dynamics of the atmospheric pollutants during a winter month. The main goal of the research work presented in this chapter was to understand the ozone chemistry and to study the effect of fog/ haze on tropospheric ozone and other pollutants. Simultaneous measurements of surface O_3 , CO, NO_x and CH_4 along with vertical distribution of ozone and other meteorological parameters were made during December 2004 at Kanpur (26.03N, 80.04E), an urban site in the IGP. Such extensive simultaneous measurements have not been made over this region. During the winter season mainly in December and January, the whole part of the northern India experiences western disturbances moving eastward which leads to intense fog and haze in this region. In winter, the relationship between ozone and westerlies is found to be positive especially in locations which are more influenced by westerlies. It is suggested that these relationships reflect the importance of vertical exchange from the free troposphere/stratosphere to the surface in winter months. Previous studies have identified transport of atmospheric pollutants from the IGP during winter and occasionally these pollutants are transported downwards and result in substantial ozone concentrations at the surface.

4.1. Significance of the study site

Asia is one of the most anthropogenically active areas in the world and provides an interesting study field for tropospheric ozone build up. The aged air masses associated with the continental outflow from the IGP carry with them anthropogenic air pollutants emitted from the industrial and urban neighborhoods of Kanpur under favorable meteorological conditions for photochemical ozone formation. Emissions of ozone precursors are expected to multiply in the next few years in India and the level of photo-oxidants may increase substantially.

There have been several field campaigns to study the transport of pollutants over the marine regions surrounding India such as INDOEX, BOBEX, and BOBPS [Lelieveld et al., 2001; Chand et al., 2003; Lal et al., 2006; Sahu et al., 2006; Lal et al., 2007]. However, there were limited measurements by individual groups to study levels of aerosols and trace gases over the IGP [Singh et al., 1997; Fishman et al., 2003; Jain et al., 2005; Sahoo et al., 2005; Beig and Ali, 2006; and Tripathi et al., 2006]. In view of the importance of this region, a campaign was organized by Indian Space Research Organization-Geosphere Biosphere Programme (ISRO-GBP) to study levels and variations of pollutants (aerosols and trace gases) at eight different sites covering wide regions of the IGP from west to east during December 2004. The month of December was chosen, as it is the period when both clear days and foggy days occur. Thus, the changes in trace gases and aerosols could be studied during clear as well as foggy days. These measurements were made by a large number of groups covering all these sites.

Measurements using balloon-borne ozonesonde provide a unique data set to study the vertical changes in the troposphere and effects of transport. This is the first time that vertical distribution of ozone was made from this site over the Gangetic basin, except the measurements made by the Indian Meteorological Department (IMD) from Delhi regularly. There are some measurements of ozone as a part of MOZAIC (measurement of ozone by air bus in-service aircraft) at Delhi. However, they are highly irregular in frequency and limited to a height below 300 mb [Kunhikrishnan et al., 2006]. Results of

distribution of surface level CO , NO_x , and CH_4 and vertical profiles of ozone are presented in this chapter.

4.2. Site description

The balloon flight experiments were conducted at the Indian Institute of Technology (IIT) campus at Kanpur in North India (Fig. 4.1). This campus is located about 16 km away from the city centre in the upwind direction. It is an industrially polluted city with a population of about 2 million. Foggy conditions often prevail during the winter season in this region [Tripathi et al., 2006].

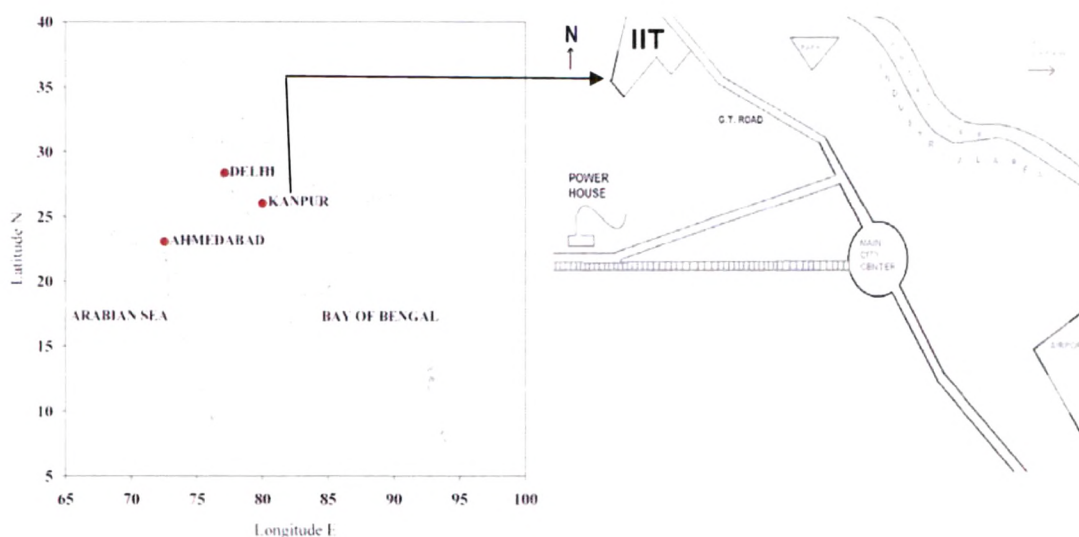


Figure 4.1. Geographical location of Kanpur city and location of Indian Institute of Technology (IIT), where measurements were made during December 2004.

4.3. Experimental details

Continuous surface level measurements of O_3 were made using an analyzer (Table 4.1), which is based on the absorption of UV radiation at 253.7 nm by O_3 . The absolute accuracy of this analyzer is 5%. Detailed description of the analyzer, including

calibration methodology, is given by Lal et al. [1998]. A Teflon tube was used as an inlet line for air sample, which was taken from the top of the building. Ozone data, averaged for every 5-min interval, were stored in a data acquisition system. A total of nearly 60 air samples were collected in glass bottles through a 2 m long stainless steel tube (1/4" OD) using an oil free compressor (Metal Bellow, USA). Analyses of CH₄ and CO were performed by a gas chromatograph (Varian Vista 6000, USA) using a molecular sieve packed column of 5 m length. Calibration mixtures supplied by NIST (Gaithersburg, USA) (1.0-0.01 ppmv; Sample 1223-E) and Matheson (Texas, USA) (2.1 0.01 ppmv; Lot 04-96-07670) were used to calibrate CH₄ and CO, respectively. Analyses of CH₄ and CO showed better than 1% and 3% of reproducibility, respectively. A detailed description of calibration and measurement methodology for analyses of CO and CH₄ are given by Sahu and Lal [2006b]. Instruments and parameters measured during land-campaign at Kanpur by PRL group are given in Table 4.1.

Table 4.1. Instruments operated and parameters measured during land-campaign at Kanpur

Instruments used	Company	Parameters	Specifications
Ozone analyzer	Environment S.A, France	Ozone	Surface
CO analyzer	Environment S.A, France	CO	Surface
NO _x analyzer	Environment S.A, France	NO and NO ₂	Surface
Gas chromatograph	Varian, USA	CO and CH ₄	Surface
Radiation flux	Solar Light, USA	UVB	At ground
Ozonesonde	EN-SCI, USA	Ozone	Maximum 35 km
Radiosonde	Vaisala, Finland	T, RH, and P	Maximum 35 km

4.4. Meteorological conditions, back trajectory and potential vorticity analysis

The regional surface winds, based on the National Center for Environmental Prediction (NCEP) reanalysis data, were found to be mainly northwesterly (Fig. 4.2). However, the surface winds varied from northwesterly to southwesterly [Tripathi et al., 2006].

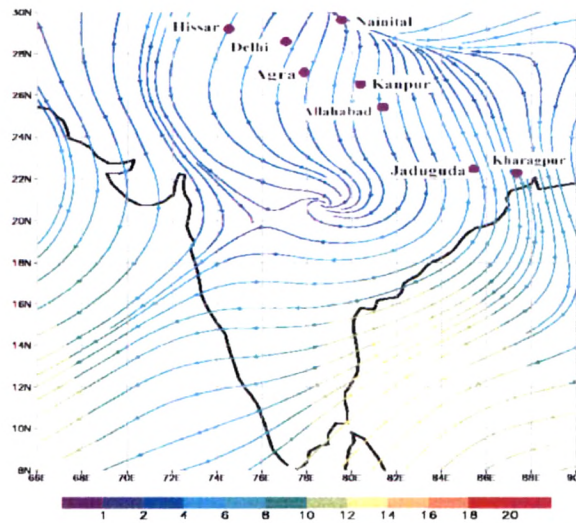


Figure 4.2. Synoptic monthly averaged wind at 925 hPa from NCEP showing northwesterly wind direction at Kanpur.

Very low wind speeds along with shallow boundary layer height during the foggy days were observed. Although, the winter season in the North India is dry, when the cold air from higher latitudes mixed with the moist air from surrounding marine regions, strong haze and fog conditions were observed in the Gangetic basin. The relative humidity (RH) soared above 75% during nighttime and in the early morning hours during these events. During foggy days, RH remained high (46%) throughout the day but it dipped down to about 40% during clear sky mid-day period. Transport of air and local meteorological conditions play an important role in changing the weather condition in this region. Low surface temperature (down to 8°C) and high humidity (up to 95%) made favorable

conditions for fog formation during 18–25 December 2004 at this site (Fig. 4.3). The average boundary layer height, based on temperature profiles from radiosonde data, was about 800 m on foggy days while it reached up to about 1.5 km on non-foggy days. The isentropic seven-day back air trajectories used in this study were obtained from Hybrid Single-Particle Lagrangian Integrated Trajectory (HYSPLIT), version 4 [Rolph and Draxler, 2003]. Back trajectory analyses are used to examine potential source regions of the air parcel and transport pathways, although the exact origin of a specific air parcel cannot be determined. The European Centre for Medium-Range Weather Forecasts (ECMWF) data are used to estimate potential vorticity (PV). This parameter is used to trace the origin of the air. PV is expressed in PV units where one PV unit is $10^6 \text{ m}^2 \text{ s}^{-1} \text{ Kg}^{-1}$. Air with potential vorticity of 2 PV units or more is taken to be of stratospheric origin [Appenzeller and Davies, 1992; Holton et al., 1995; Newell et al., 1997].

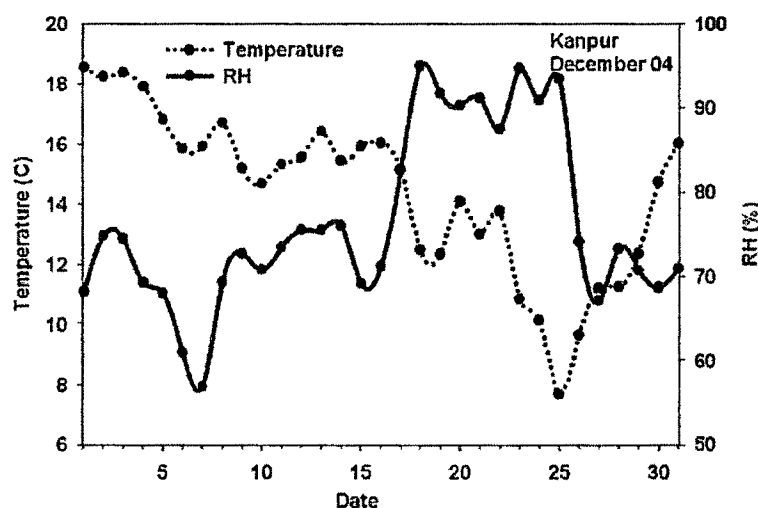


Figure 4.3. Surface temperature and relative humidity observed over Kanpur during the land campaign (11–29 December 2004).

4.5. Results and discussion

4.5.1. Time series analysis

Figure 4.4a depicts the variation of hourly averaged O_3 mixing ratios observed during the entire campaign. Ozone mixing ratios showed a large range (10–60 ppbv) of variability during the campaign. During the first half of the campaign its average value was ~55 ppbv and then it decreased to 20 ppbv during the foggy days.

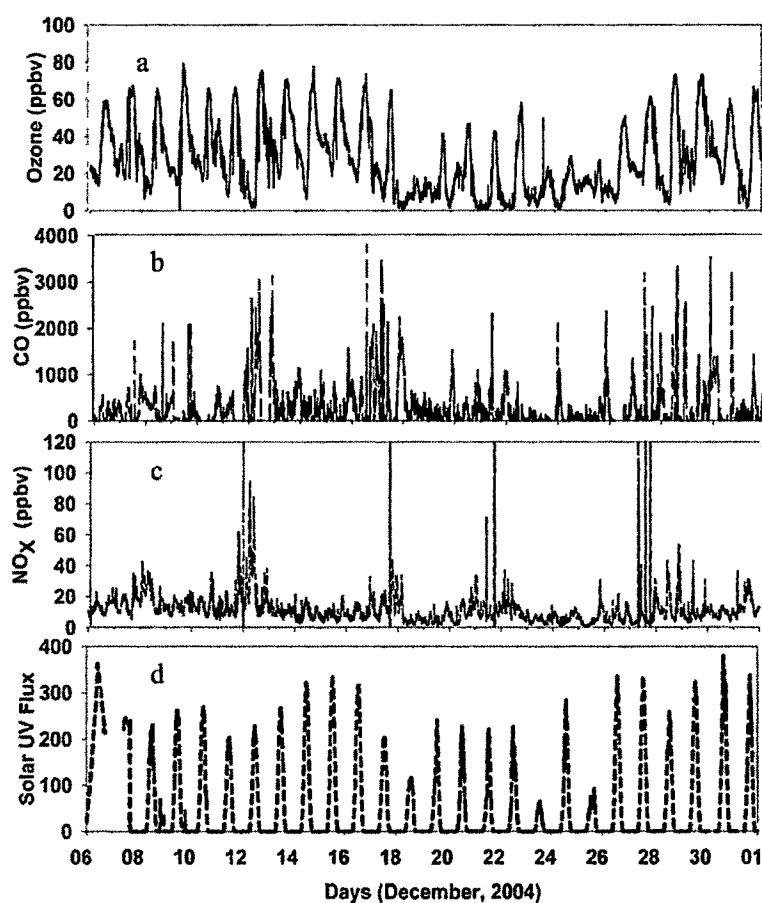


Figure 4.4. Time series of surface ozone, CO and NO_x along with UVB flux (in arb units) observed at Kanpur during December 2004.

Figure 4.4b depicts the variations in CO mixing ratios. CO varied from 200 to 1000 ppbv. High CO concentrations were observed on 12 December and 16 December. Variations in concentrations of NO_x are shown in Figure 4.4c. It varied between 5 to 50 ppbv during the campaign. Except for some small variations, the overall trend in NO_x is somewhat similar to those in CO mixing ratios. The mixing ratios of NO_x showed peaks on 12 and 16 December as for CO. Figure 4.4d shows the variations in pyro-measured flux. The flux ranged from 20 to 350. It depicts lows on 18, 24, and 26 December when heavy fog events were observed.

4.5.2. Frequency distributions

Frequency distributions of O₃, NO_x, and CO based on the data averaged for 5 minutes are shown in Figure 4.5, in bins of 2, 1, and 25 ppbv, respectively. A total of about 7500 data points were obtained. Most of the data points of ozone lied in the range of 5 to 25 ppbv. Out of the total data points, maximum numbers of data points in a single bin were in the 8 ppbv bin. Similarly most of the data points for CO were in the range of 25 to 400 ppbv. The maximum number of data points lied in the 25 ppbv bin. In case of NO_x, most of the data points are in the range of 0 to 20 ppbv, however the 10 ppbv bin had the highest number (550) of data points.

4.6. Diurnal variations in ozone and its precursors

Average mixing ratios of surface O₃, CO and NO_x at Kanpur during clear sky days were 34.99 ± 15.12 ppbv, 337.68 ± 169.9 ppbv, and 13.86 ± 2.5 ppbv, respectively while on foggy days these were 14.35 ± 8.7 ppbv, 191.87 ± 135.6 ppbv, and 7.93 ± 1.7 ppbv.

4.6.1. Foggy days

From 18 –26 December 2004, there was an intense fog over Kanpur as well as over the Indo- Gangetic Plain [Gupta et al., 2007]. Atmospheric visibility was very poor during the morning and evening hours. Diurnal variations of ozone show a very different pattern from its normal pattern since no afternoon peak was observed during the foggy days. This observation suggests high suppression in ozone concentration due to heavy fog.

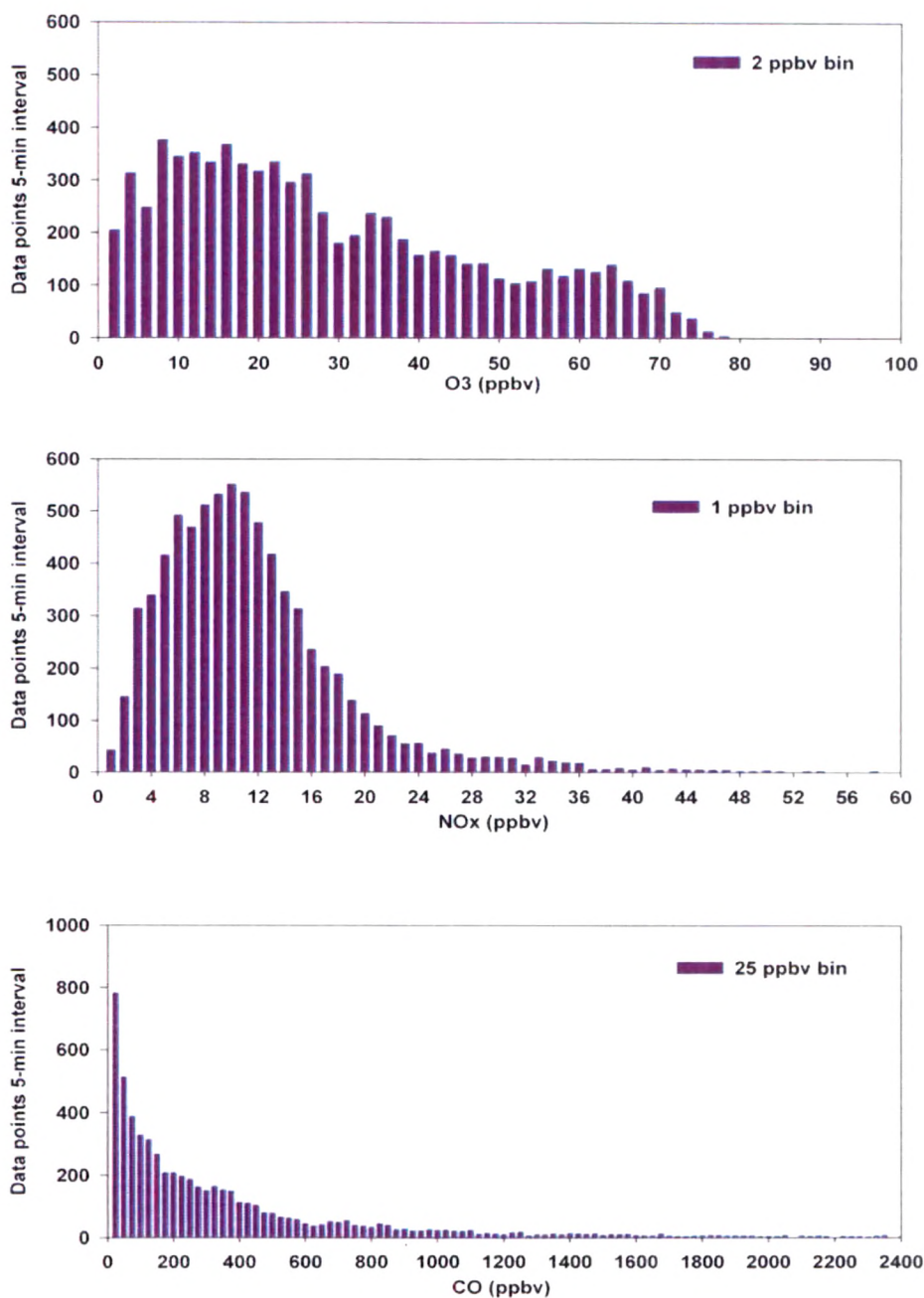


Figure 4.5. Frequency distribution of ozone (ppbv), carbon monoxide (ppbv) and NO_x (ppbv) at Kanpur during December 2004.

There were no changes in the diurnal patterns of CO and NO_x except that there was a decrease in the concentrations compared to clear sky days (Fig. 4.6). These results indicate that in spite of significant levels of precursors, ozone does not show its diurnal pattern due to the absence of photochemistry during heavy foggy condition. Pyro flux was reduced to 2 μWcm^{-2} compared to 6 μWcm^{-2} on a clear sky day. Measurements during clear sky days showed stronger diurnal variations in the trace gas distributions as compared to foggy days. The levels and variabilities of trace gases were suppressed on foggy days due to the lack of photochemical production.

4.6. 2. Clear days

Concentrations of trace gases at Kanpur also show large diurnal variations like other urban and industrial sites. Typical diurnal distributions of O₃, CO and NO_x are shown in Figure 4.7. The maximum amplitudes of about 75 ppbv, 3.5 ppmv and 80 ppbv were observed for O₃, CO, and NO_x concentrations, respectively. The diurnal variation in O₃ showed a maximum in the afternoon with low values during early morning and late night hours. An increasing trend was observed between early morning hours and noon, while a decreasing trend was observed between noon and evening. Day-to-day variations in ozone increasing and decreasing trends were negligible. The diurnal variations in CO and NO_x were opposite to that of ozone. Observed diurnal and day-to-day variabilities in the distributions of anthropogenically emitted trace gases like CO and NO_x could be due to significant differences in their local emissions considering that solar irradiance induce variations are minimal during clear days within a month.

Average diurnal variations of O₃, CO, NO_x and UVB measured during clear sky of observations are shown in Figure 4.6. The diurnal peak in ozone occurs at 1500 hrs in the afternoon, while the radiation peaks around 1300 hrs. Mixing ratio of ozone was observed to be lowest at 0900 hrs. There is an increase in ozone mixing ratio due to lifting of boundary layer height in the forenoon and due to photochemical production of ozone and after 1500 hrs, loss of ozone starts dominating due to decrease in solar radiation. Diurnal patterns observed in CO and NO_x shows two peaks in the morning and

evening hours. Morning peak occurs at around 0800-0900 hrs and evening peak at around 2100 hrs. Both of these peaks coincidence with the morning and evening rush hours as well as decrease in boundary layer height. These variations are typical of an urban/semi - urban site [Sahu and Lal, 2006a].

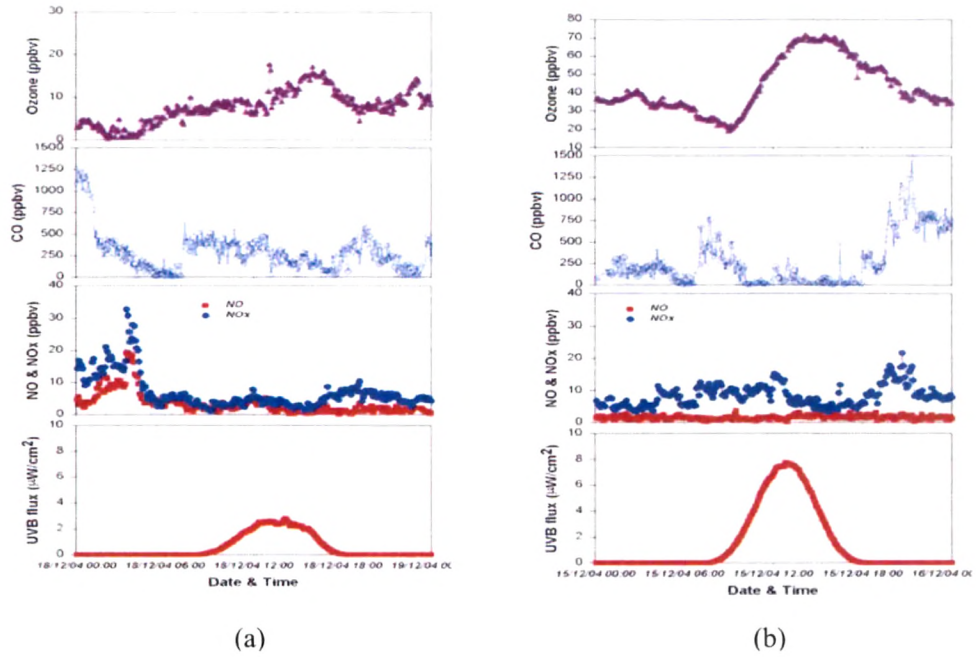


Figure 4.6. Diurnal variations of ozone, CO, NO & NO_x and UVB flux on (a) a foggy day (b) and on a clear day at Kanpur

4.7. Vertical distribution of ozone

4.7.1. Average vertical profiles of ozone and temperature over Kanpur

Six balloon flights were conducted of which three were on clear days (December 11, 15 and 29) while the other three were on foggy days (December 18, 22 and 25). Average peak ozone concentration of 140 nb was observed around 25 km (Fig. 4.7). The cold point tropopause temperature ranged from -70°C to -77°C and the tropopause height ranged from 16.5 to 18.9 km with an average and standard deviation of 17 ± 0.7 km as shown in Figure 4.8. Large variability in tropopause height was observed from flight to flight (Fig. 4.8). A layer of high ozone was observed in the free troposphere from 3 to 7 km on December 18. Similarly, three sharp layers of high ozone were observed in the height range of 10–18 km on December 25. On the contrary, depleted ozone was observed in the height range of 11–14 km on December 29. These results are discussed in detail in the following section.

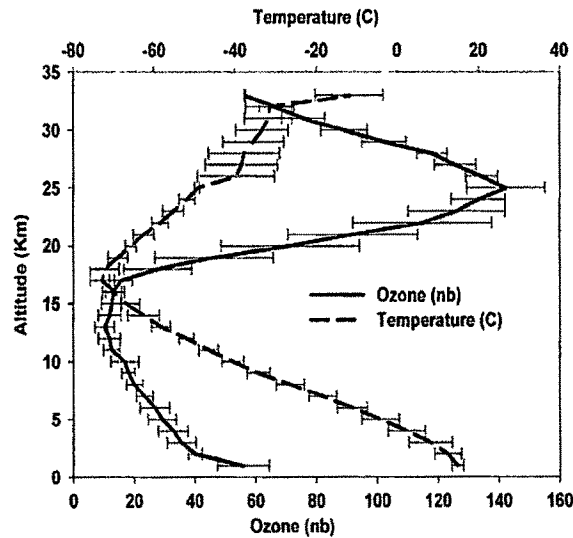


Figure 4.7. Mean vertical profile of ozone (nb) and temperature up to 35 km observed from six balloon flights made from Kanpur during December 2004.

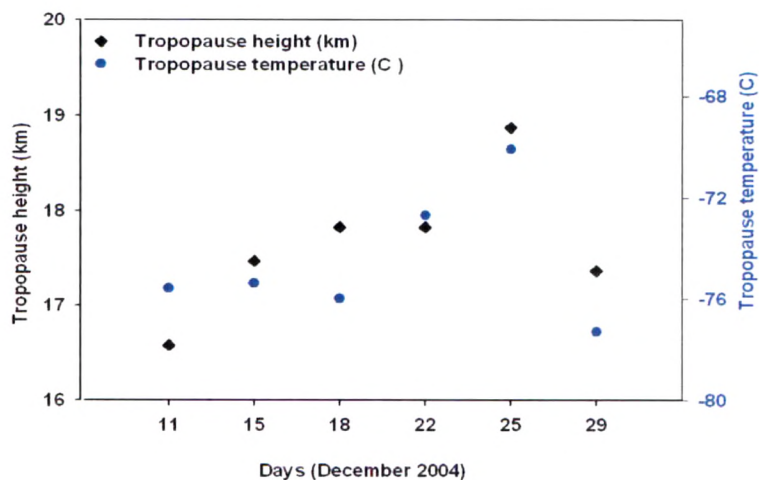


Figure 4.8. Tropopause temperature and height over Kanpur during December 2004.

4.7.2. Observed features

Columnar total ozone was obtained by integrating individual profiles up to the balloon burst altitude which was generally around 32–35 km, and further extending it up to 60 km using the method described by McPeters et al. [1997]. These integrated columnar ozone for the balloon flight days show good correlation ($r = 0.74$) with the corresponding total ozone values obtained from total ozone mapping spectrometer (TOMS) (Fig. 4.9). The average TOMS total ozone for six flights was 249 ± 20 DU, whereas the average balloon flight total ozone was 266 ± 13 DU. There was a bias of about 22 DU in the satellite data.

The average of all the observational tropospheric ozone content was obtained by integrating individual observed profiles up to the tropopause height, which was calculated from the temperature profile measured by the radiosonde. Total columnar and tropospheric columnar ozone variability are shown in Figure 4.10. The average tropospheric column ozone was 41 ± 3 DU but it was much higher (53 DU) on 25 December.

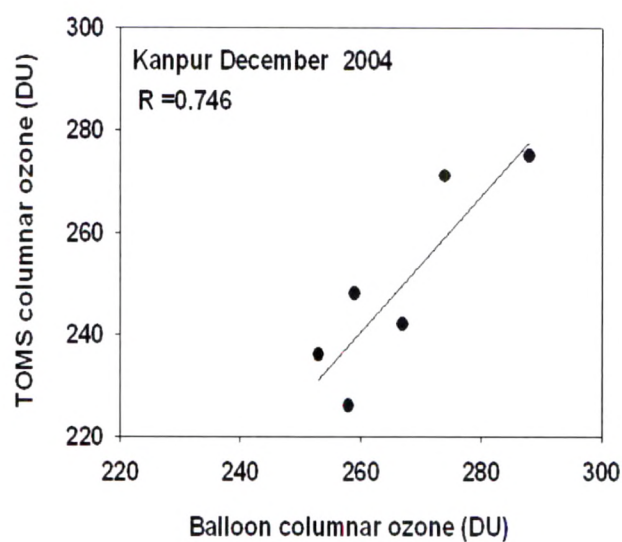


Figure 4.9. Comparison between total columnar ozone computed from balloon data and TOMS columnar ozone.

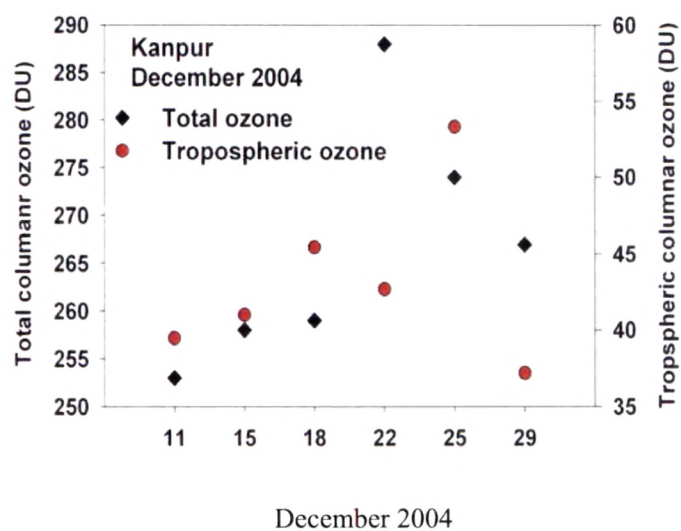


Figure 4.10. Total columnar and tropospheric columnar ozone amounts computed from ozonesonde data.

4.7.3 Case 1: Higher ozone concentration in the lower troposphere

Higher ozone (70 ppbv) with respect to the average of six balloon profiles on December 18 was observed in the altitude region of 3–7 km (Fig. 4.11). Average ozone concentration of all the six balloon flights in the height range of 3–7 km was 50 ppbv. The strong inversion at the bottom of the layer suggests that the higher concentration was not due to mixing upwards from the local boundary layer (Fig. 4.12). Seven-day back trajectories were calculated at the altitude levels of 3, 4, and 5 km. This trajectory analysis clearly indicates that the air parcel in the enhanced ozone layer over Kanpur passed over the region of intensive seasonal burning in Africa and higher pollutants (e.g., CO, CH₄) region of the Gulf as seen from the MOPITT data (Fig. 4.13a). The humidity in the enhanced layer was found to be lower, which indicates that the air mass passed through a dry region. CO data obtained from measurements of pollution in the troposphere (MOPITT) at 850 hPa shows higher concentration of CO along the trajectory path for 18 December 2004 (Fig. 4.13b).

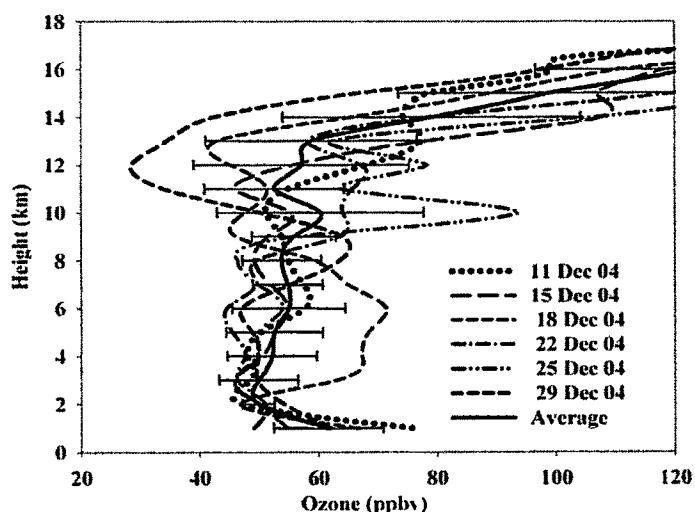


Figure 4.11. Vertical distribution of ozone (ppbv) with $\pm 1\sigma$ standard deviation along with six balloon profiles.

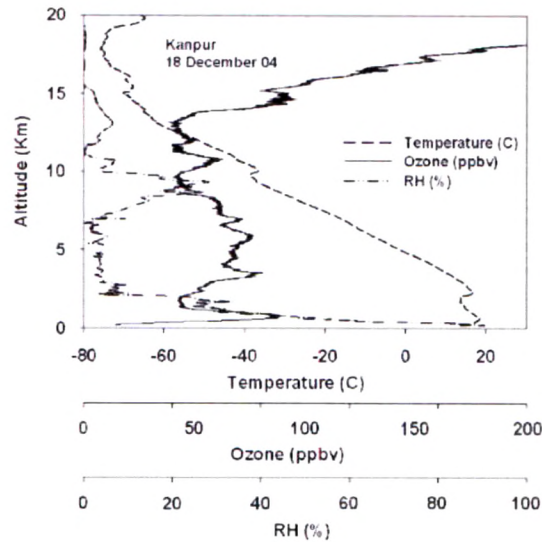


Figure 4.12. Vertical profile of ozone, temperature and RH for December 18, 2004.

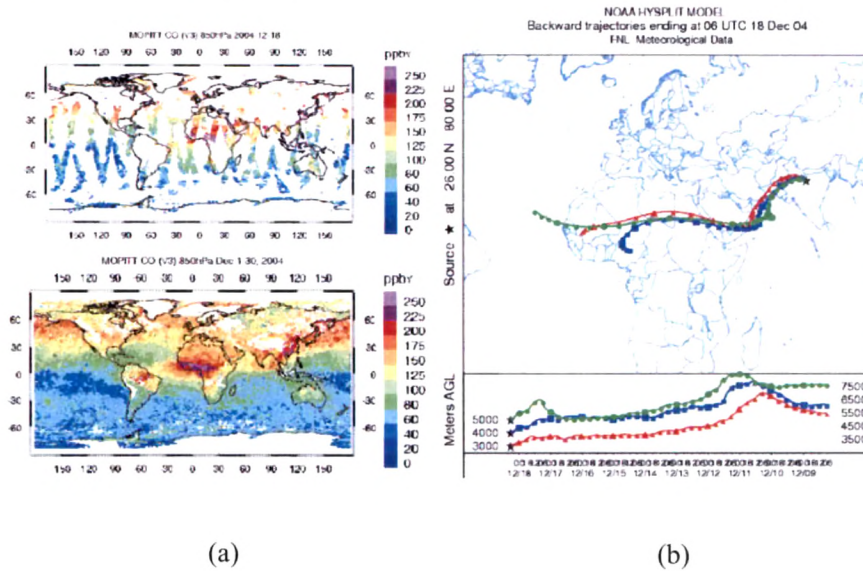


Figure 4.13. CO obtained from MOPITT (measurements of pollution in the troposphere) at 850 hPa shows higher concentration of CO along the trajectory path for 18 December, 2004 (a). Seven day back trajectory analysis from HYSPLIT model at 3, 4 and 5 km for December 18. The upper plate shows the horizontal movement of air parcel while the lower plate shows the vertical movement of air parcel (b).

During this month northern tropics experience a dry season where precipitation is rare and biomass burning is frequent in regions like Central Africa and Southeast Asia as shown in the Figure 4.13a.

The NASA earth observatory (<http://earthobservatory.nasa.gov/NaturalHazards/>) has captured this intense burning during 1-12 December 2004. Although back trajectory analysis is a tool to track the path of air mass, it is not possible to locate the origin and exact location of the source. Both the meteorological data obtained along with ozone profile and the air parcel trajectory information were consistent in showing that the layer of high ozone values could be due to transport of ozone as well as its precursors and subsequent photochemical production of ozone. PV data obtained from ECMWF do not show any evidence of its origin from the stratosphere (not shown here). Local pollutants measured simultaneously with the balloon launchings at this location i.e. surface ozone, (25 ppbv) carbon monoxide (300 ppbv) and nitrogen oxides (20 ppbv) could not get mixed from the local boundary layer to the free troposphere due to the strong boundary layer inversion. These observations further suggest that this ozone rich air can only be due to lateral transport.

4.7.4. Case 2: Ozone intrusion from the stratosphere

Enhanced ozone peaks were observed between 10 and 18 km on December 25, compared to the average ozone profile based on all the six balloon flights. The peak in the Tropical Tropopause Layer (TTL) region (14–18 km) shows enhanced ozone by 35–55 ppbv compared to the average ozone profile values, while the peaks at lower heights of 10 and 12 km show enhanced ozone by 20 and 35 ppbv, respectively (Fig. 4.14).

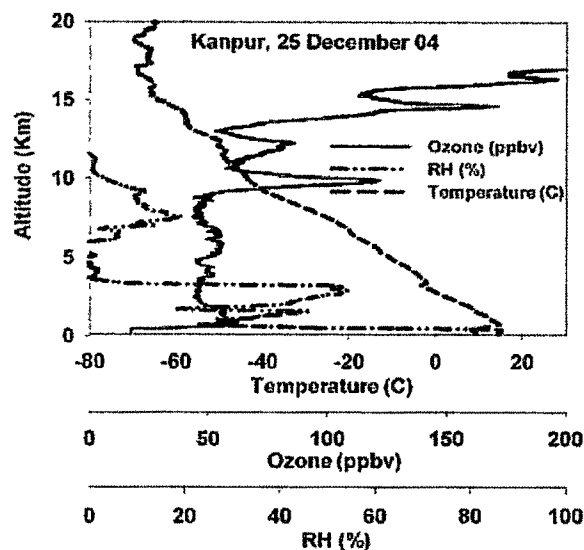


Figure 4.14. Vertical profiles of ozone, relative humidity and temperature observed on 25 December 2004 over Kanpur.

The temperature profile on this day showed double tropopause (Fig.4.14), which suggest that these high ozone layers below the tropopause may be due to its transport from the stratosphere resultant of the weakening of the tropopause.

Wind data obtained from NCEP show extremely high (60 ms^{-1}) wind around 12 km of altitude on this day (Fig. 4.15). Seven-day back trajectories for the height range of 9–15 km obtained from HYSPLIT model suggest that wind was coming from higher latitudes at this site (Fig. 4.16).

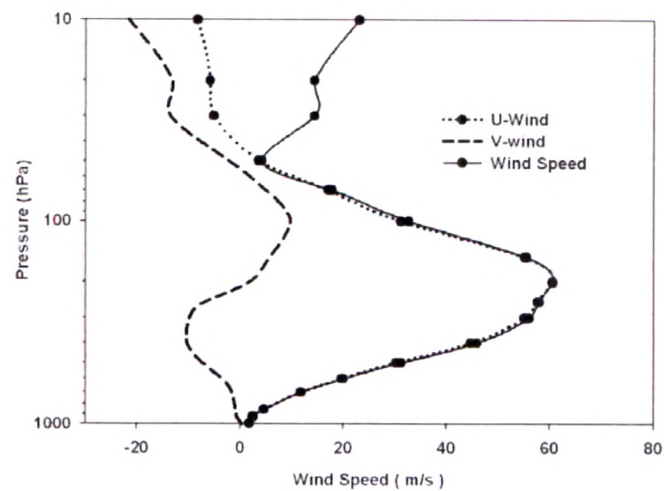


Figure 4.15. Vertical profile of mean wind speeds along with the U and V components.

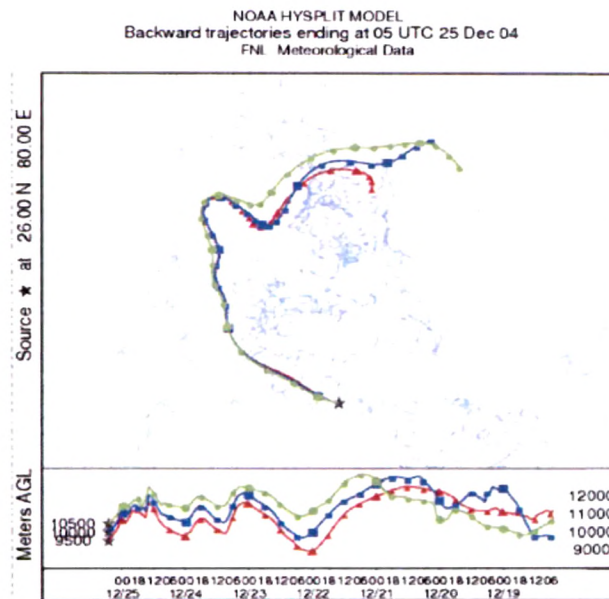


Figure 4.16. Seven-day back trajectory analysis from HYSPLIT model at 10, 11 and 12 km for 25 December 2004. The upper plate shows the horizontal movement, whereas the lower plate shows the vertical movement of air parcels.

There was a very dense fog event on December 25. Furthermore, due to low convective activity over this region, vertical transport from the polluted continental boundary layer was less likely. PV from the ECMWF analyzed wind and temperature fields was estimated at 0600 GMT on December 25 (Fig. 4.17). A jet stream was observed to be coming from the mid latitude in the southeast direction towards this site through the isentropic surface of 350 K. Noticeably, there was a sharp PV gradient along the subtropical jet stream around 20–30N, which is the location where active stratosphere–troposphere exchange can occur [Chan et al., 2004]. Cross-sectional view of PV (Fig. 4.18) showed a tongue of air with PV of more than 2 PV units between about 300 hPa (9.5 km) and 100 hPa (17 km). These altitudes coincide with the ozone enhanced peak levels and indicate that the air at these altitudes had its origin in the stratosphere. Enhanced ozone layers were also observed by Chan et al. (2004) over Xining (36.4N, 101.4E), Beijing (39.8N, 116.4E) and Hong Kong (22.3N, 114.2E) in January, 2002. These observations suggested that these enhancements were due to intrusion of stratospheric ozone from the Indo-Burmese region of Southeast Asia, where subsidizing downward motion were observed during winter. A study by Waugh and Polvani [2000] using NCAR/NCEP (National Center for Atmospheric Research/National Center for Environmental Prediction) reanalysis data for the period between 1980 and 1997 also showed that in the northern hemisphere, stratospheric intrusions occur mainly during the northern winter

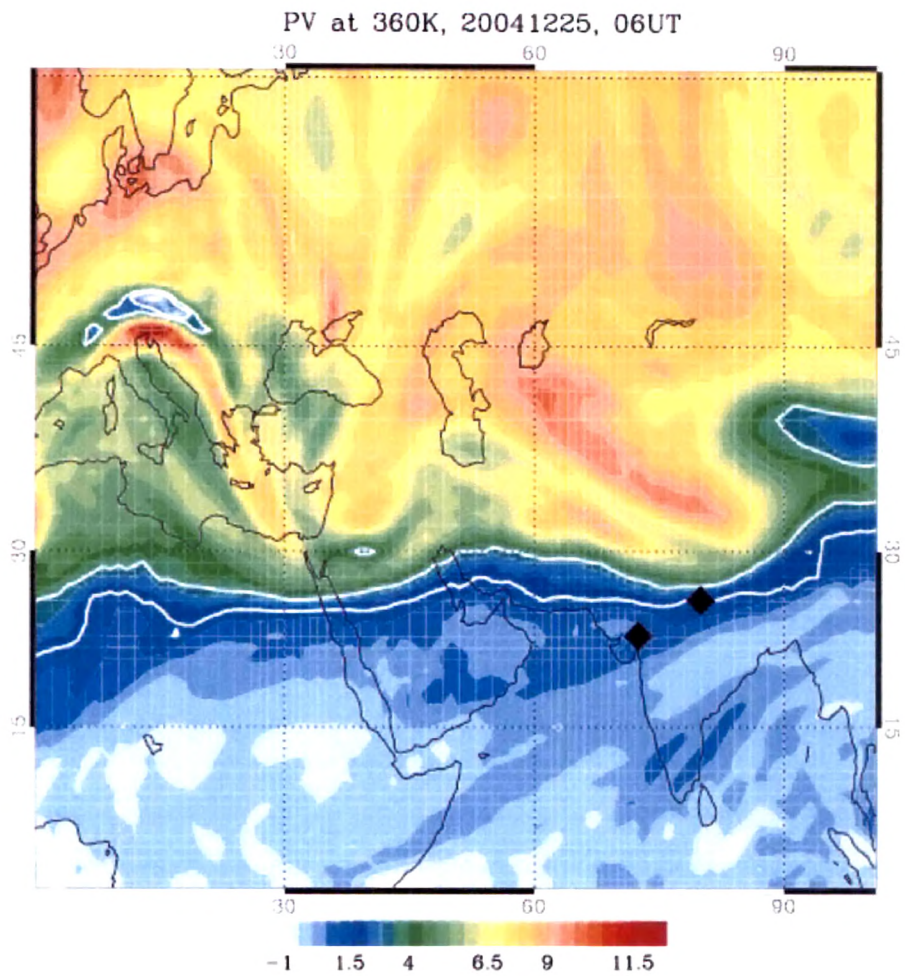


Figure 4.17. Latitude–longitude cross-section of potential vorticity (PV) derived from ECMWF for 06 UT on 25 December 2004 at 350K potential temperature.

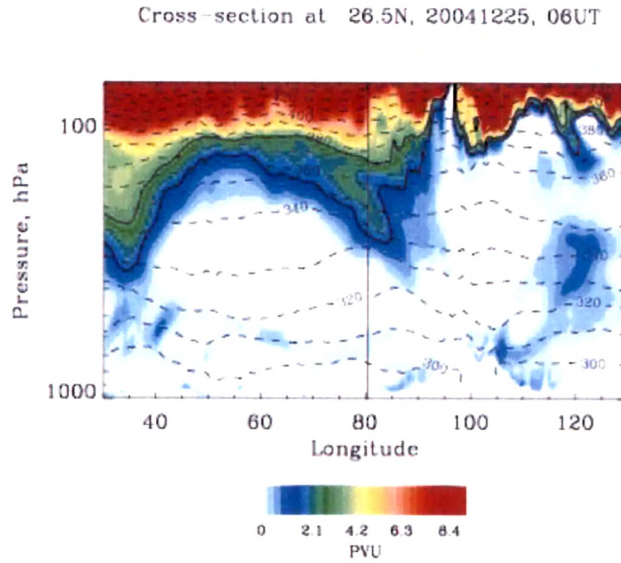


Figure 4.18. Longitude–pressure cross-section view of potential vorticity at 26.5N for 25 December 2004.

The Atmospheric Infrared Sounder (AIRS) data were also able to capture this event of ozone transport from high latitude to low latitude on 25 December 2004 (Fig. 4.19). Figure 4.18 depicts the Latitude-Pressure cross sectional view of ozone variation on 80 E longitude on 25 December 2004. This indicates a subsidence of air mass at 100 hPa pressure level at 26 N to 30 N.

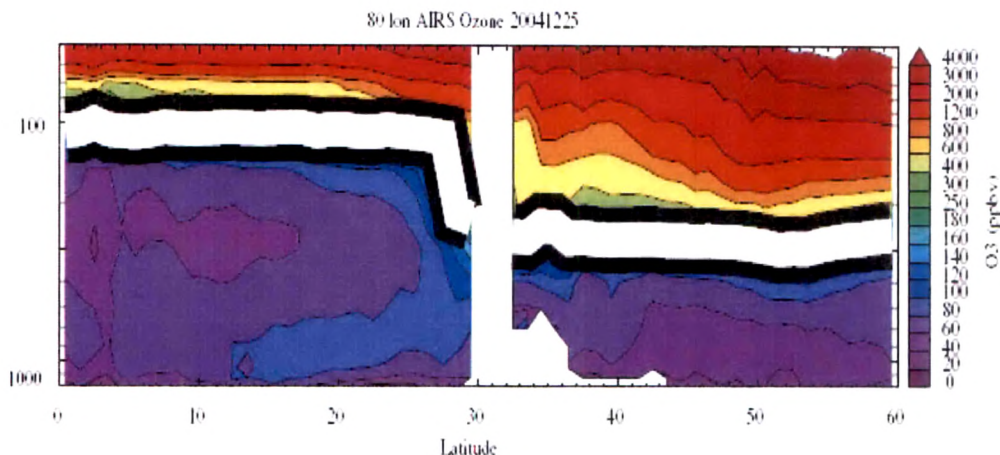


Figure 4.19. Latitude-pressure cross section of ozone at 80 E longitude on 25 December, 2004 at Kanpur based on the results from AIRS.

4.7.5. Case 3: Lower ozone concentration

Lower ozone concentrations by 35–40 ppbv compared to the average concentrations in the height range of 11–14 km were observed on December 29. Back trajectory analysis (Fig. 4.20) suggest that the air mass originated from a pristine marine region near the equator and had traveled across the Indian Ocean, where generally low ozone values were observed as reported in earlier studies [deLaat et al., 1999; Taupin et al., 1999; Zachariasse et al., 2000]. Since ozone lifetime is long in the free troposphere it can get transported far away from the source regions. The back trajectory analysis suggests that the low ozone air on December 29 originated from the free troposphere over the Arabian Sea and the Indian Ocean.

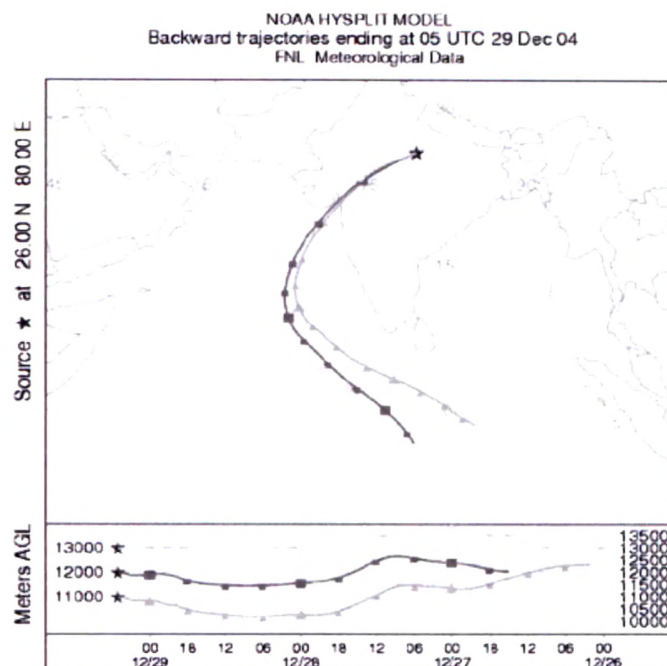


Figure 4.20. Back trajectories at 11, 12 and 13 km for 29 Dec. 04. Upper panel shows the horizontal movement while the lower panel shows the vertical movement.

4.8. Comparison with MATCH-MPIC model

4.8.1. Surface ozone

The global atmospheric off line model, MATCH-MPIC (Model of Atmospheric Transport and Chemistry - Max Planck Institute for Chemistry version), was developed for studies of atmospheric photochemistry. The, MATCH-MPIC is driven by wind, temperature, pressure, surface heat flux, and wind stress data from the NCEP -GFS analysis, at T42 horizontal resolution (roughly 2.8 degrees in latitude and longitude), and with 42 vertical levels (from the surface to about 2 hPa). The details of this model are discussed elsewhere [Lawrance et al., 1999, 2003; Von Kulmann et al., 2003]. Diurnal



cycle obtained from MATCH-MPIC modeled output agrees quite well with the observational data for Kanpur (Fig. 4.21). However, it is not able to reproduce low ozone during foggy days. This observation is due to the fact that these are short term local effects and the model is a global model.

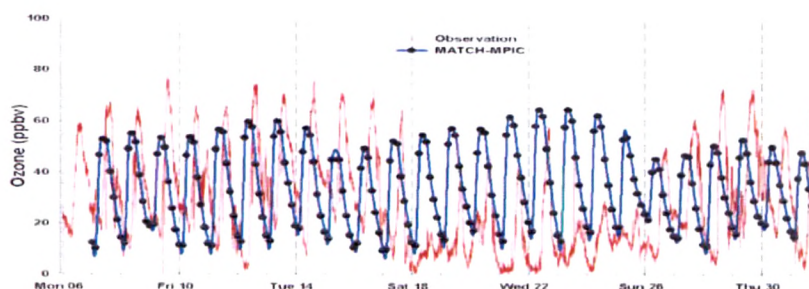


Figure 4.21. Comparison of surface ozone measured at Kanpur during December 2004 and MATCH-MPIC model simulated results.

4.8.2. Vertical distribution of ozone

The vertical profiles of ozone obtained from ozonesonde were compared with the profile obtained from MATCH-MPIC model (Fig. 4.22). Among all the six profiles, model was able to reproduce major features in the ozone profiles which were observed in ozonesonde profiles. However, model was not able to reproduce the small features observed in the ozone profiles. Model did a poor job in reproducing the STE and LRT enhancements on 25 as well as on 18 December although there was a weak signal in both of them. The model did a much better job with the 29 December low ozone in the upper troposphere.

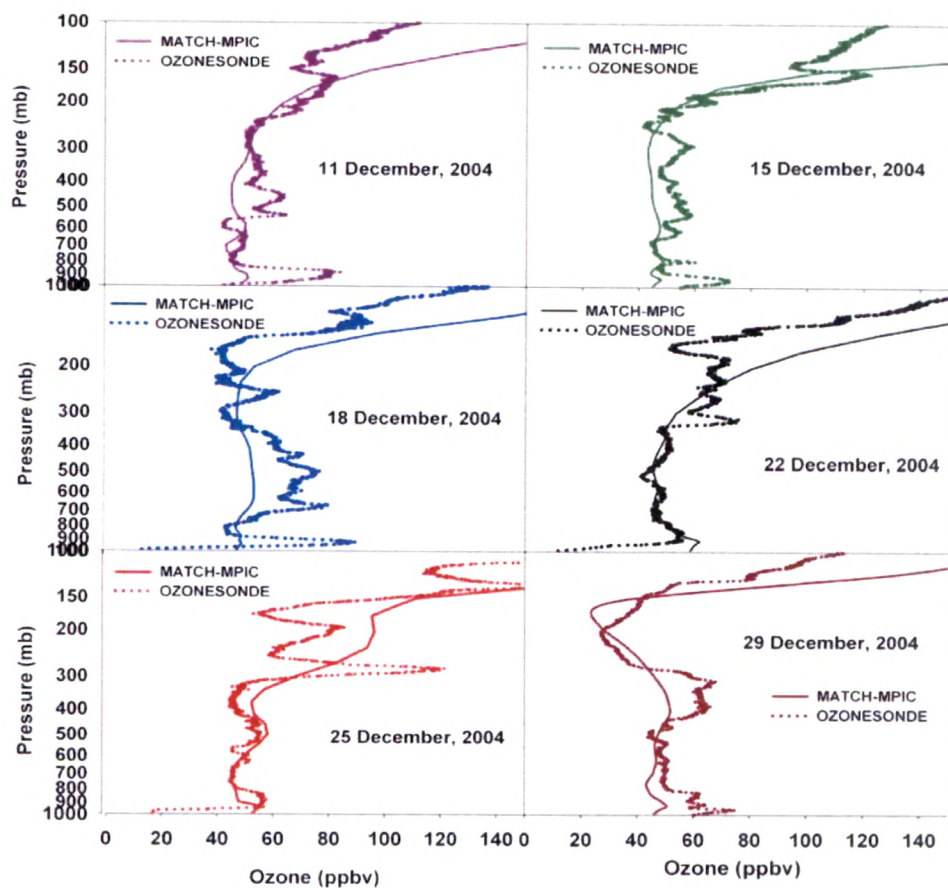


Figure 4.22. Comparison of the vertical profiles of ozone measured from ozonesonde and MATCH-MPIC model computed for December 2004 over Kanpur.

4.9. Summary of the results

As a part of a major campaign, six balloon flights carrying ozone and radiosondes were conducted from Kanpur during December 2004. Measurements showed large variability in tropospheric ozone distributions over this subtropical site. Average total ozone from the six balloon flights data was 262 ± 16 DU. But the TOMS data had a bias and gave

lower total ozone by about 22 DU. The average columnar tropospheric ozone estimated was 41 ± 3 DU which accounted for about 16% of the total column ozone. The average profile based on six balloon flights showed 60 ppbv below 2 km height and about 50 ppbv upto about 13 km. There after there was a sharp increase in ozone. The average available MOZAIC profile for December 1999 over Delhi showed mixing ratios of about 60–80 ppbv within 1–2 km of altitude and about 50 ppbv in the free troposphere [Kunhikrishnan et al., 2006]. This average profile closely matched the profile observed over Kanpur. There are significant variations in ozone profiles observed on December 18, 25 and 29. On December 18, there was a broad layer of higher ozone in the height range of 3–7 km. This increase was by 40% as compared to the average profile. The PV analysis on this day did not show any evidence of air coming from the stratosphere, also the strong boundary layer temperature inversion ruled out the convection from the boundary layer. Hence, this increase seemed to be due to lateral transport from Africa and the Gulf countries as indicated by back trajectory. The results also revealed multiple layers of enhanced ozone on December 25 in the upper troposphere. These enhancements from the average profile range from 2.4 to 1.3 for height 10 to 17 km. Based on PV analysis, these peaks are linked to transport from the stratosphere. These observations confirmed that this region was susceptible to the influence of stratospheric intrusions, which can lead to large ozone enhancements in the upper troposphere in winter. However, there is a need to quantify the impact of such intrusions on ozone distribution. In addition to the elevated events, one event of lower ozone (60%) compared to the average in the height range of 10–14 km was also observed on December 29. This was a result of transport of pristine air from the free troposphere over the Arabian Sea and the Indian Ocean. These are the first observations of ozone distribution from this site in the Indo-Gangetic plain in India. This data set is valuable for validating models and satellite ozone profiles for this region. Ozone data on 25 December 2004, retrieved from AIRS was also able to capture the intrusion of stratospheric air to the troposphere. However, for better understanding of these variations in ozone and role of transport, there is a need to make measurements for a longer period to quantify the occurrence and exchange

amount of ozone in different seasons over the Indian region. This study has also indicated the fact that surface ozone is not affected by the elevated ozone concentrations in the upper troposphere but it is mainly affected by the local meteorological conditions due to strong temperature inversion. Isentropic back trajectory analyses were applied to sort out the influence of the air mass exchange in the winter month and the regional scale photochemical build up of ozone.

A comparison of these results was made with that of MATCH-MPIC results. The model is able to reproduce general features of the observed ozone profiles but it is not able to capture local effects.

CHAPTER- 5

Distribution of ozone over the marine regions surrounding India

Study of vertical distribution of ozone is critical to the understanding of photochemistry and dynamical processes that are operating in the atmosphere and contributing to its tropospheric budget. Photochemistry of ozone is dominated by its precursors (NO_x , CH_4 and CO) over land, while over the marine region it mainly depends on the distribution of HO_x radicals. The lifetime of ozone in the Marine Boundary Layer (MBL) is longer due to its lower loss as compared to over land regions. Ozone in the MBL has a lifetime of the order of several days [Fishman et al.,1991], whereas in the free troposphere it may last for several months due to the drier atmosphere and the absence of other removal mechanisms such as surface deposition [Liu et al.,1987]. Cyclone formation generally takes place only over the marine region which can change the vertical distribution of ozone and other species. Organized convection associated with these cyclones enhances vertical exchange between the boundary layer and the free troposphere thereby causing extended effects covering lower as well as upper troposphere. Deep convection constitutes a very efficient mechanism to redistribute trace gases from surface to the free troposphere followed by faster horizontal transport spreading these gases over vast areas [Chatfield and Crutzen, 1984]. Few investigators have reported vertical ozone distributions in the free troposphere over tropical oceans where low ozone values in the free troposphere and latitudinal decrease towards lower latitudes were observed [Kley et al., 1996; Weller et al., 1996; Thompson et al., 2000]. Particularly intriguing features were the extremely low ozone mixing ratios below 10 ppbv observed in the MBL and free troposphere as obtained from soundings made over the equatorial Pacific in March, 1993 [Kley et al.,1996]. Since 1998 the SHADOZ (Southern Hemisphere Additional Ozonesondes) network of ozone sounding stations mainly

located in the tropics, have provided climatology of the vertical distribution of ozone in the tropical belt [Thompson et al., 2003]. The SHADOZ stations located in the Atlantic region have recorded low ozone concentrations in the entire troposphere during the March-April period and enhanced ozone concentrations during the September-October period. Only in certain regions of the tropics, especially the Indonesian archipelago, deep convective transport can be so vigorous that it can even penetrate into the stratosphere [Newell and Gould-Stewart, 1981]. Atmospheric convection in the tropics is particularly important for rapidly transporting material from near the surface to the upper troposphere [Thompson et al., 1996]. In situ observations during convective updrafts are limited due to sporadic nature of convection as well as the paucity of continuous measurements of ozone. The current focus is to determine the variations in the distribution of tropospheric ozone and related trace gases. A number of observational campaigns have been conducted over the Indian subcontinent and surrounding oceanic regions in recent times to investigate the role of transport in altering the distribution of trace gases. These include Indian Ocean Experiment (INDOEX) and some other campaigns over the Bay of Bengal [Leliveld et al., 2001; Stehr et al., 2002; Chand et al., 2003; Sahu and Lal., 2006b; and Lal et al., 2007]

The sharp rise in temperature and increasing solar insulation during springtime over this region lead to rapidly increasing photochemical activity. This rise coincided with the annual peak in emissions of ozone precursors from biomass burning sources in Southeast Asia, contributing to large variability in ozone abundances over the Arabian Sea region. Furthermore, the flux of stratospheric air into the troposphere in the northern Hemisphere is greatest in spring, and much of this in flux occurs in tropopause folds associated with deviations of jet stream that are most common over northeast Asia in springtime [Austin and Midgley, 1994; Wild et al., 2003].

An Integrated Campaign for Aerosol, gases and Radiation Budget (ICARB) was conducted during March-May 2006 over the Bay of Bengal (BOB) and Arabian Sea (AS). The region and period of the ICARB campaign were very important due to frequent passage of low pressure systems and high photochemical activity. As a part

of this campaign, measurements of ozone profiles along the cruise track were made. This is the first systematic study of the vertical distribution of ozone covering the entire BOB region.

Although there have been many observations for surface measurements of ozone and other trace gases during different seasons over these regions (e.g. INDOEX, BOBEX) but there has been no such extensive measurement for vertical distribution of ozone over this region. The ICARB mission focused on understanding the chemical processes and the transport. This aim cannot be achieved without the knowledge of pollutant emissions and distributions over this region. Most of the observations of surface ozone concentration over the ocean are in campaign mode for a small period only over Atlantic Ocean [Winkler, 1988] as well as over the Pacific Ocean [Routhier et al., 1980; Liu et al., 1983; Piotrowicz et al., 1991; and Singh et al., 1995]. Vertical distribution of ozone using ozonesonde have been made over the Atlantic Ocean by [Smit et al., 1991; and Weller et al., 1996] and over the Pacific Ocean by [Thompson and Witte, 1999]. Measurements of vertical distribution of ozone over the marine region surrounding Indian subcontinent for a long period are rare. There is very little extensive measurement over the marine region around the Indian peninsula. We are only aware of few reports on the vertical distribution of ozone over the AS during INDOEX [Rasch et al., 2001; Lelieveld et al., 2001; Stehr et al., 2002]. Extensive measurement of vertical distribution of ozone over the AS were made from April 18 to May 10, 2006 to study the transport from continent to pristine marine region surrounding Indian Sub continent.

This chapter discusses the spatial and temporal distribution of ozone and trace species measured during ICARB on board a ship cruise over the BOB and the AS. Vertical distribution of tropospheric ozone and some special case studies are discussed. The stratospheric contribution to the tropospheric ozone measured over the BOB and the AS are estimated and inferences are drawn.

5.1. Cruise track

The ICARB cruise expedition was conducted on the Oceanographic Research Vessel (ORV) Sagar Kanya from 18 March to 10 May, 2006. It started on the east coast of India from Chennai port (13.1N, 80.3E) on 18 March. The cruise track over the marine region around the Indian sub-continent is shown in Fig.5.1.

The cruise initially proceeded in the north-east/eastward direction and reached the farthest point on the north (20.69°N, 90.18°E) near Bangladesh on 21 March 2006, which was the maximum latitude covered over the BOB during the cruise and on the east (14.8N, 92.6E) over BOB on 26 March. After covering various parts of BOB it reached Kochi port (9.9N, 76.2E) on the west coast on 12 April 2006 while traversing through some part of the northern Indian Ocean. Thus the first leg of observations conducted over the BOB during March–April 2006 was for 24 day. Climate of the Bay of Bengal is influenced by three types of air flow, flow from Indian Subcontinent, flow South-East Asia, and from the Indian Ocean.

The second leg started on the west coast from Kochi on 18 April to cover the AS and concluded after 23 days at Goa port (15.4N, 73.8E) on 11 May. It reached its northern most point (21.37°N, 69.51°E) on 9 May and western point (14N, 59.4E) on 3 May 2006.

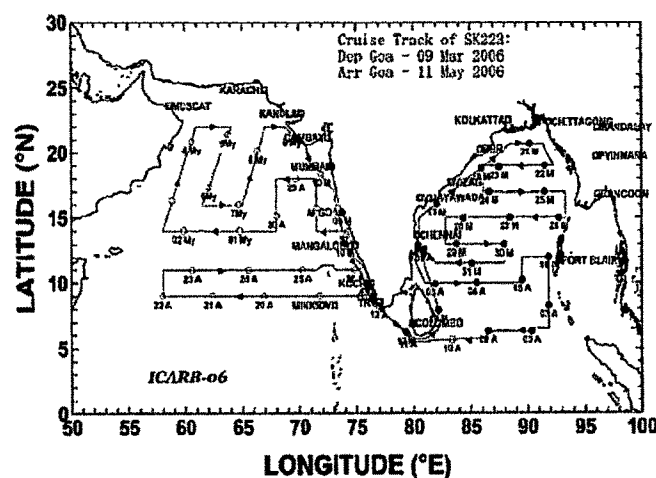


Figure 5.1. Cruise track for the Integrated Campaign for Aerosols, gases and Radiation Budget (ICARB).

The track of the ship cruise was designed in such a way that maximum possible marine regions were covered during the period for observations. The total duration of the cruise including both the phases was 55 days

5.2. Experimental details

Vertical profiles of ozone, humidity and temperature were obtained using balloon borne ozonesondes coupled to the radiosonde. Measurement details are given in Chapter 2. These sondes were typically launched at nearly 1000 hrs (local time) but some were launched during the night time to examine the difference between the daytime and the night time profiles. A total of 15 ozonesondes along with radiosondes were launched from March 18 to April 12, 2006 from the ship covering an extensive area of the BOB (5-22N, 80-95E) and some parts of the Indian Ocean as a part of ICARB. Details of the balloon flights are given in Table 5.1. In addition to these, 60 samples of surface air were also collected in pre-evacuated glass bottles for the analyses of carbon monoxide and methane during the campaign period. These samples were analyzed for CO and CH₄ using a gas chromatograph technique described by Sahu et al. [2006]. Samples were collected daily at 0800 hrs in the morning and at 2000 hrs (local time) in the evening.

Table 5.1a. Details of balloon flights conducted during ICARB campaign over Bay of Bengal.

Bay of Bengal (BOB)			
Date	Latitude (N)	Longitude (E)	Time (IST)
20 March 06	18.77	85.92	1010
22 March 06	19.00	91.52	1000
24 March 06	17	86.53	0955
26 March 06	15	92.73	1000
28 March 06	14.99	84.37	1000
30 March 06	12.39	87.92	1515
01 April 06	12.55	80.91	1000
02 April 06	12.65	80.38	1228
04 April 06	9.99	85.54	1030
06 April 06	11.99	91.83	1030
08 April 06	6.29	90.33	1310
10 April 06	5.62	83.36	1030
12 April 06	8.49	76.74	1000

Table 5.1b. Details of balloon flights conducted during ICARB campaign over the Arabian Sea.

Arabian Sea (AS)			
Date	Latitude (N)	Longitude (E)	Time (IST)
19 April 06	9	71.77	0945
21 April 06	9	62.39	1030
23 April 06	11	61	1015
25 April 06	11	70.27	1000
27 April 06	13.94	74.26	1020
28 April 06	17.59	71.5	2215
29 April 06	18	69.74	1015
01 May 06	14	64.78	1030
03 May 06	16.33	58.86	1041
04 May 06	20.85	60.6	1110
05 May 06	21.4	63.75	1045
05 May 06	20.72	63.42	1530
07 May 06	16	64.67	1030
09 May 06	21	68.08	0435
09 May 06	21.08	69.85	1400

5.3. Meteorology

5.3.1. General wind patterns

The regional winds at 850 hPa, based on data obtained from the NCEP (National Center for Environmental Prediction) reanalysis were found to be arriving mainly from Africa and the Gulf countries during 19 - 30 April (Figure 5.2a) while the wind pattern changed from ocean to land during the month of May. While at 200 hPa regional winds were found to be from Africa and the Gulf countries up to 25 April while in the next week (26 April - 3 May) (Figure 5.2 b) it was of both land as well as oceanic origin. In the last week (4 - 9 May) it was mainly of oceanic origin (not shown here). The region and period of the campaign provide particularly challenging conditions. The meteorological conditions in springtime over the Arabian Sea are characterized by the frequent passage of low-pressure systems, which mix continental air masses with cleaner marine air.

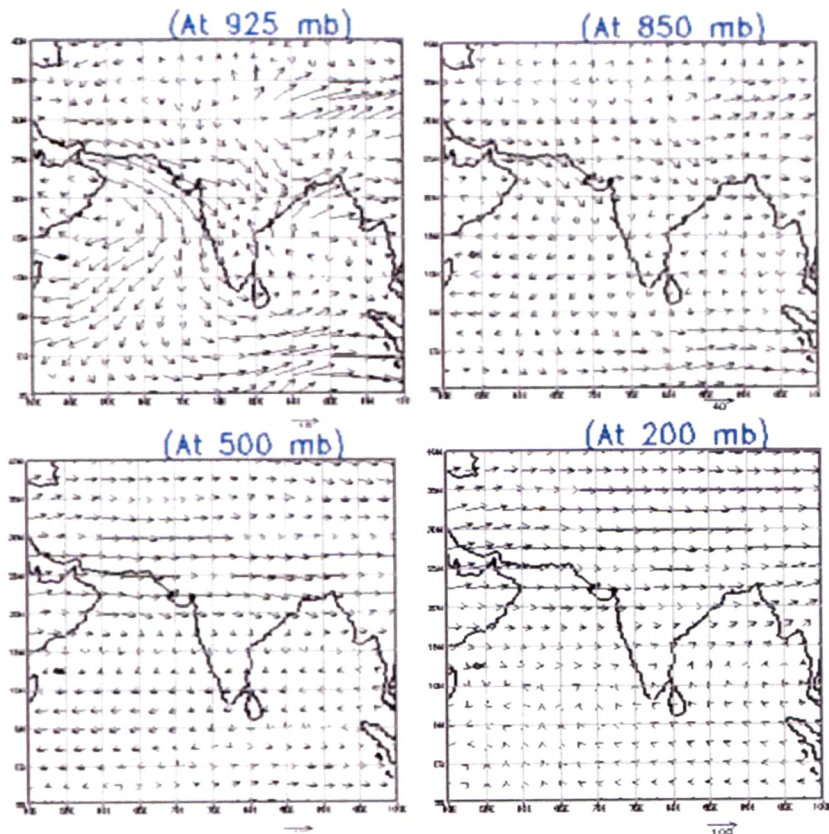


Figure 5.2a Mean winds at different pressure levels for the period during 18 March- 12 April 2006.

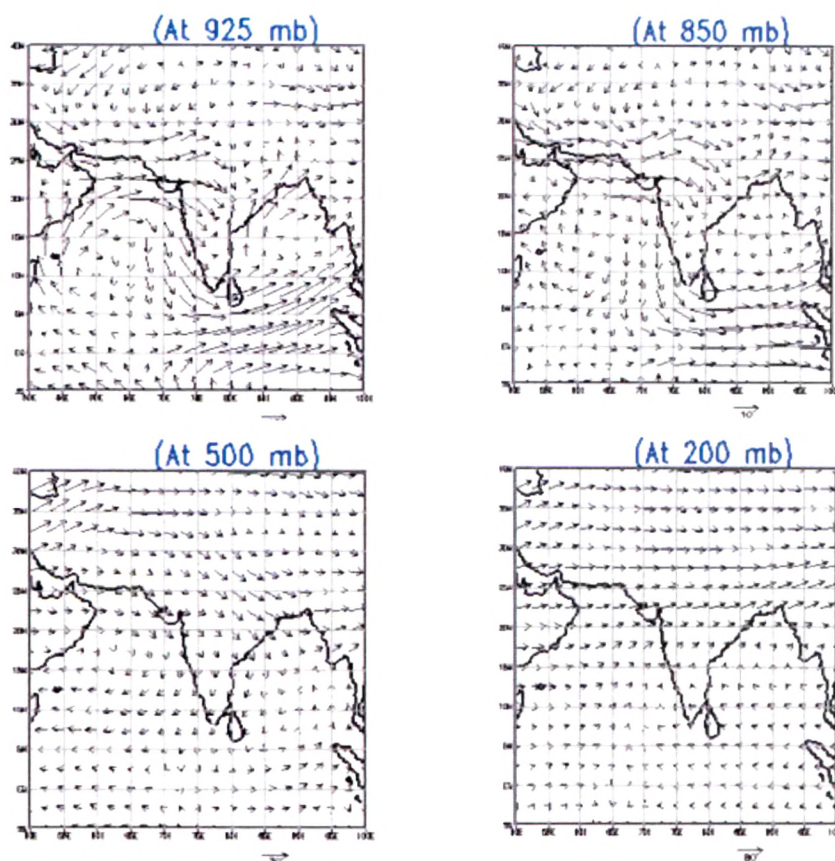


Figure 5.2b Mean winds at different pressure levels for the period during 18 April-10 May 2006

5.3.2 Variation of meteorological parameters

Meteorological parameters (temperature, wind speed and relative humidity) were measured on board the ship at 1-hour interval during the ICARB period. The daily means calculated from the hourly data are plotted in Figure 5.3. The daily average surface air temperature over the Bay of Bengal ranged from 30 C on 17 March to a minimum of 27.2 C on 22 March when the ship was around 20 N. Later the temperature was around 29-30 C when the ship was in the Southern BOB region. Relative humidity was mostly in the range of 65-80 % with small variations. The wind speed was in the range of 2-7 ms^{-1} during most of the cruise period over this region. However, the wind direction was changing as shown in Fig 5.3. The sky

conditions were generally clear, while on some days cloud patches were seen. Large convective clouds were observed on 30 March, 2006.

The daily average air temperature over the Arabian Sea during the cruise period was in the range of 28-30 C. It was minimum on 5 May when the ship was around 21 N, which was the northern most point of the cruise over this region (Figure 5.4).

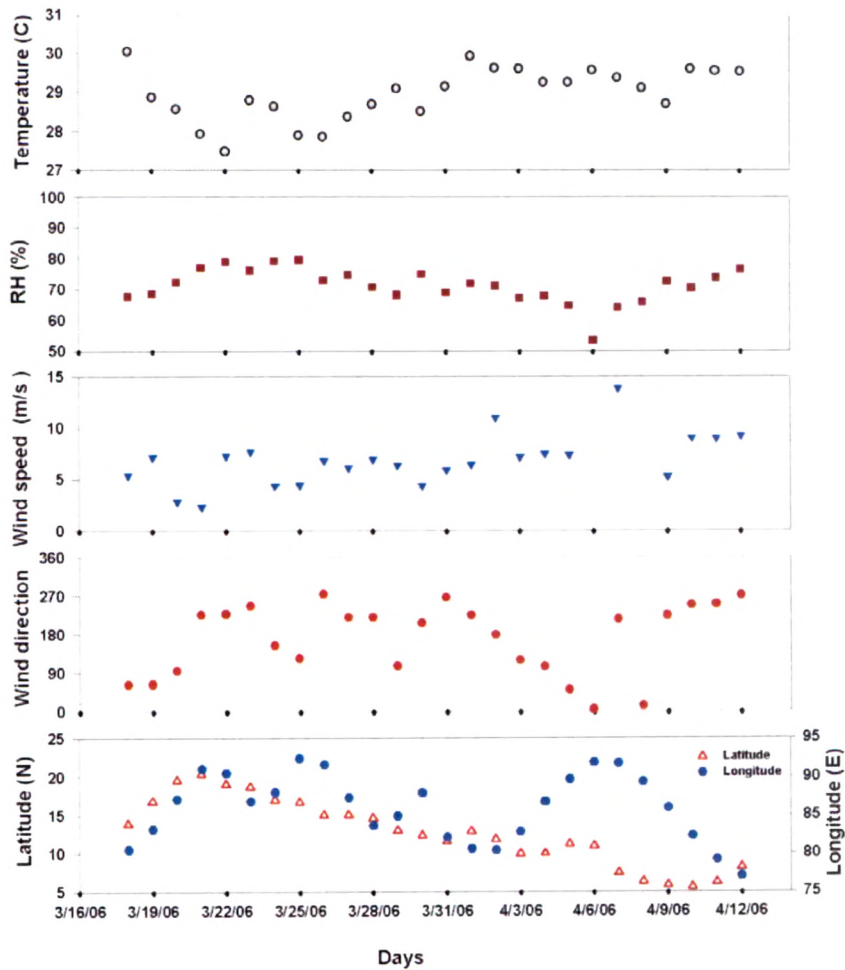


Figure 5.3. Daily average temperature, relative humidity (RH %), wind speed, wind direction and cruise track (latitude and longitude) measured at the ship's deck during 18 March- 12 April 2006 over the Bay of Bengal.

The relative humidity was higher (85-90 %) in the northern AS. The wind speed was mostly around 5 ms^{-1} except during 27-28 April, when it reached almost 12 ms^{-1} . The wind direction was mostly around 270° except during 21-25 April, when it changed to 45° .

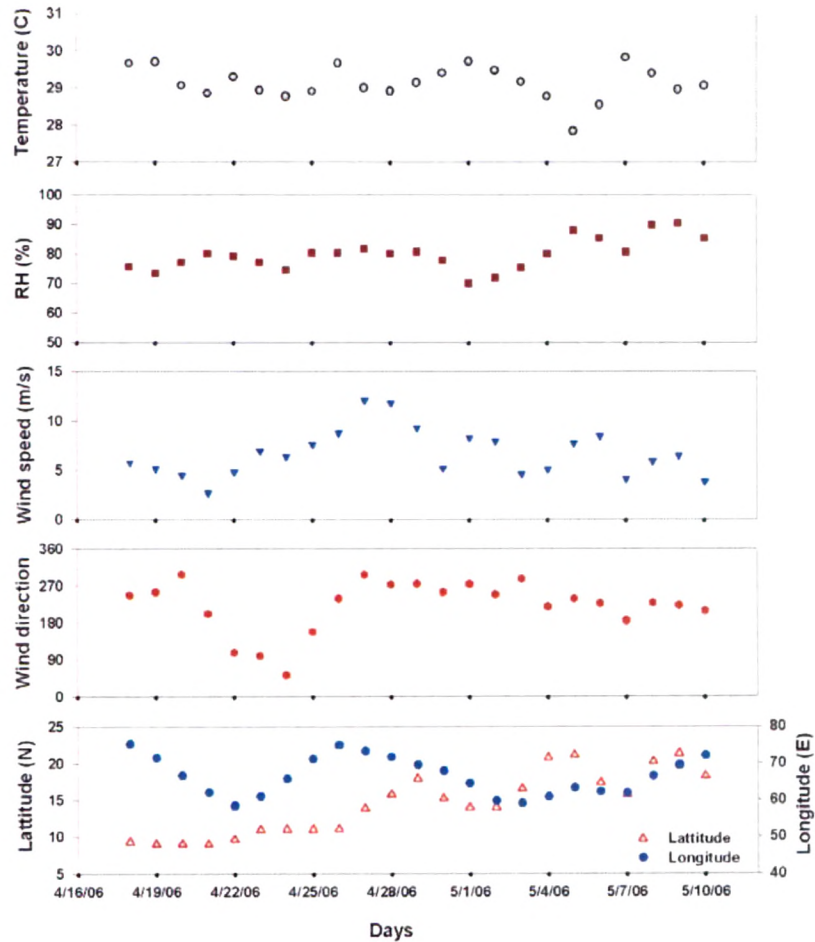


Figure 5.4. Daily average temperature, relative humidity (RH%), wind speed, wind direction and position of the ship (latitude and longitude) measured at the ship's deck during 18 April-10 May 2006 over the Arabian Sea.

5.4. Variation of trace gases during ICARB

Figure 5.5 shows the variations of O_3 , CO and CH_4 observed during the first part of the cruise over Bay of Bengal. The O_3 values correspond to surface level for each balloon flight. CO and CH_4 are the average values of the two samples collected each day. Levels of these trace gases were higher in the beginning of the cruise from 17 March to 25 March. This is the region along the eastern coast of India, when the ship moved from Chennai to the north most point. During this period, O_3 , CO and CH_4 values were found in the ranges of 50-60 ppbv, 175-225 ppbv and 1.8 -1.9 ppmv, respectively. After 27 March, levels of these trace gases were lower around 20 ppbv for O_3 , 100-130 ppbv for CO and around 1.8 ppmv for CH_4 . This clear difference in the levels is due to prevailing winds and vicinity to emission sources.

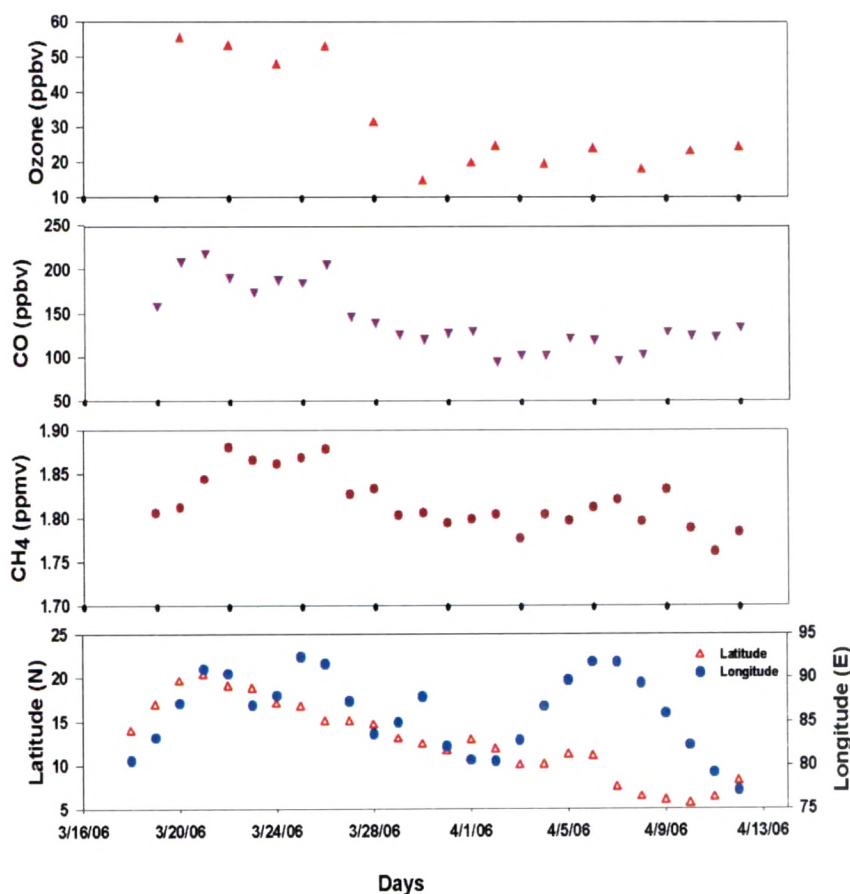


Figure 5.5. Variations of trace gases (O_3 , CO and CH_4) and position of the ship (latitude and longitude) over the Bay of Bengal from 18 March to 12 April, 2006.

Similar data set is shown for the Arabian Sea in Figure 5.6. Surface O_3 values for the first three flights, which were conducted in the southern AS, are low (30-35 ppbv). However, after 25 April O_3 values increased to about 40 ppbv. On the contrary, levels of CO and CH_4 were high up to 23 April but decreased later (Fig 5.6). This is somewhat abnormal as one expects higher levels of pollutants over northern AS as compared to the southern regions. Such opposite trends between O_3 and CO / CH_4 have not been reported during all the four INDOEX cruises over the AS. Due to the existence of anti-cyclonic system, there is a descending motion of air over this region. Since the horizontal wind speed in this region is very low, the effect of vertical motion could be dominating. This may bring higher levels of ozone and lower levels of other gases from the free troposphere

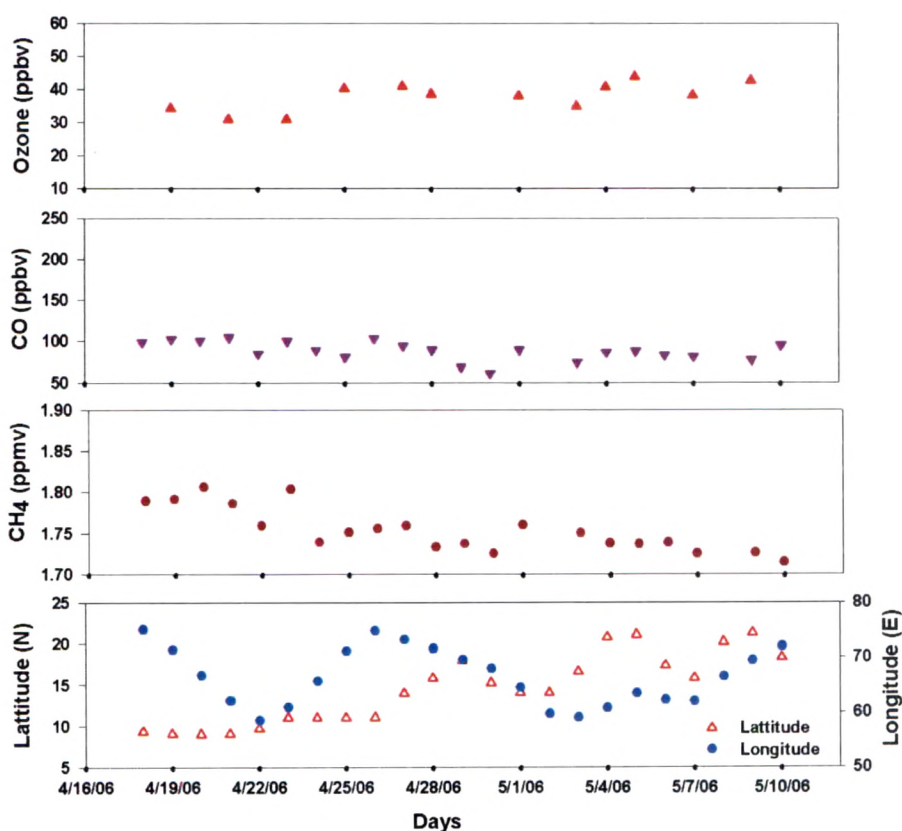


Figure 5.6. Variations of trace gases (O_3 , CO and CH_4) and position of the ship (latitude and longitude) over the Arabian Sea from 18 April to 10 May, 2006.

5.5. Possible loss of ozone due to dust

In the southern AS, in spite of the presence of higher concentration of CO, CH₄ and other trace gases, ozone is found to be lower. Atmospheric abundance of mineral dust was observed in the range of 2.7 - 23.7 μgm^{-3} over the AS during this campaign [Kumar et al., 2008]. A decreasing dust concentration was found (from south to north) during the campaign period. Ozone and dust levels show anti-correlation (Fig. 5.7). This could be due to the deposition of ozone on dust surface as discussed in the article [Dentener et al., 1996]. The presence of minerals (eg. carbonate) enhance the alkalinity of dust and accelerate the uptake of acidic species (eg SO₂/SO₃) followed by O₃ to form sulphate due to the increase in hygroscopic nature of dust. This is a new feature observed over this region, attesting to the fact that heterogeneous chemistry has a role to play in the marine atmosphere.

Several studies have shown that dust particles from Sahara can impact atmospheric processes during the course of their transport by providing reactive sites for heterogeneous chemical reactions [Jacob, 2000; Martin et al., 2003; Michel et al., 2003; Bauer et al., 2004 and Tie et al., 2005]. These reactions can deplete gas phase species by condensation or deposition on aerosol.

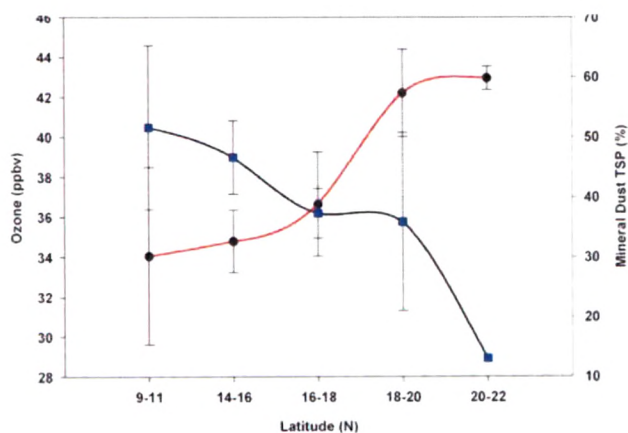


Figure 5.7. Variations of surface level ozone (given in red) and mineral dust (%) over Arabian Sea.

5.6. Vertical distribution ozone over the Bay of Bengal

5.6.1. Variation of Integrated total and tropospheric ozone

Columnar total ozone is obtained by integrating individual profiles up to the balloon burst altitude which was generally around 32–35 km, and further extending it up to 60 km of height using the method described by McPeters et al. [1997]. These integrated columnar ozone for the balloon flight days show similar trends with corresponding total ozone values obtained from TOMS (Figure 5.8 left). The total content based on the balloon data varies from 225–248 DU, with highest value of 248 DU on 20 March. The average total ozone based on TOMS data for flight days is 264 ± 7 DU, whereas the average total ozone from balloon flight data is 234 ± 5 DU (Figure 5.8 left). Thus there seems to be a bias between the two sets with the TOMS higher by about 30 DU. However the variability seems to be similar.

The tropospheric ozone content is obtained by integrating individual observed profiles up to the tropopause height which was calculated from the temperature profile measured by radiosondes. The ozone content varies from 22 to 45 DU, with a minimum of 22 DU on 30 March in the central BOB and a maximum of about 45 DU near the coast in the northern BOB (Figure 5.8 right). The average tropospheric column ozone with standard deviation was 36.7 ± 5.7 DU. This accounted for 15.6 % of the total column ozone.

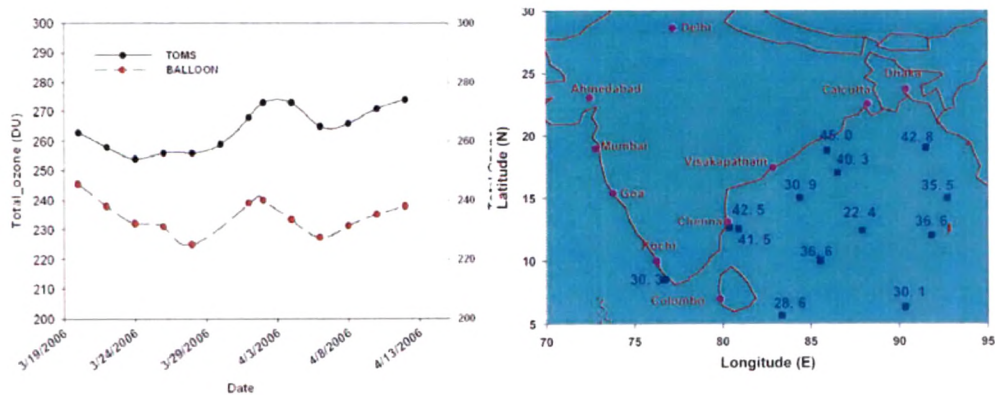


Figure 5.8 Time series of total ozone from TOMS and balloon (left), spatial distributions of integrated total column and tropospheric ozone (right).

5.6.2. Low ozone in the troposphere on 30 March, 2006.

The average integrated tropospheric ozone was observed to be 36.7 DU over the entire cruise period, while at a location (12.39N, 87.92E) on 30 March, it was found to be only 22.4 DU, which is approximately 60 % only of the average value. Vertical profiles of O₃ along with relative humidity and temperature as well as estimated potential temperature and equivalent potential temperature observed on 30 March, 2006 are shown in Figure 5.9. Potential temperature and equivalent potential temperature both indicate the stability of the atmosphere.

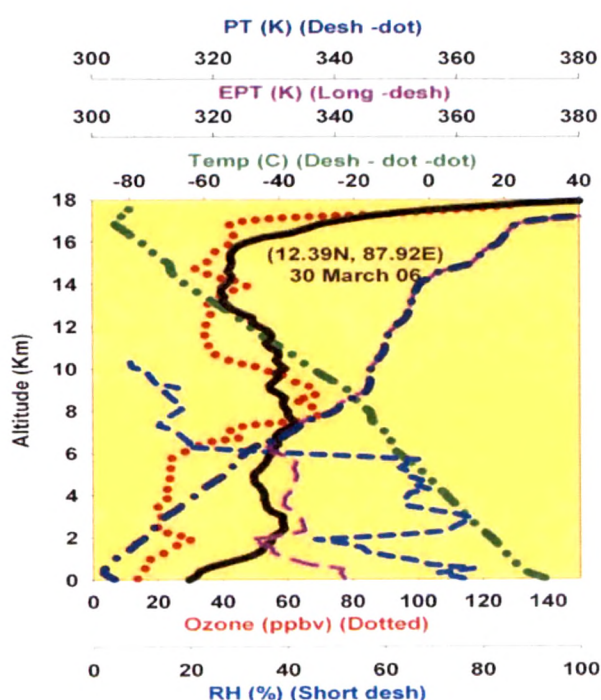


Figure 5.9. Altitude profiles of ozone, temperature and relative humidity (RH) observed on 30 March.

Also both become equal after 6 km, which indicates the presence of deep convection up to 6 km. The surface ozone on this day was found to be 14.6 ppbv, which is also less by 57% from the average value. During a convection event ozone deficient air is lifted from the MBL to the upper troposphere (10-16 km). But higher ozone in middle troposphere (6 -10 km), requires a supply of ozone rich air after the convection has occurred from some high ozone regions like stratosphere or a polluted land region.

The advection of an air mass from the surrounding continents can be the cause of this sharp increase in ozone concentration. At maritime locations characterized by persistent deep convection, the fraction of air parcels with O_3 mixing ratios less than 20 ppbv have been used as a proxy for the frequency of convective outflow [Folkens et al., 2002, 2006; Solomon et al., 2005]. The increase in convective outflow reduces upper tropospheric O_3 by a proportional amount at higher altitudes. Outgoing Longwave Radiation (OLR) represents a measure of convective activity and it is an indicator of both how warm the earth's surface is and the degree of transparency of the overhead atmosphere. When OLR is low it represents the presence of upper level clouds i.e. cumulonimbus convection in the region [Willicki and Green, 1989]. It will reduce the OLR by about $50\text{-}100\text{ Wm}^{-2}$ compared to a clear sky day OLR [Harrison et al., 1990]. Regions of a deep convective activity are indicated by OLR value typically below 250 Wm^{-2} .

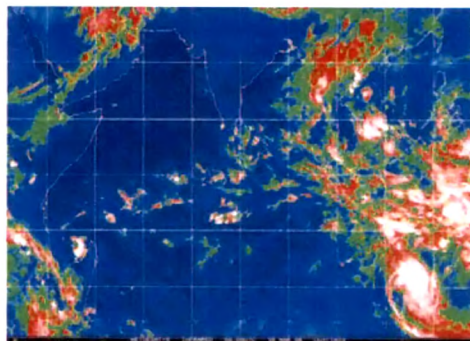


Figure 5.10. Satellite image of clouds over Bay of Bengal on 30th March 2006

The OLR over this region was observed to be about 250 Wm^{-2} on 30 March. Presence of clouds from satellite images also confirm significant convective activity during this period (<http://caos.iisc.ernet.in/weather.html>) as shown in Figure 5.10.

Satellite observations of trace gases in the troposphere are more difficult to make due to cloud interference. Observation of convection within the MBL are limited to Atlantic Ocean [Smit et al., 1989 and Piotrowicz et al., 1990], Indian Ocean [Rhoads et al., 1997] and Pacific Ocean [Thompson et al., 1993; Oltmans and Levy, 1994;

Kley et al.,1996 and Hoell et al.,1999]. Some of the results have been discussed in detail by Kley et al. [1996] and by Folkins et al. [2002, 2006].

5.6.3. Back trajectory analysis

Back trajectory analysis from HYSPLIT (www.arl.noaa.gov/ready/hysplit4.html) has been used as a second proxy to study transport of air. The wind field analysis and back trajectory analysis do not reveal any evidence of transport from the land on 30th March except at 1 km from India and for the height of 7-9 km from Africa (Figure 5.11 left). These results show long range transport from Africa (non-convective region) for the height range of 6-10 km. On the contrary, trajectories for the height range of 2 to 6 km and 10 to 18 km show transport from the Pacific Ocean side where a small cyclonic formation took place during that time. The height information from the back trajectories shows lateral transport for the height range from 1 to 6 km and downward transport in the height range of 6 to 10 km whereas from 10 to 18 km it shows up lift of air mass from 4-5 km of altitude range (Figure 5.11 right). The interaction of deep convection with long range advection seems to account for the possibility of confluence of dry air on deep convection.

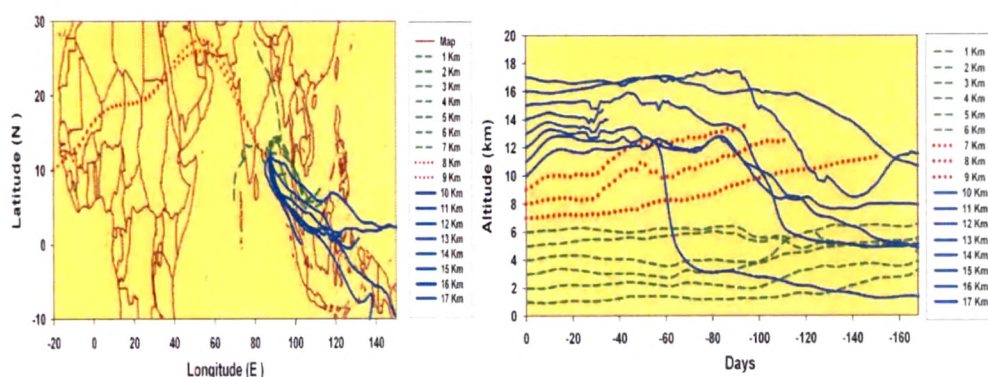


Figure 5.11. Back trajectory from HYPSPPLIT showing the horizontal transport at different altitude levels from 1 to 17 km on 30 March (left) and vertical transport of air mass from 1 to 17 km (right).

Convection of free tropospheric air has resulted in low O_3 in most of the troposphere, which could have substantial impact on the local photochemistry and its budget in the troposphere. Since the lifetime of ozone in the free troposphere is larger, change in ozone in the troposphere can change the OH concentration, which can lead to change in tropospheric chemistry. Regular measurements of O_3 and its precursors in the upper tropical troposphere are needed to study the frequency of convection events and their impact on ozone budget.

5.6.4 Comparison with a photochemical model

Figure 5.12 shows the surface ozone variation from 25 March to 5 April from MATCH- MPIC (Model of Atmospheric Transport and Chemistry - Max Planck Institute for Chemistry version) for the same location (12.39N, 87.92E) where convection has been captured by ozonesonde.

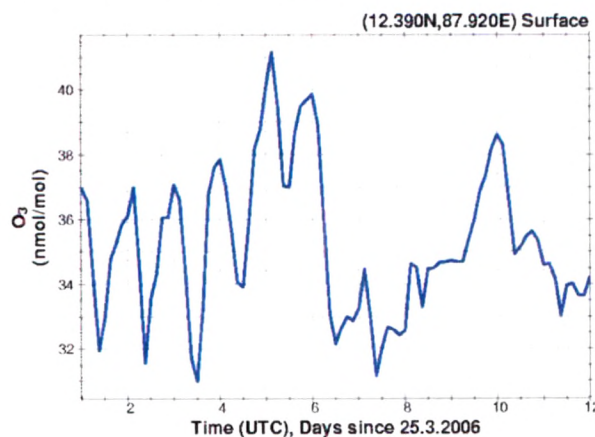


Figure 5.12. Surface ozone obtained from MATCH-MPIC model at location (12.39N, 87.92E) from 25 March to 5 April, 2006.

Some of the details of this model were discussed in Chapter 4. However, the model is described completely by Lawrence et al., [1999] and von Kuhlmann et al., [2003]. Surface ozone values calculated from this model also show low ozone mixing ratio at this location for the same time period

5.6.5. Distribution of ozone at different pressure levels

Distributions of ozone at three different pressure ranges, viz, Surf -700 hPa, 700 -400 hPa and 400- 200h Pa are depicted in Figure 5.13. In the lower troposphere, ozone concentration is minimum (20 ppbv) on 30 March.

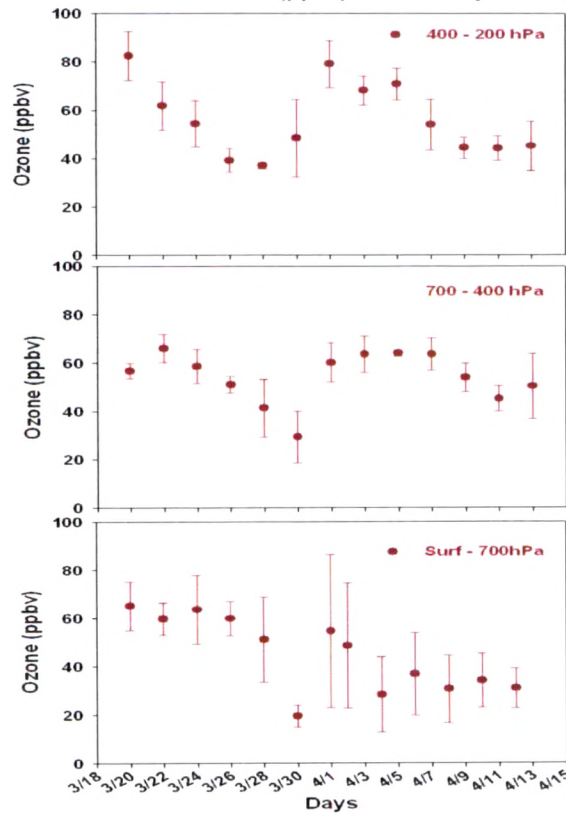


Figure 5.13. Distribution of ozone at different pressure ranges in the troposphere observed over the Bay of Bengal.

On this day, lowest ozone values are observed in the other two levels also. In the middle level ozone varied from 25 to 65 ppbv while in the upper level it varies from 35 to 80 ppbv.

5.7. Vertical distribution of ozone over the Arabian Sea

5.7.1. Variation of Integrated total and tropospheric ozone

Column integrated ozone amount for different flights made over the Arabian Sea are shown in Figure 5.14 (left). The total content varies between 233 DU and 263 DU. The lowest value of 233 DU was obtained on 1 May at 14 N, 64.5 E, while the highest total content was observed on 23 April(11 N, 61 E) as well as on 9 May (21 N, 69 E). The average is about 250 DU. The total content from TOMS ranged between 280 DU and 290 DU with an average of 285 DU. TOMS again showed a value of total ozone content by about 35 DU. This is similar to what was obtained over the BOB.

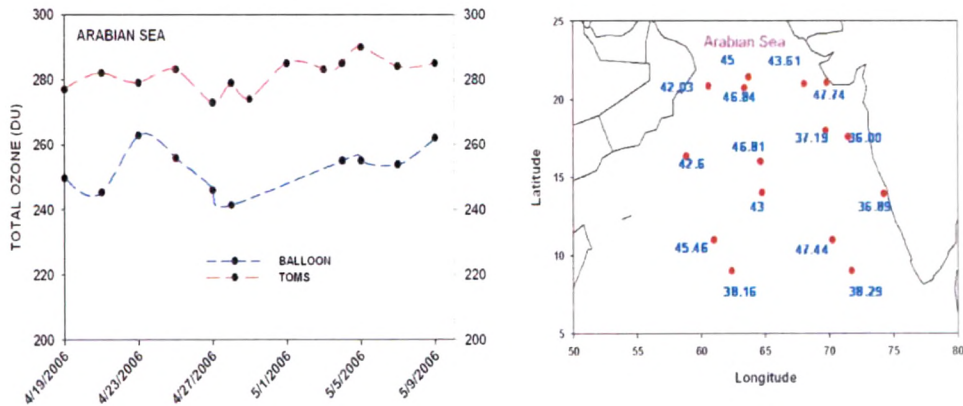


Figure 5.14. Time series of total ozone from TOMS and balloon over the Arabian sea(left). Spatial distribution of integrated total column and tropospheric ozone (right).

The total tropospheric content over this region varies from 36 DU to about 47 DU with an average of 42 DU (Figure 5.14 right). High content is generally observed in the northern AS. The average tropospheric content is high over this region compared to that over the BOB. These results are discussed further in this section.

5.8. Latitudinal distribution of ozone

The profiles have been divided into three major groups A, B, and C on the basis of their locations from 8-12N, 12-16N, and 16-20N respectively. This categorization has been done on the basis of the change in meteorological conditions along the cruise track.

5.8.1 Group A: 8-12N

There are four profiles in the latitude range between 8-12 N (Figure 5.15). Surface level trajectories obtained from HYSPLIT show that air came mainly from the African and Gulf countries during this time of observation (18 - 25 April, 2006). Higher ozone and low RH have been observed from 6 km to 11 km with an ozone peak at around 10 km on 19 April 06. Above 12 km, all the back trajectories originated from the Indian Ocean and the surrounding oceanic regions.

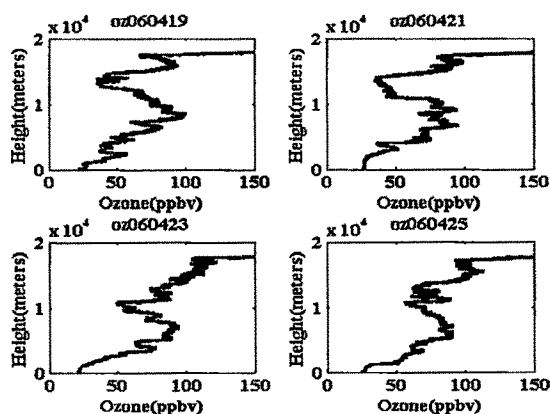


Figure 5.15. Vertical profiles of ozone in the troposphere observed over the AS in the 8-12 N latitude belt (format of the flight date is ozyymmdd).

Total integrated CO from MOPITT (<http://mopitt.eos.ucar.edu/mopitt/>) data was found to be high over Africa along with high fire counts along the back trajectory path in the height range of 5 to 11 km on 21 April 06. Back trajectories in the 5 - 9 km range on 23 April 06 originated from the region of high total CO as well as high fire

counts. However from 10 km onwards trajectories originated from the Indian Ocean region. Similar features were observed on 25 April 06 for the 5-9 km altitude range.

5.8.2. Group B: 12-16N

This group contains the four balloon profiles in 12N-16N latitude range (Figure 5.16). Higher ozone levels from 200 meters to 12 km were obtained on 27 April 06. Total integrated CO was high over eastern Africa, Indian region and also over the Gulf region. Cyclonic winds were observed on 1 May 06 in the height range of 1 to 6 km altitude range. However, winds in the 7 to 9 km altitude range originated over the oceanic region while those at 10-12 km were from South America and passed over African region on their way. Many fire counts were reported along the trajectory on this day.

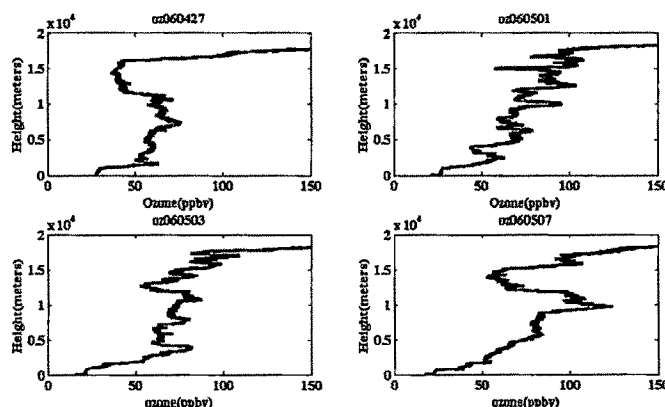


Figure 5.16. Vertical profiles of ozone in the troposphere observed over the AS in the 12-16 N latitude belt.

Ozone profile for this day shows a continuous increase. Potential Vorticity at 200 hPa also shows slight subsidence over this region on 1 May. High ozone at 3-4 km of altitude was observed on 3 May 06. Not many fire counts were reported along the trajectory. Very high ozone peak was originated from 6 to 12 km on 7 May 06. At this height back trajectories are mainly originated from the Atlantic Ocean and passed over Africa and the Gulf countries, up to 12 km of altitude range. Just above 12 km

wind patterns changed and trajectories were arriving from the Pacific Ocean and the Bay of Bengal. Few fire counts were reported.

5.8.3. Group C: 16-20 N

This group consists of seven ozone profiles in the 16- 20N latitude range (Figure 5.17). Back trajectories in the 1 to 11km altitude range originated from Africa and passed over the Gulf countries on their way to the sampling location on 28 April 06. High ozone from 3 km to 10 km was observed on 29 April 06. 3-7 km back trajectories originated from Africa and came via the Gulf countries while those in the 8 to 12 km range originated from the same region but passed over the Arabian Sea. Trajectories for the heights 13, 14 and 15 km also came from the African region while those at 16, 17 and 18 km came from the BOB region. All the back trajectories for 4 May 06 originated again from the same region. Few fire counts were reported along the path of the back trajectories. Ozone profile of this day shows a continuous increase. Potential Vorticity (PV) at 200 hPa also shows slight subsidence over this region on 4 May. Back trajectories for 5 May 06 show long range transport of ozone from Pacific Ocean via United States, Atlantic Ocean, and Africa up to 16 km of altitude while above 16 km these originated from the Bay of Bengal region.

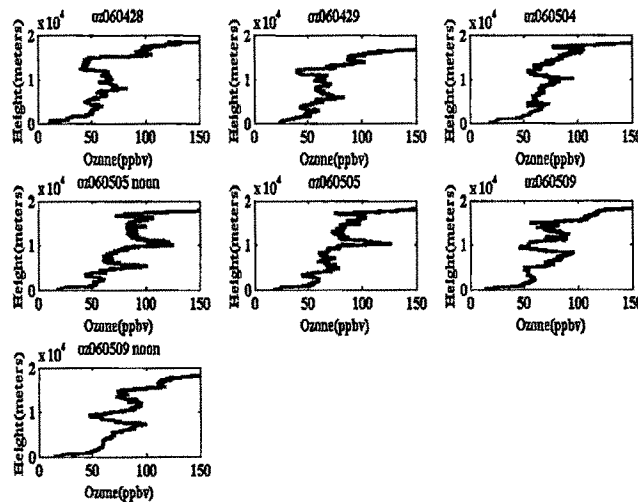


Figure 5.17. Vertical profiles of ozone in the troposphere observed over the AS in the 16-20 N latitude belt.

Total CO concentration were observed to be higher in eastern part of Africa while high fire counts were reported over Afghanistan and some parts of the Gulf region. This indicates that high ozone could be because of photo chemistry and transport from the higher latitudes. Potential Vorticity at 200 hPa also shows subsidence over this region on 5 May 06.

5.9. Day/night change in ozone vertical distribution

Two pairs of day-night balloon flights were made over the Arabian Sea (27 and 28 April) and two flights on 9 May to understand the effect of photochemistry on day and night profiles. Among these, one launch was made near the coast and the other one was made far from the coast. There was no appreciable change in ozone profiles in the free troposphere except within the MBL due to deposition and chemistry. In the first few kilometers on 28 April, ozone concentration was found to be lower than the day time value (Figure 5.18) when the ship was near the coast. However, on 9 May both the profiles seem to be similar even in the boundary layer except the slight change in the ozone structure in the profile (Figure 5.18) when the ship was away from the coast. This indicates that photochemical origin of ozone played minor roles in comparison with the dynamical mechanism. Similar results were obtained by Kley et al., [1996] and Folkins et al., [2000] over the Pacific Ocean.

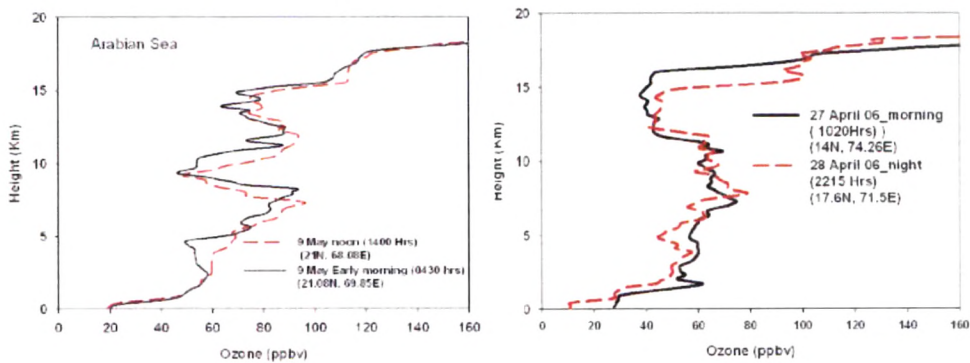


Figure 5.18. Day night change in ozone profile 9 May 06 (left) and 27 April 06 (right).

5.10. Stratosphere-Troposphere Exchange over the Arabian Sea

Average integrated tropospheric ozone was observed to be 42.5 DU over the Arabian Sea. Higher levels of tropospheric column ozone was observed in the north Arabian Sea (47 DU) compared to the average value, as discussed earlier. Enhanced ozone peaks are observed between 12 and 15 km on 1 May 06, compared to the average ozone profile based on all the 15 balloon flights data. The peak just below the tropopause shows enhanced ozone by 2.08 DU from the average ozone profile. While the peaks at higher heights 15 to 16.5 km show enhanced ozone by 1.47 DU. Similarly on 5 May enhanced ozone by 5.3 DU from the average profile was observed from 10 to 17 km (Figure 5.19). Seven day back trajectories for the height range of 10-15 km obtained from HYSPLIT model suggest that wind was coming from higher latitudes at this site. Potential Vorticity (PV) is used to trace the origin of the air. It is expressed in PV units where one PV unit = $10^{-6} \text{ m}^2 \text{ s}^{-1} \text{ K kg}^{-1}$. Air with potential vorticity of 2 PV unit or more is taken to be of stratospheric origin [Pan et al., 2004]. It has been estimated from NCAR data at 05 GMT from 1 to 9 of May (Figure 5.20). A jet stream was observed to be coming from the mid latitude in the southeast direction towards this site through the isentropic surface of 350K. Noticeably, there was a sharp PV gradient along the subtropical jet stream around 20–30N, which is the location where active stratospheric-tropospheric exchange occurs.

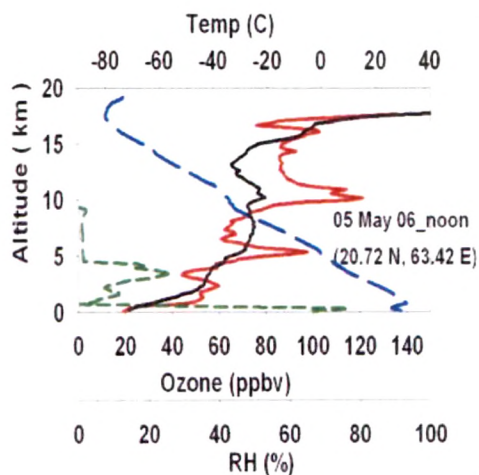


Figure 5.19. Ozone profile observed on 5 May 06 over northern AS

Cross-sectional view of PV (Figure 5.20) shows a tongue of air with PV of more than 2 PV units indicate that the air at these altitudes has its origin in the stratosphere. Both PV and back trajectory analysis suggest that the observed ozone peaks were associated with air of stratospheric origin. Enhanced ozone layers have also been observed over Xining (36.4N, 101.4E), Beijing (39.8N, 116.4E) and Hong Kong (22.3N, 114.2E) in January 2002 [Chan et al., 2004] and over Kanpur (26N, 80E) in December 2004 [Gupta et al., 2007]. They suggested that these enhancements were due to intrusion of stratospheric ozone from the Indo-Burmese region of SE Asia, where subsidizing downward motion had been observed.

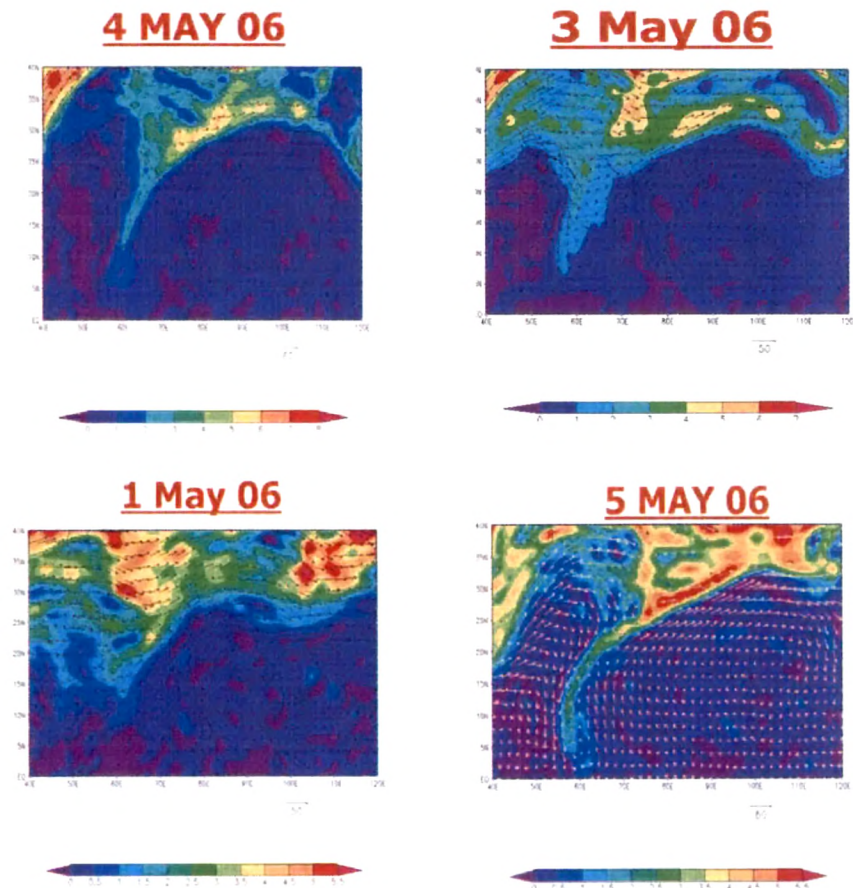


Figure 5.20. Potential Vorticity (in PV units) estimated from the NCEP GFS model.

A study done by Waugh and Polvani [2000] using NCAR/NCEP (National Center for Atmospheric Research/National Center for Environmental Prediction) reanalysis data for the period between 1980 and 1997 also showed that in the northern hemisphere stratospheric intrusions occur mainly during the northern winter.

5.9. Summary and Conclusions

Around 30 balloon flights carrying ozonesondes and radiosondes were conducted over the Bay of Bengal and Arabian Sea during the ICARB campaign (18 March – 9 May 2006) to study variability in tropospheric ozone distribution. In addition to these balloon flights, 60 samples of surface air were also collected which were analyzed for CO and CH₄. Higher levels of surface ozone were observed over the Bay of Bengal as compared to that over the Arabian Sea. However, for CO and CH₄, the reverse trend was observed (Table 5.2). Higher levels of surface ozone, CO and CH₄ were observed along the east coast of India over the BOB as compared to over the open marine region (Figure 5.21). In general, there is not much difference in the average levels of these gases observed during this study and with earlier studies in these regions.

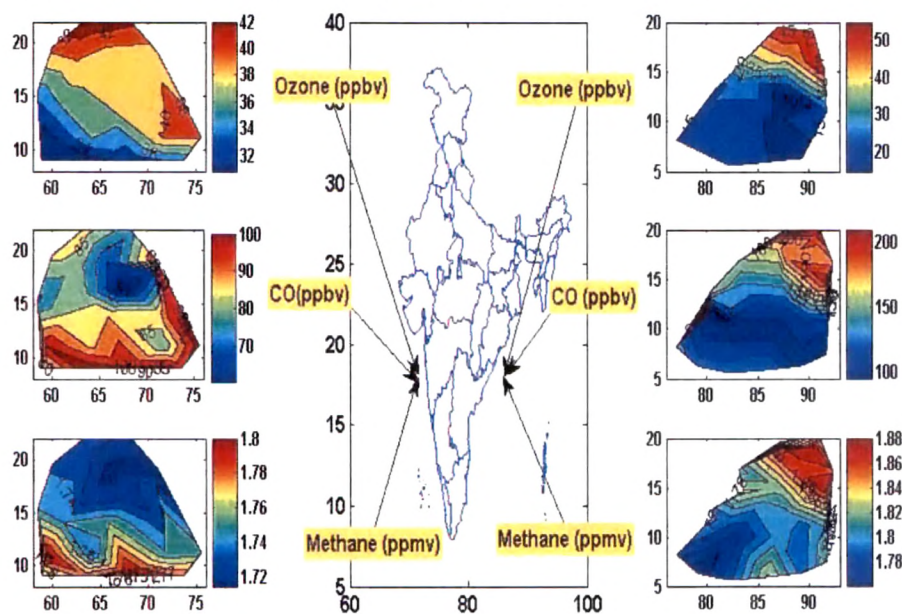


Figure 5.21 Spatial variations of surface O₃, CO and CH₄ over the Bay of Bengal (Right panel) and the Arabian Sea (left panel) from March 18 to May 10, 2006.

Table 5.2. Comparison of the average concentrations of surface O₃, CO, CH₄ and meteorological parameters measured during different campaigns (ICARB, INDOEX, BOBEX) over the Bay of Bengal and the Arabian sea.

Species	ICARB AS (5- 22N) (this study)	ICARB BOB(5- 20N) (this study)	BOBEX 2001 (Sahu et al., 2005) AS	INDOEX 1999 (Winter Monsoon) IO & AS Chand et al., 2003	Summer monsoon (5-12N) AS (Stehr et al., 2002)
Ozone (ppbv)	37.3±4.0	31.2±15.1	43.1±4.2	17.71±3.85	35.9± 3.0
CO (ppbv)	87.2±12.6	143.4±37.5	91±15		146.1±18.9
CH ₄ (ppmv)	1.75±0.02	1.82±0.03	1.8±0.02		
RH(%)	79.9±5.3	71.4±5.7	72.0±4.7		
Wind speed (m/s)	6.7±2.4	6.8±2.5	5.5±1.9	5.63± 1.93	

Over the southern AS, low surface ozone was observed where CO and CH₄ were still high. This feature has been examined further using observed levels of mineral dust in air. There seems to be an anti-correlation between the ozone and dust levels indicating heterogeneous loss of ozone on mineral dust.

Vertical distribution of ozone over the two marine regions is compared with the measurements made over Ahmedabad (Figure 5.21). Peak stratospheric ozone is lower over Ahmedabad (130 nb) as compared to either that of BOB (140 nb) and AS (150 nb).

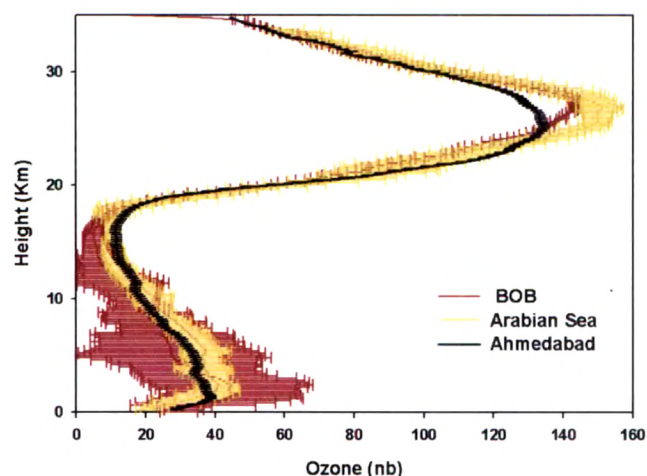


Figure 5.21. Comparison of the observation made over the Bay of Bengal and the Arabian Sea during SK223A and SK223B

However, there is no appreciable difference in ozone values within the troposphere. The average ozone partial pressures are highest (40-44 nb) around 2-3 km in the lower troposphere and minimum (5-10 nb) near the tropopause. Average values ozone partial pressure over the two marine regions are given in the Table 5.3.

The total integrated tropospheric columnar ozone shows extremely low values on 30 March 06 over BOB. This is due to strong convection which occurred during that period in this region. The vertical profile observed on this day show lower ozone values due to convection in the height region of 1 km except in the height region of 1 to 6 and 12 to 18 km. The height region on 6 to 11 km shows higher ozone values. Back trajectory analysis show that this plume of higher ozone is due to transport of ozone as well as its precursors from north Africa. Details of tropopause height, total columnar and total tropospheric ozone for all the balloon ascents are given in Table 5.4

Table 5.3. Average ozone partial pressure at each km height observed over BOB and AS during the ICARB 2006

Height (km)	Ozone (nb) Bay of Bengal	Ozone (nb) Arabian Sea
1	32.7±3.0	25.6±4.2
2	43.6±1.4	37.5±2.8
3	43.7±0.9	40.0±0.9
4	36.8±2.9	37.4±0.8
5	30.5±2.1	36.7±0.6
6	27.4±0.2	36.7±0.8
7	26.0±0.8	33.6±1.0
8	24.5±0.9	30.0±1.2
9	20.9±1.2	25.8±1.3
10	17.3±0.5	22.5±0.6
11	15.5±0.9	20.6±1.2
12	12.6±0.6	16.7±1.3
13	9.5±1.1	13.2±0.8
14	6.9±0.5	11.3±0.3
15	6.1±0.3	10.5±0.3
16	5.3±0.2	10.9±0.3
17	6.1±0.6	10.2±0.3
18	8.5±1.4	11.6±1.7
19	18.5±5.6	24.1±6.8
20	39.9±8.7	48.5±9.1
21	64.0±6.8	77.8±6.8
22	83.4±4.4	91.4±3.2
23	99.4±6.2	106.5±4.7
24	113.3±3.6	124.9±6.5
25	127.5±4.5	140.4±3.9
26	137.0±1.6	149.1±1.2
27	141.9±1.4	150.4±0.6
28	143.1±0.8	146.3±2.7
29	133.6±5.0	134.3±5.4
30	115.5±5.8	115.0±6.7
31	97.5±5.3	98.2±4.8
32	82.2±4.0	85.5±3.0
33	70.3±3.3	74.4±3.6
34	59.9±4.4	61.9±5.2
35	47.1±6.8	

Table 5.4. Observed tropopause height and estimated values of total columnar and total tropospheric ozone values during the ICARB 2006 campaign over the two marine regions.

Date	Latitude (N)	Longitude (E)	Tropo pause Height (km)	Total Tropo spheric Ozone (DU)	Total columnar Ozone (DU)
Bay of Bengal (BOB)					
20 Mar 06	19.6	87.0	17.5	45.0	245.4
22 Mar 06	19.0	90.4	17.7	42.8	238
24 Mar 06	17.0	87.9	16.9	40.3	232
26 Mar 06	15.0	91.5	18.1	35.5	231
28 Mar 06	14.6	83.6	17.5	30.9	225
30 Mar 06	12.3	87.8	16.9	22.4	----
1 April 06	12.9	80.6	17.0	42.5	239
2 April 06	11.8	80.4	17.4	41.5	240
4 April 06	10.0	86.7	17.5	36.7	233.3
6 April 06	11.0	91.7	17.8	36.6	227.4
8 April 06	6.3	89.3	16.7	30.1	231.3
10 April 06	5.6	82.2	17.4	28.6	235.1
12 April 06	8.2	77.0	17.5	30.3	238
Average			17.4±0.4	35.6±6.8	261.9±6.4
Arabian Sea (AS)					
19 April 06	9.0	71.4	17.2	38.3	249.7
21 April 06	9.0	62.1	17.2	38.2	245.3
23 April 06	11	61.0	17.5	45.5	262.8
25 April 06	11	71.1	17.5	47.4	255.8
27 April 06	10.6	56.1	17.2	36.9	246

28 Apr06	13.6	61.8	17.7	36	241.4
1 May 06	14.0	64.5	18.1	37.2	233
3 May 06	16.6	59	17.7	43	235
4 May 06	20.8	60.7	17.5	42.6	255
5 May 06	21.1	63.3	18.0	42	255
			17.5	45	257
7 May 06	15.8	61.8	18.1	46.8	253.8
9 May 06	21.3	69.4	17.7	43.6	262.1
			18.9	47.7	256.3
Average			17.7±0.5	41.7±4	250.1±9.5

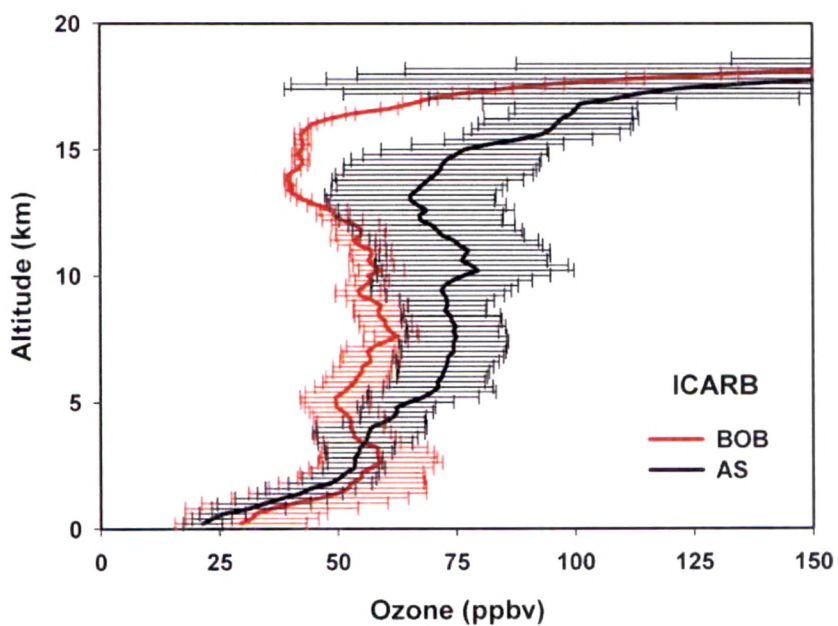


Figure 5.22. Average vertical distribution of ozone over BOB and AS observed during the ICARB 2006

Vertical distribution of tropospheric ozone mixing ratios show higher levels in the free troposphere over AS as compared to over BOB (Figure 5.22). This seems to be due to two factors viz: strong convective activities over BOB transporting low levels of ozone from the marine boundary layer into the free troposphere and intrusion of stratospheric air into the upper troposphere over the northern AS. The upward motion over the BOB could be a part of the major Walker circulation. The downward motion over AS has been identified using Potential Vorticity as well as back trajectory analysis.

CHAPTER- 6

Summary with general conclusions and outlook

Tropospheric ozone plays an important role in the chemistry and radiation budget of the atmosphere. It is a major source of OH radicals and was also a greenhouse gas. Measurements over the northern tropical region are very limited. The aim of this work is to study the variability in the distribution of ozone in the tropical troposphere over different sites representing different environments.

Fortnightly measurements of ozone profile were made at Ahmedabad, an urban location in the western part of India during 2003-2007 using a standard ECC ozonesonde coupled with a radiosonde (RS80). As a part of a major campaign over the Indo-Gangetic Plain (IGP) in December 2004, similar measurements were made from Kanpur, which is located in central IGP, using these sondes. The aim of this campaign was to study effects of foggy conditions on the distributions of trace gases including ozone. Another major campaign was conducted over the marine regions surrounding India namely, Bay of Bengal (BOB) and Arabian Sea (AS). A total of 30 balloon flights carrying these two sondes were launched from the ship, which covered both these marine region during March-May 2006. This study provided an opportunity to study the effects of dynamics on the distribution of ozone. These results are used to get the average distribution of ozone in the troposphere as well as to study the effects of advection, convection, and transport from the stratosphere on ozone distribution. Results from the three sets of measurements are summarized below.

6.1. Variations in vertical distribution of ozone over Ahmedabad

Ahmedabad is a semi-arid region in western India (23.03 N, 72.54 E). While, ozone soundings do not give information on the day-to-day changes associated with a particular synoptic event they provide a quantitative measure of variation in ozone throughout the troposphere. Over 80 profiles on the vertical distribution of ozone were obtained over this site from June 2003 to July 2007. These data obtained over Ahmedabad are classified into four major seasons viz winter (DJF), pre-monsoon (MAM), monsoon (JJAS) and post-monsoon (ON). Boundary layer ozone was maximum during winter and minimum during monsoon. This observation could be due to shallow boundary layer height during winter and wash out of pollutants during monsoon. The summer monsoon ozone minimum in the lower troposphere is attributed to the onset of summer monsoon when polluted air from the Asian continent is replaced by cleaner air from the tropical Indian Ocean.

The middle troposphere ozone was at its highest during the rainy season and at a minimum during post-monsoon. Near tropopause, large variability was observed during pre-monsoon and winter due to intrusion of ozone from the stratosphere. A frequently observed feature during pre-monsoon and winter was high ozone (80-170 ppbv) in the upper troposphere (from about 9 to 16 km). Integrated ozone increase due to STE for the month of March was 5 DU (Dobson unit) and for April it was 15 DU. This phenomenon is generally observed at higher latitudes in the months of March and April. However, this phenomenon was also observed at the study location. This is the first experimental study to estimate the contribution of ozone due to STE process over Ahmedabad. In the stratosphere highest peak ozone concentration was observed during rainy season and minimum during winter.

Average integrated total ozone was 261 DU and average integrated tropospheric ozone was 39.4 DU. Higher lifetime of ozone in the free troposphere increases the importance of long range transport. In the lower and mid-troposphere, higher concentrations of O₃ in the spring season could be due to long-range transport of pollutants by northwesterly

winds associated with the winter monsoon circulation. This circulation transports the ozone-rich polluted air masses from the Asian continent to this site. Conversely, low ozone (as low as 15 ppbv) values are observed over Ahmedabad during summer season (July to September). This is related to summer monsoon circulation, advecting cleaner and moist air from the Indian Ocean.

Elevated O_3 values of around 100-450 ppbv were observed in the middle and upper troposphere (10-14 km) during the spring season over Ahmedabad. Occurrences of high O_3 tongues in the spring season follow the propagation of dry air with low relative humidity, suggesting that O_3 is transported from higher heights, probably of stratospheric origin.

Case study of vertical profiles over Ahmedabad reveals significant day-to-day variability in the vertical structure of O_3 and relative humidity. These studies also revealed influences of convection and advection of various air masses within the troposphere.

Dynamics plays a major role in the seasonal distribution over Ahmedabad. In the lower and middle regions of the troposphere, low O_3 values with high water vapor concentrations in the summer monsoon season are pronounced. While in the upper region of the troposphere, high O_3 values with very low amount of water vapor in the spring season are pronounced. In the spring season, elevated O_3 levels over this location reflect the influence of photochemical production from precursors. Back trajectory analysis suggests that this enhancement resulted from the transport of air masses arriving at the altitudes of O_3 peaks in the middle troposphere passed over regions of biomass burning during this season.

6.2. Study of ozone distribution over the Indo-Gangetic Plain (IGP) during a winter month

Vertical distributions of ozone and other meteorological parameters were measured at Kanpur, an urban site in the Indo-Gangetic Plain (IGP) during December 2004 to study

the processes affecting their levels. This campaign was organized to study the effect of fog/haze on tropospheric ozone and other pollutants. During the foggy days, wind speed was very low along with shallow boundary layer height. In general, the winters in the North Indian region are dry. Six balloon flights were conducted from this site during December 2004. Three were on clear days (December 11, 15 and 29) while the remaining were on foggy days (December 18, 22 and 25).

Large variability in tropospheric ozone was observed from flight to flight. Temperature profile suggested that the average boundary layer height was about 800 m on foggy day and 1.5 km on non-foggy days. The average tropopause height was observed to be 17 ± 0.7 km. The average tropospheric column ozone was 41 ± 3 DU. It increased to 53 DU on December 25 due to intrusion of air mass from the stratosphere, which accounted for 15 – 20% of the total tropospheric ozone column.

In the lower troposphere (3-7 km) ozone concentration was higher (70 ppbv) as compared to an average of 50 ppbv based on the six balloon profiles. Back-trajectory analysis suggests that the air parcels in the enhanced ozone layers over Kanpur passed over the region of intensive seasonal burning in Africa and higher pollutant region of the Gulf.

Enhanced ozone peaks were observed between 10 and 18 km on December 25, compared to the average ozone profile based on all the six balloon flights data. The peak in the TTL region (14-18 km) showed an enhancement of ozone by 35-55 ppbv over the average ozone profile. The peaks at lower heights of 12 and 10 km show enhanced ozone by 20 ppbv and 35 ppbv respectively from the average ozone profile. Seven day back trajectories for the height range of 9-15 km obtained from HYSPLIT (Hybrid Single-Particle Lagrangian Integrated Trajectory) model suggest that the air came from high latitudes at this site. Further, the Potential Vorticity (PV) values indicate that a jet stream came from the mid latitude in the southeast direction towards this site through the isentropic surface of 350K. Noticeably, there was a sharp PV gradient along the subtropical jet stream around 20-30 N, which is the location of active stratospheric-

tropospheric exchange. Cross-sectional view of PV shows a tongue of air with PV of more than 2 PV units between about 300 hPa (9.5 km) and 100 hPa (17 km). These altitudes coincide with the ozone enhanced peak levels and indicate that the air at these altitudes has its origin in the stratosphere. Lower ozone levels by 35-40 ppbv as compared to the average profile in the height range of 11 to 14 (December 29) were observed. Back trajectory analysis suggests that the air mass originated from a pristine marine region near the equator and traveled across the Indian Ocean, where generally low ozone values were observed as reported in earlier studies. Since ozone lifetime is higher in the free troposphere, it can get transported far away from the source regions.

A comparison of vertical profile of ozone obtained from ozonesonde with that obtained from MATCH-MPIC (Model of Atmospheric Transport and Chemistry - Max Planck Institute for Chemistry version) model was made. Among all the six profiles, model was able to reproduce large variations in the ozone profiles (e.g., high ozone on 25th December and low ozone on 29th December).

6.3. Cruise study of ozone distributions over the marine regions

Simultaneous measurements of vertical distributions of ozone and meteorological parameters were made to study variations in ozone distribution and its relationship with meteorology over the Bay of Bengal (BOB) and Arabian Sea during a cruise from 18 March to 9 May, 2006. This is the first systematic study of the vertical distribution of ozone covering both these marine regions fully during the pre-monsoon season. The northern and western Arabian Sea regions are the least studied. Most of the earlier studies e.g. INDOEX (Indian Ocean Experiment)) focused on the eastern/southern Arabian Sea and attention was only on winter season (NE monsoon).

Variations in the vertical distribution of ozone and meteorological parameter show evidence of deep convection on 30 March over the central BOB (12.39N, 87.92E). The average integrated tropospheric ozone over the BOB was 36.7 ± 5.7 DU, while on 30 March at the location 12.39N, 87.92E it was only 22.4 DU (which is approximately 60%

of the average value) due to strong convective activity. Depleted ozone profile with mixing ratio of 20 ppbv up to around 6 km of altitude and 35 ppbv in the height range of 10 to 16 km were observed. However, high ozone concentrations (50-60 ppbv) from 6 - 10 km were observed. Outgoing Long wave Radiation (OLR) and the presence of clouds from satellite images indicated significant convective activity during this period, while seven day back-trajectories showed that superimposition of long range transport on this activity. The confluence of deep convection with advected dry air was a new observation. Computation of surface ozone estimated using MATCH -MPIC model also showed low ozone concentrations in this region.

The wind field analysis and back trajectory analysis did not reveal any evidence of transport from the land on 30 March except at 1 km height from India and for the height range of 7-9 km from Africa. For the height range of 7-9 km, these results show long range transport from Africa (non convective region), on the contrary trajectories for the height range of 2 to 6 km and 10 to 18 km show transport from the Pacific Ocean where a small cyclonic formation took place during that time. The back trajectories computation show lateral transport for 1 to 6 km and downward transport in the height range of 6 to 10 km whereas from 10 to 18 km it shows uplift of air mass from 4 -5 km altitude range.

Surface ozone in north-west Arabian Sea was observed to be higher as compared to south-east Arabian Sea, while the reverse was true for ozone precursors line CO, and CH₄. These observations in combination with simultaneously observed dust levels suggest the loss of ozone through heterogeneous chemistry on dust particles. However, the anti-correlation between ozone and dust concentrations was weak.

Higher concentration of ozone in the upper troposphere was observed in the north Arabian Sea during first week of May. This increase was due to intrusion from the stratosphere and transport of air from the higher latitudes. It is known that incidence of stratospheric contribution is frequent and strong during spring. Average integrated

tropospheric ozone is found to be 42.5 DU which was higher than that obtained over the Bay of Bengal.

Comparison of the day-night profiles of ozone does not show any difference in the free troposphere but showed differences in the boundary layer for the profiles near the coast only. These results indicate that photochemistry played a minor role compared to the dynamics of the free troposphere.

Figure 6.1 shows average tropospheric ozone profiles observed Ahmedabad for the entire period of measurements (May 2003- September 2007), over Kanpur for the campaign period of December 2004 and over the two marine regions, Bay of Bengal and Arabian Sea during 18 March -12 April 2006 and 18 April - 10 May 2006 respectively. Even though these are for different periods, average ozone over Arabian Sea is clearly higher not only compared to over the BOB but also over urban sites of Ahmedabad and Kanpur. Higher ozone values over the Arabian sea appears to be due to transport from the stratosphere/ higher latitudes during the observation period.

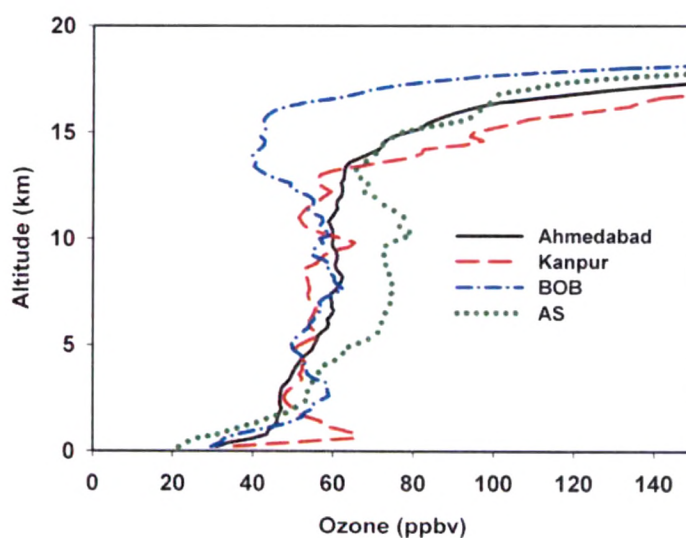


Figure 6.1 Average tropospheric ozone profiles over land sites (Ahmedabad and Kanpur) and marine regions (Bay of Bengal and Arabian Sea).

6.4. Future directions and scope

The present study characterized the spatial and temporal distributions of ozone in the lower atmosphere and provided an unique opportunity to study the influence of meteorological events and long range transport. Ozone together with the meteorological parameters helps in the elucidation of stratosphere-troposphere exchange across the tropopause. Tropopause structure, temperature profile and potential vorticity are required to calculate the increase in tropospheric ozone flux from the stratosphere and its implication to its tropospheric budget.

Ozone together with available relative humidity and temperature profiles help to study the effects of convection events and change in photochemistry. Since lifetime of ozone in the free troposphere is large, once ozone gets lifted from the boundary layer into the troposphere, it can get transported to long distances. This can have significant implications on a global scale. It is also observed that in the free troposphere dynamical processes dominate over photochemistry in altering the distribution of ozone while in the boundary layer photochemistry dominates the dynamical processes. Regular measurements of ozone and its precursors in the tropical troposphere are needed to study the integrated effects of stratospheric tropospheric transport, long range transport and convection events.

This study also brings out the need to validate models to understand quantitative contribution of different chemical and dynamical processes. Due to regional nature of the sources/sinks, there is a significant spatial variability in tropospheric ozone, which makes modeling of tropospheric ozone extremely difficult. It is necessary that observations and modeling studies should complement each other for further improvement in our understanding of chemistry-transport coupling, long term changes and influence of ozone on the climate.

The marine regions are affected by transport of pollutants from the continental regions. It is also important to make regular measurements of ozone along with its precursors in the

troposphere. Limited observations during INDOEX campaign were made using aircraft borne sensors. Aircraft based studies are needed over the Indian subcontinent to understand chemistry and transport.

Numerical models in combination with field measurements have proven to be useful tools in studying the complex interactions of chemical species and meteorology in the atmosphere. Development of photochemical air quality models, which will be helpful to predict spatially and temporally resolved ambient pollutant concentrations are essential.

A network of stations for long term, simultaneous measurements of ozone and its precursor gases will be important to account for the regional contributions in the model simulations. As tropical data are still scarce, measurements at Ahmedabad should continue for a long period.

So far the focus of ozone research was mainly on stratospheric ozone, but during the last decade it has changed to tropospheric ozone. While ozonesondes provide high-resolution vertical profiles from limited sites there is a need for satellite measurements of tropospheric ozone for global coverage.



- Akimoto, H. (2003), Global air quality and pollution, *Science*, 302, 1716-1719.
- Aneja, V.P., B. Bunton, J.P. Chauhan, B.P. Malik, J. Walker, Y. Li, and George C. Murray, Jr. (1999), Ammonia emissions from swine waste operations in North Carolina, International Workshop on Atmospheric Nitrogen Compounds II: Emissions, Transport, Transformation, Deposition and Assessment, Chapel Hill, NC, June 7-9.
- Appenzeller, C. and H. C. Davies (1992), Structure of stratospheric intrusions into the troposphere. *Nature*, 358, 570–572.
- Austin, J.F. and Midgley, R.P. (1994), The climatology of the jet stream and stratospheric intrusions of ozone over Japan. *Atmospheric Environment* 28 A, pp. 39–52
- Bates, D.R. and M. Nicolet, (1950), The photochemistry of the atmospheric water vapor, *J. Geophys. Res.*, 55, 301,
- Bauer, S. E., Y. Balkanski, M. Schulz, D. A. Hauglustaine and F. Dentener (2004), Global modeling of heterogeneous chemistry on mineral aerosol surfaces: Influence on tropospheric ozone chemistry and comparison to observations, *J. Geophys. Res.*, 109, D02304, doi:10.1029/2003JD003868.
- Beig, G. and K. Ali (2006), Behaviour of boundary layer ozone and its precursors over great alluvial plain of the world: Indo-Gangetic Plains. *Geophys. Res. Lett.* 33, L24813 doi:10.1029/2006GL028352.
- Benson, S. W. and Axworthy, A. E., (1965), Reconsiderations of the rate constants from the thermal decomposition of ozone, *J. Chem. Phys.*, 42, pp. 2,614-2,615.
- Bey, I., D.J., Jacob, J.A. Logan, and R.M. Yantosca (2001), Asian chemical outflow to the Pacific in spring Origins, pathways and budgets, *J. Geophys. Res.*, 106, 23097-23113.
- Brasseur, G.P., Susan Solomon (1985), *Aeronomy of the middle Atmosphere*, Atmospheric and oceanographic sciences library, Springer.
- Brasseur, G. P., D. A. Hauglustaine, S. Walters, P.J. Rasch, J.F. Muller, C. Granier and X. X. Tie (1998), MOZART A global chemical transport model for ozone and related chemical tracers, Part 1. Model description. *J. Geophys. Res.*, 103, 28,265-28,290.
- Brasseur, G.P., R. Cox, D. Hauglustaine, et al. (1998), European scientific assessment of the atmospheric effects of aircraft emissions. *Atmos. Environ.*, 32, 2329-2418.
- Brasseur, G.P., J.J. Orlando, and G.S. Tyndall (1999), *Atmospheric Chemistry and Global Change*, Oxford University Press, New York.

- Brewer, A.W. and J. R. Milford (1960), The Oxford-Kew Ozone Sonde, Royal Society of London Proceedings Series A, 256, 470—495.
- Brewer, A. W. (1949), Evidence for a world circulation provided by the measurements of helium and water vapour distribution in the stratosphere, Quart. J. Roy. Meteor. Soc., 75, 351-363.
- Cebula, R. P., M. T. DeLand, and E. Hilsenrath (1998), NOAA 11 Solar Backscattered Ultraviolet, model 2 (SBUV/2) instrument solar spectral irradiance measurements in 1989–1994 1. Observations and long-term calibration, J. Geophys. Res., 103(D13), 16,235–16,249.
- Chakrabarty, D. K., Peshin, S. K., Pandya, K. V., and Shah, N. C. (1998), Long-term trend of ozone column over the Indian region, J. Geophys. Res., 103, 19 245–19 251.
- Chameides, W. L. & Walker, J. C. G. (1973), J. geophys. Res. 78, 8751–8760.
- Chameides, W.L. (1987), Acid dew and the role of chemistry in the dry-deposition of reactive gases to wet surfaces, (), J. Geophys. Res., 92, 11,895-11908.
- Chameides, W.L., D.D. Davis, G.L. Gregory, G. Sachse and A.L. Torres (1989), Ozone precursors and ozone photochemistry over the eastern North Pacific Ocean in spring, based on the GTE/CITE 1 1984 airborne observations, (), J. Geophys. Res., 94, 9799-9808.
- Chameides, W.L., P.S. Kasibhatla, J. Yienger and H. Levy II (1994), Growth of continental-scale metro-agro-plexes, regional ozone pollution, and world food production, Science 264, pp. 74
- Chameides, W.L. Xingsheng, L. Xioyan, T. Xiuji, Z. Chao, L. Kiang, C.S. St. John, J. Saylor, R.D. Liu, S.C. Lam, K.S. Wang, T. and F. Giorgi (1999), Is Ozone Pollution Affecting Crop Yields in China, Geophys. Res. Lett., 26, 867-870.
- Chan, C. Y., et al. (2004), Vertical profile and origin of wintertime tropospheric ozone over China during the PEACE-A period, J. Geophys. Res., 109, D23S06, doi:10.1029/2004JD004581.
- Chan, L. Y., H. Y. Liu, K. S. Lam, T. Wang S. J. Oltmans and J. M. Harris (1998), Analysis of the seasonal behavior of tropospheric ozone at Hong Kong , Volume 32, Page 159-168.
- Chand, D., K.S. Modh, M. Naja, , S. Venkatramani and S. Lal (2001), Latitudinal trends in O₃, CO, CH₄ and SF₆ over the Indian Ocean during the INDOEX IFP-1999 cruise, Current Sci., 80, 100-104.
- Chand, D., (2002), Study of trace gases in the tropical troposphere. Ph.D. Thesis, MLS University, Udaipur, India.
- Chand, D., S. Lal, M. Naja (2003), Variations of ozone in the marine boundary layer over the Arabian Sea and the Indian Ocean during the 1998 and 1999 INDOEX campaigns. J. Geophys. Res. 108 doi:10.1029/2001JD001589.

- Chandra, S, J. R. Ziemke, P. K. Barthia, R. V. Martin (2002), *J. Geophys. Res.* 107, 4188, 10.1029/2001JD000447.
- Chatfield, R.B. and P.J. Crutzen (1984), Sulfur dioxide in remote oceanic air: Cloud transport of reactive precursors, *J. Geophys. Res.*, 89,7111-7132.
- Crutzen, P.J. (1970), The influence of nitrogen oxide on the atmospheric ozone content, *Quart. J. R. Met. Soc.*, 96, 320-325.
- Crutzen, P.J., (1974), Photochemical reaction initiated by and influencing ozone in unpolluted tropospheric air, *Tellus* 26, pp. 44-55.
- Crutzen, P.J. (1979), The role of NO and NO₂ in the chemistry of the troposphere and stratosphere, *Annual Review of Earth and Planetary Sciences*, 7,443-472, 10.1146/annurev.ea.07.050179.002303.
- Crutzen, P. J. (1988), Tropospheric ozone: an overview, in *Tropospheric Ozone, Regional and Global Scale Interactions*, edited by I.S.A. Isaksen, pp. 185-216, D.Reidel Publ. Comp., Dordrecht.
- Crutzen, P. J. (1995), Ozone in the troposphere, *Von Nostrand Reinold Publ.*, New York, chapter 10, 349-393.
- Danielsen, E. F. (1968), Stratospheric-tropospheric exchange, based upon radioactivity, ozone and potential vorticity, *J. Atmos. Sci.*, 25, 502-518.
- Danielsen, E.F. and V.A. Mohnen (1977), Project Dustorm report - Ozone transport, in situ measurements and meteorological analyses of tropopause folding, *J. Geophys. Res.*,82,5867-5877.
- Davis, D. D., et al. (1996), Assessment of ozone photochemistry in the western North Pacific as inferred from PEM-West A observations during the fall 1991, *J. Geophys. Res.*, 101(D1), 2111-2134.
- De Laat, A. T. J., M. Zachariasse, G. J. Roelofs, P. van Velthoven, R. R. Dickerson, K. P. Rhoads, S. J. Oltmans, and J. Lelieveld (1999), Tropospheric ozone distribution over the Indian Ocean during spring1995 evaluated with a chemistry-climate model, *J. Geophys. Res.*, 104, 13,881-13,894.
- Dentener, F., G. Carmichael, Y. Zhang, J. Lelieveld and P. Crutzen (1996), Role of mineral dust aerosol as a reactive surface in the global troposphere, *J. Geophys. Res.*101 D17 (1996) 22869-22889.

- Derwent, R. G., Simmonds, P.G., and Collins, W. J., (1994), Ozone and carbon monoxide measurements at a remote maritime location, Mace Head, Ireland, from 1990 to 1992, *Atmos. Environ.* 28, 2623–2637.
- Desqueyroux, H, Pujet JC, Prosper M, Squinazi F, Momas I. (2002), Short-term effects of low-level air pollution on respiratory health of adults suffering from moderate to severe asthma. *Environ Res* 89(1):29-37.
- Dobson, G. M. B 1931 *Proc. Phys. Soc.* 43 324.
- Draxler, R.R. and G.D. Hess (1998), An overview of the Hysplit_4 modeling system for trajectories, dispersion, and deposition, *Australian Meteorological Magazine* 47, pp. 295–308.
- Duce, R. A., Unni, C. K., Ray, B. J., Prospero, J. M., and Merrill, J. T. (1980), Long-range atmospheric transport of soil dust from Asia to the Tropical North Pacific: Temporal variability, *Science*, 209, 1522–1524.
- Fabian, P. and Chr. E. Junge. (1969), Max-Planck-Institut für Aeronomie, Institut für Stratosphärenphysik, Lindau/Harz, and Max-Planck-Institut für Chemie, Mainz, BRD Global Rate of Ozone Destruction at the Earth's Surface Received November 18.
- Fabian, P., R. Borchers, B. C. Krüger, and S. Lal (1985), The Vertical Distribution of CFC-114 (CClF₂-CClF₂) in the Atmosphere, *J. Geophys. Res.*, 90(D7), 13,091–13,093.
- Fabian, P., R. Borchers, B. C. Krüger, and S. Lal (1987), CF₄ and C₂F₆ in the Atmosphere, *J. Geophys. Res.*, 92(D8), 9831–9835.
- Fishman, J. and Crutzen, P.J. (1991), A numerical study of tropospheric photochemistry using a one-dimensional model. *J. Geophys. Res.*, 82, 5897–5906.
- Fishman, J., Hoell, M. Jr., Bendura, R. D., McNeal, R. J., and Kirchoff, V. W. J. H. (1996), NASA GTE TRACE A Experiment (September–October 1992): Overview, *J. Geophys. Res.*, 101, 23 865–23 879.
- Fishman, J. and V.G. Brackett (1997), The climatological distribution of tropospheric ozone derived from satellite measurements using version 7 Total Ozone Mapping Spectrometer and Stratospheric Aerosol and Gas Experiment data sets, *J. Geophys. Res.*, 102, 19275–19278.
- Fishman, J., A.E. Wozniak and J.K. Creilson (2003), Global distribution of tropospheric ozone from satellite measurements using the empirically corrected tropospheric ozone residual technique: Identification of the regional aspects of air Pollution. *ACP* 3, 893– 907.

- Folkens, I., M. Loewenstein, J. Podolske, S.J. Oltmans and M. Proffitt (1999). A barrier to vertical mixing at 14 km in the tropics: Evidence from ozonesondes and aircraft measurements, *J. Geophys. Res.*, 104, 22095-22102, 10.1029/1999JD900404.
- Folkens, I., C. Braun, A.M. Thompson and J.C. Witte (2002), Tropical ozone as an indicator of deep convective outflow, *J. Geophys. Res.*, 107, D13, doi: 10.129/2001JD001178.
- Folkens, I., P. Bernath, C. Boone, L. J. Donner, A. Eldering, G. Lesins, R. V. Martin, B.-M. Sinnhuber, and K. Walker (2006), Testing convective parameterizations with tropical measurements of HNO₃, CO, H₂O, and O₃: Implications for the water vapor budget, *J. Geophys. Res.*, 111, D23304 doi:10.1029/2006JD007325.
- Fonrobert, E. (1916), In *chemie in Einzeldarstellungen*, Ferdinand Enke, Germany, 16.
- Fortuin, J.P.F. and Kelder, H. (1998), An ozone climatology based on ozonesonde and satellite measurement, *J. Geophys. Res.*, 105(D24), 31,709-31,734.
- Gidel, L.T. (1983), Cumulus cloud transport of transient tracers, *J. Geophys. Res.*, 88, 6587-6599.
- Graedel, T.E. and P.J. Crutzen (1993), *Atmospheric Change: An Earth System Perspective*. W.H. Freeman, New York, 446 pp.
- Grassian, V. H., (2002), Chemical reactions of nitrogen oxides on the surface of oxide, carbonate, soot, and mineral dust particles: Implications for the chemical balance of the troposphere. *J. Phys. Chem. A*, 106, 860-877.
- Gupta, Shilpy; S. Lal, S.Venkataramani, T.A. Rajesh and Y.B.Acharya, Variability in the vertical distribution of ozone over a subtropical site in India during a winter month *Journal of Atmospheric and Solar-Terrestrial Physics*, 69, 1502-1512.
- Haagen-Smit, E F Darley, M Zaitlin, H Hull, W Noble A.J. (1952), Investigation on Injury to Plants from Air Pollution in the Los Angeles Area. *Plant Physiol.*, 18-34.
- Hahn, J. F., C. T. McElroy, E. W. Hare, W. Steinbrecht, and A. I. Carswell (1995), Intercomparison of Umkehr and differential absorption lidar stratospheric ozone measurements, *J. Geophys. Res.*, 100(D12), 25,899–25,911.
- Hampson, J. (1965), Chemiluminescent emission observed in the stratosphere and mesosphere, 'Les problèmes météorologiques de la stratosphère et de la mésosphère, Presses Universitaires de France, pp. 393-440.
- Harrison, E.F., P. Minnis, B.R. Barkstrom, V. Ramanathan, R.D. Cess and G.G. Gibson (1990), Seasonal variation of cloud radiative forcing derived from the Earth radiation budget experiment, *J. Geophys. Res.*, 95, 18687- 18703.

- Hoell, J. M., D. D. Davis, D. J. Jacob, M. O. Rodgers, R. E. Newell, H. E. Fuelberg, R. J. McNeal, J. L. Raper, and R. J. Bendura (1999), Pacific Exploratory Mission in the tropical Pacific: PEM-Tropics A, August-September 1996, *J. Geophys. Res.*, 104(D5), 15567-15584.
- Holton, J. R., P. H. Haynes, M. E. McIntyre, A. R. Douglass, R. B. Rood, and L. Pfister (1995), Stratospheric-tropospheric exchange, *Rev. Geophys.*, 33, 403-439.
- Hoskins, Brian J. (2003), Climate Change at Cruising Altitude? *science*, 301, 469-470.
- Hudson, R.D. and A.M. Thompson (1998), Tropical tropospheric ozone from total ozone mapping spectrometer by a modified residual method, *J. Geophys. Res.*, 103, 22129-22145.
- Hunt, B. G., (1966), Photochemistry of ozone in a moist atmosphere, *J. Geophys. Res.*, 71, pp. 1,385-1,398
- IGAC (2003), Atmospheric Chemistry in a Changing World, An integration and synthesis of a decade of tropospheric chemistry Research, Eds, G.P. Brasseur, R.G. Prinn, A.A.P. Pszenny, Springer, Verlag, Berlin.
- Intergovernmental Panel on Climate Change (IPCC) (1995), The science of Climate Change. Cambridge University Press, Cambridge, UK.
- Intergovernmental Panel on Climate Change (IPCC) (2007), The science of Climate Change, Cambridge University Press, Cambridge, UK.
- Jacob, D.J., B.G. Heikes, S. M. Fan, J.A. Logan, D.L. Mauzerall, J.D. Bradshaw, H.B. Singh, G.L. Gregory, R.W. Talbot, D.R. Blake and G.W. Sachse (1996), Origin of ozone and NO_x in the tropical troposphere: A photochemical analysis of aircraft observations over the South Atlantic basin, *J. Geophys. Res.*, 101, 24235-24250, 10.1029/96JD00336.
- Jacob, D.J., (2000), Heterogeneous chemistry and tropospheric ozone. *Atmospheric Environment*, 34, 2131-2159.
- Jain, S.L., B.C. Arya, A. Kumar, S.D. Ghude and P.S. Kulkarni (2005), Observational study of surface ozone at New Delhi, India. *Int. J. Remote Sens.* 26, 3515-3524 doi:10.1080/01431160500076616.
- Jiang, Y. B., et al. (2007), Validation of Aura Microwave Limb Sounder Ozone by ozonesonde and lidar measurements, *J. Geophys. Res.*, 112, D24S34, doi:10.1029/2007JD008776.
- Johnson, J.E., R.H. Gammon, J. Larsen, T.S. Bates, S.J. Oltmans and J.C. Farmer (1990), Ozone in the marine boundary layer over the Pacific and Indian Oceans: Latitudinal gradients and diurnal cycles. *J. Geophys. Res.*, 95, 11847-11856.

- Junge, C. E. (1962), Global ozone budget and exchange between stratosphere and troposphere, *Tellus* 14, 363–377.
- Kerr, J.B., H. Fast, C.T. McElroy, S.J. Oltmans, J.A. Lathrop, E. Kyro, A. Paukkunen, H. Claude, U. Kohler, C.R. Sreedharan, T. Takao and Y., Tsukagoshi (1994), The 1991 WMO International Ozone Sonde Intercomparison at Vanscoy, Canada, *Atm. Ocean*, 32, 685-716.
- Kim, Y. K., H. W. Lee, J. K. Park, and Y. S. Moon (2002), The stratospheric-tropospheric exchange of ozone and aerosols over Korea, *Atmos. Environ.*, 36, 449–463
- Kley, D., P. J. Crutzen, H. G. J. Smit, H. Vomel, S. J. Oltmans, H. Grassl and V. Ramanathan (1996), Observations of near-zero ozone concentrations over the convective Pacific Effects on air chemistry, *Science*, 274, 230-233.
- Kley, D., H. G. J. Smit, H. Vomel, H. Grassl, V. Ramanathan, P. J. Crutzen, S. Williams, J. Meywerk, and S. J. Oltmans (1997), Tropospheric water vapor and O₃ cross sections in a zonal plane over the central equatorial Pacific, *Q. J. R. Meteorol. Soc.*, 123, 2009-2040.
- Komhyr, W.D. (1967), Nonreactive gas sampling pump, *Rev. Sci. Inst.*, 38, 981-983.
- Komhyr, W.D. (1969), Electrochemical concentration cells for gas analysis, *Ann. Geoph.*, 25, 203-210.
- Komhyr, W.D. (1971), Development of an ECC-Ozone Sonde NOAA Techn. Rep. ERL 200-APCL 18ARL 149.
- Komhyr, W.D. (1986), Operations handbook – Ozone measurements to 40 Km altitude with model 4A ECC- ozone sondes, NOAA Techn. Memorandum ERL-ARL-149.
- Komhyr, W.D., R.A. Barnes, G.B. Brothers, J.A. Lathrop and D.P. Oppermann (1995), ECC Ozone Sonde performance evaluation during STOIC 1989, *J. Geophys. Res.*, 100, 9231-9244.
- Khemani, L.T., G.A. Momin, P.S.P. Rao, R. Vijaykumar and P.D. Safai (1995), Study of surface ozone behaviour at urban and forest sites in India, *Atmospheric Environment* 29 (16), pp. 2021–2024.
- Kumar, A., M.M. Sarin, A.K. Sudheer (2008), Mineral and anthropogenic aerosols in Arabian Sea–atmospheric boundary layer: Sources and spatial variability, *Atmospheric Environment*, Volume 42, 5169-5181.
- Kunhikrishnan, T., M.G. Lawrence, R. Kuhlmann, A. Richter, A. Ladstätter-Weissenmayer and J.P. Burrows (2004), Analysis of tropospheric NO_x over Asia using the model of atmospheric transport and chemistry (MATCH-MPIC) and GOME-satellite observations, *Atmospheric Environment* 38, pp. 581–596.

- Kunhikrishnan, T., M. G. Lawrence, R. von Kuhlmann, M. O. Wenig, W.A. H. Asman, A. Richter, and J. P. Burrows (2006), Regional NO_x emission strength for the Indian subcontinent and the impact of emissions from India and neighboring countries on regional O₃ chemistry, *J. Geophys. Res.*, 111, D15301, doi:10.1029/2005JD006036.
- Lal, S., Naja, M., Jayaraman, A. (1998), Ozone in the marine boundary layer over the tropical Indian Ocean. *J. Geophys. Res.* 103, 18907–18917.
- Lal, S., Naja, M., Subbaraya, B.H. (2000), Seasonal variations in surface ozone and its precursors over an urban site in India. *Atmos. Environ.* 34, 2713–2724.
- Lal, S., D. Chand, L.K. Sahu, S. Venkataramani, G. Brasseur and M. Schultz (2006), High levels of ozone and related gases over the Bay of Bengal during winter and early spring of 2001. *Atmos. Environ.* 40, 1633–1644 (2006) doi:10.1016, *J. Atmos. Env.* 2005.10.060.
- Lal, S., L. K. Sahu, and S. Venkataramani (2007), Impact of transport from the surrounding continental regions on the distributions of ozone and related trace gases over the Bay of Bengal during February 2003, *J. Geophys. Res.*, 112, D14302, doi:10.1029/2006JD008023.
- Lawrence, M. G., P. J. Crutzen, P. J. Rasch, B. E. Eaton, and N. M. Mahowald (1999), A model for studies of tropospheric photochemistry: Description, Global Distributions, and Evaluation, *J. Geophys. Res.*, 104, 26,245-26,278.
- Lawrence, M. G., R. von Kuhlmann, M. Salzmänn, and P. J. Rasch (2003), The balance of effects of deep convective mixing on tropospheric ozone, *Geophys. Res. Lett.*, 30(18), 1940, doi:10.1029/2003GL017644.
- Lelieveld, J., and P. J. Crutzen (1994), Role of deep cloud convection in the ozone budget of the troposphere, *Science*, 264, 1759-1761.
- Lelieveld, J., and F.J. Dentener (2000), What controls tropospheric ozone?, *J. Geophys. Res.*, 105, 3531–3551.
- Lelieveld, J., et al (2001), The Indian Ocean Experiment: widespread air pollution from south and southeast Asia. *Science* 291, 1031–1036 Medline doi:10.1126/science.1057103.
- Levy, H. (1971), Normal atmosphere: Large radical and formaldehyde concentrations predicted, *Science*, 173,141-143.
- Liu, S.C., M. Mc Farland, D. Kley, O. Zafiriou, and B. Huebert (1983), Tropospheric NO_x and O₃ budgets in the equatorial Pacific, *J. Geophys. Res.*, 88, 1360-1368.

- Liu, S. C., M. Trainer, F. C. Fehsenfeld, D. D. Parrish, E. J. Williams, D. W. Fahey, G. Ubler and P. C. J. Murphy (1987), Ozone production in the rural troposphere and the implications for regional and global ozone distributions, *J. Geophys. Res.*, 92, 4191-4207.
- Liu, X., et al. (2006), First directly retrieved global distribution of tropospheric column ozone from GOME: Comparison with the GEOS-CHEM model, *J. Geophys. Res.*, 111, D02308, doi:10.1029/2005JD006564.
- Logan, J. A., M. J. Prather, S. C. Wofsy and M. B. McElroy (1981). Tropospheric chemistry a global perspective, *J. Geophys. Res.*, 86, 7210-7254.
- Logan, J. A. (1985), Tropospheric Ozone: Seasonal Behavior, Trends, and Anthropogenic Influence, *J. Geophys. Res.*, 90(D6), 10,463–10,482.
- Logan, J.A. (1994), Trends in the vertical distribution of ozone: an analysis of ozonesonde data. *Journal of Geophysical Research* 99, pp. 25553–25585.
- Logan, J. A. (1999), An analysis of ozonesonde data for the troposphere recommendations for testing 3-D models and development of a gridded climatology for tropospheric ozone, *J. Geophys. Res.*, 104, 16115-16149.
- Londhe, A. L., Bhosale, C. S., Kulkarni, J. R., Padma Kumari, B. and Jadhav, D. B., Space-time variability of ozone over Indian region for the period 1981–1998. *J. Geophys. Res.*, 2003, 108.
- Madronich, S (1994), Increases in biologically damaging UV-B radiation due to stratospheric ozone reductions: A brief review, *Arch. Hydrobiol. Beih: Ergebn. Limnol.*, 43, 17-30.
- Mandal, T. K., D. Kley, H. G. J. Smit, S. K. Srivastava, . K. Peshin, and A. P. Mitra (1999), Vertical distribution of ozone over the Indian Ocean (15°N-15°S) during First Field Phase I NDOEX-1998, *Indian Sci.*, 76, 938-943.
- Martin, R., D. Jacob, R. Yantosca, (2003), Global and regional decreases in tropospheric oxidants from photochemical effects of aerosols. *J. Geophys. Res.*, 108(D3), 4097, 10.1029/2002JD002622.
- McPeters, R. D., and G. J. Labow (1996), An assessment of the accuracy of 14.5 years of Nimbus 7 TOMS Version 7 ozone data by comparison with the Dobson Network, *Geophys. Res. Lett.*, 23, 3695-3698, 1996.
- McPeters, et al., (1997), An SBUV ozone climatology for balloonsonde estimation of total column ozone. *Journal of Geophysical Research* 102, pp. 8875–8885.

- Mauzerall, D.L., D. Narita, H. Akimoto, L. Horowitz, S. Walters, D.A. Hauglustaine and G. Brasseur (2000), Seasonal characteristics of tropospheric ozone production and mixing ratios over East Asia: a global three-dimensional chemical transport model analysis, *Journal of Geophysical Research* 105, pp. 17895–17910.
- Mauzerall, D.L. and X. Wang (2001), Protecting agricultural crops from the effects of tropospheric ozone exposure: reconciling science and standard setting in the United States, Europe, and Asia, *Annual Review of Energy and the Environment* 26, p. 237.
- Mickley, L. J., P. P. Murti, D. J. Jacob, J. A. Logan, D. Koch, and D. Rind (1999), Radiative forcing from tropospheric ozone calculated with a Unified Chemistry-Climate model, *J. Geophys. Res.*, 104, 30,153–30,172.
- Michel, A.E., C.R. Usher, V.H. Grassain, (2003), Reactive uptake of ozone on mineral oxides and mineral dusts. *Atmospheric Environment*, 37, 3201–3211.
- Mohnen, V. A., W. Goldstein and W.C. Wang. (1993), Tropospheric ozone and climate change, *Air & Waste* 43, 1332–1344.
- Molina, M. J., and F. S. Rowland, (1974), Stratospheric sink for chlorofluoromethanes: Chlorine atom catalyzed destruction of ozone. *Nature*, 249, 810.
- Myhre, G., A. Myhre and F. Stordal (2001), Historical evolution of radiative forcing of climate, *Atmos. Environ.*, 35, 2361–2373.
- Nair, P.R., Chand, D., Lal, S., Modh, K.S., Naja, M., Parameswaran, K., Ravindran, S., Venkataramani, S. (2002), Temporal variations in surface ozone at Thumba (8.6°N, 77°E): a tropical coastal site in India. *Atmos. Environ.* 36, 603–610.
- Naja, M. and S. Lal. (1996), Changes in surface ozone amount and its diurnal and seasonal patterns, from 1954–55 to 1991–93, measured at Ahmedabad (23°N), India, *Geophys. Res. Lett.*, 23, 81–84.
- Naja, M. (1997), Tropospheric Chemistry in tropics, Ph.D. Thesis, submitted in Gujarat University.
- Naja, M., S. Lal and D. Chand (2003), Diurnal and seasonal variabilities in surface ozone at a high altitude site Mt. Abu (24.6°N, 72.7°E, 1680 m asl) in India, *Atmospheric Environment* 37.
- Naja, M., Hajime Akimoto (2004), Contribution of regional pollution and long-range transport to the Asia-Pacific region: Analysis of long-term ozonesonde data over Japan, *J. Geophys. Res.*, 109, D21306, doi:10.1029/2004JD004687.

- Nassar, R., et al. (2008), Validation of Tropospheric Emission Spectrometer (TES) nadir ozone profiles using ozonesonde measurements, *J. Geophys. Res.*, 113, D15S17, doi:10.1029/2007JD008819.
- Newell, R.E., and S. Gould-Stewart (1981), A stratospheric fountain, *J. Atmos. Sci.*, 38, 2789-2796.
- Newell, R.E., Y. Zhu, E.V. Browell, W.G. Read and J.W. Waters (1996), Walker circulation and tropical upper tropospheric water vapor. *Journal of Geophysical Research* 101, pp. 1961– 1974.
- Newell, R. E., E. V. Browell, D. D. Davis, and S. C. Liu (1997), Western Pacific tropospheric ozone and potential vorticity: Implications for Asian pollution, *Geophys. Res. Lett.*, 24, 2733–2736
- Newell, R. E., Thouret, V., Cho, J. Y. N., Stoller, P., Marenco, A., and Smit, H. G. (1999), Ubiquity of quasi-horizontal layers in the troposphere, *Nature*, 398, 316–319.
- Oksanen, E., Holopainen T. (2001), Responses of two birch (*Betula pendula* Roth) clones to different ozone profiles with similar AOT40 exposure. *Atmospheric Environment* 35: 5245-5254.
- Oltmans, S. J. and Levy II, H. (1994), Surface ozone measurements from a global network. *Atmos. Environ.* 28, pp. 9–24.
- Pan, L. L., W. J. Randel, B. L. Gary, M. J. Mahoney, and E. J. Hintsa (2004), Definitions and sharpness of the extratropical tropopause: A trace gas perspective, *J. Geophys. Res.*, 109, D23103, doi:10.1029/2004JD004982
- Pashin, et al., (2001), Observations of vertical distribution of tropospheric ozone over Indian ocean and its comparison with continental profile during INDOEX FFP-1998 and IFP-1999.
- Philander, S.G. (1990), El Nino, La Nina and the Southern oscillation, Academic press, San Diego.
- Piotrowicz, S.R., C.J. Fischer, and R.S. Artz (1990), Ozone and Carbon monoxide over the North Atlantic during boreal summer, *Global Biogeochem. Cycles*, 4, 215-224.
- Piotrowicz, S.R., H.F. Bezdek, G.R. Harvey, and M. Springer-Young (1991), On the ozone minimum over the equatorial Pacific ocean, *J. Geophys. Res.*, 96, 18679-18687.
- Prather, M., et al. (2003), Fresh air in the 21st century?, *Geophys. Res. Lett.*, 30(2), 1100, doi:10.1029/2002GL016285.
- Rajeevan, M. (1996), Climate implications of the observed changes in ozone vertical distribution. *Int J Climatol*, 16: 15–22.
- Ramanathan, V., R. J. Cicerone, H. B. Singh and J. T. Kiehl (1985), Trace Gas Trends and Their Potential Role in Climate Change. *J. Geophys. Res.*, 90, 5547-5566.

- Ramanathan, V., L. Callis, R. Cess, J. Hansen I. Isaken, W. Kuhn, A. Lacis, F. Luther, J. Mahlman, R. Reck and M. Schlesinger (1987), Climate-chemical interactions and effects of changing atmospheric trace gases, *Rev. Geophys.*, 25, 1441-1482.
- Rasch, P. J., W. D. Collins and B. E. Eaton (2001), Understanding the Indian Ocean Experiment (INDOEX) aerosol distributions with an aerosol assimilation, *J. Geophys. Res.*, 106(D7), 7337-7356.
- Regener, V.H. (1960), On a sensitive method for the recording of atmospheric ozone. *J. Geophys. Res.* 65, 3975-3977.
- Rhoads, K.P., P. Kelley, R.R. Dickerson, T.P. Carsey, M. Farmer, D.L. Savoie and J. Prospero (1997), The composition of the troposphere over the Indian ocean during the monsoonal transition, *J. Geophys. Res.*, 102, 18,981-18,995.
- Routhier, F.R., R. Denet, P.D. Davis, A. Wartburg, P. Haagenson and A.C. Delany (1980), Free tropospheric and boundary layer airborne measurements of ozone over the latitude range of 58°S to 70°N, *J. Geophys. Res.*, 85, 7307-7321.
- Rolph, R.R., G.D., 2003. HYSPLIT (Hybrid Single-Particle Lagrangian Integrated Trajectory) Model access via NOAA ARL READY NOAA Air Resources Laboratory, Silver Spring, MD.
- Russell, J.M., et al. (1993), The Halogen occultation Experiment, *J. Geophys. Res.*, 98, 10777-10,797.
- Sahoo, A., S. Sarkar, R.P. Singh, M. Kafatos, M.E. Summers (2005), Declining trend of total ozone column over the northern parts of India. *Int. J. Remote Sens.* 26, 3433-3444 doi:10.1080/01431160500076467.
- Sahu, L. K., and S. Lal (2006), Changes in surface ozone levels due to convective downdrafts over the Bay of Bengal, *Geophys. Res. Lett.*, 33, L10807, doi:10.1029/2006GL025994.
- Sahu, L. K., and S. Lal (2006), Distributions of C2-C5 NMHCs and related trace gases at a tropical urban site in India. *Atmos. Environ.*, 40, 880-891.
- Sahu, L. K., S. Lal, S. Venkataramani (2006), Distributions of O₃, CO and hydrocarbons over the Bay of Bengal: A study to assess the role of transport from southern India and marine regions during September-October 2002, *Atmospheric Environment*, Volume 40, Issue 24, Pages 4633-4645.
- Saraf, N., and G. Beig (2004), Long-term trends in tropospheric ozone over the Indian tropical region, *Geophys. Res. Lett.*, 31, L05101, doi:10.1029/2003GL018516.

- Schenkel, A. and B. Broder (1982), Interference of some trace gases with ozone measurements by the KI method, *Atmos. Environ.*, 16, 2187-2190.
- Schultz, M.G., D.J. Jacob, Y. Wang, J.A. Logan, E.L. Atlas, D.R. Blake, N.J. Blake, J.D. Bradshaw, E.V. Browell, M.A. Fenn, F. Flocke, G.L. Gregory, B.G. Heikes, G.W. Sachse, S.T. Sandholm, R.E. Shetter, H.B. Singh, and R.W. Talbot (1999), On the origin of tropospheric ozone and NO_x over the tropical South Pacific, *J. Geophys. Res.*, 104, 5829-5843.
- Schwarzkopf, M. D., and V. Ramaswamy. (1993), Radiative forcing due to ozone in the 1980s: Dependence on altitude of ozone change. *Geophysical Research Letters*, 20(2), 205-208.
- Singh, H. B. (1980), Guidance for the collection and use of ambient hydrocarbon species data in the development of ozone control strategies, final report, EPA contract 68-02-2524, Environ. Prot. Agency, Washington, D. C.
- Singh, H.B., M. Kanakidou, P.J. Crutzen and D.J. Jacobs (1995), High concentrations and photochemical fate of oxygenated hydrocarbons in the global troposphere, *Nature*, 378, 50-54.
- Singh, H. B., Gregory, G. L., Andersen, B. E., Browell, E. W. (1996), one in the marine boundary layer of the tropical Pacific Ocean: Photochemical loss, chlorine atoms, and 10 entrainment, *J. Geophys. Res.*, 101, 1907-1917, 1996.
- Singh, H. B., Viezee, W., Chen, Y., Bradshaw, J. (2000), Biomass burning influences on the composition of the remote South Pacific troposphere: Analysis based on observations from PEM-Tropics A, *Atmos. Environ.*, 34, 635-644.
- Singh, A., S.M. Sarin, P. Shanmugam, N. Sharma, A.K. Attri and V.K. Jain (1997), Ozone distribution in the urban environment of Delhi during winter months. *Atmos. Environ.* 31, 3421-3427 doi:10.1016/S1352-2310(97)00138-6.
- Smit, H.G. J., D. Kley, S. McKeen, A. Voltz and S. Gilge (1989), The latitudinal and vertical distribution of tropospheric ozone over the Atlantic Ocean in the southern and northern hemispheres, *Ozone in the Atmosphere*, edited by R.D. Bojkov, P. Fabian, 419-422, Deepak Publ.
- Smit, H. G. J., S. Gilge and D. Kley (1990), The meridional distribution of ozone and water vapor over the Atlantic Ocean between 30°S and 52°N in September/October 1988, in G. Restelli, G. Angeletti (eds.) *Physio-chemical behaviour of atmospheric pollutants*, CEC., Air Pollution Report 23, Kluwer Acad. Publ., 630-637.

- Smit, H. G. J., S. Gilge and D. Kley (1991), Ozone profiles over the Atlantic Ocean between 36°S and 52°N in March/April 1987 and September/October 1988, *Jul Berichte Nr 2567*, Forschungszentrum Julich.
- Smit, H.G. J and D. Kley (1998), JOSIE: The 1996 WMO International intercomparison of ozonesondes under quasi flight conditions in the environmental simulation chamber at Julich, WMO/IGAC Report, WMO Global Atmosphere Watch report series, No. 130, (Technical Document No. 926). World Meteorological Organization, Geneva.
- SPARC-IOC-GAW (1998), Assessment of Trends in the Vertical Distribution of Ozone, SPARC report No.1, WMO Global Ozone Research and Monitoring Project Report No. 43.
- Stehr, J. W., W. P. Ball, R. R. Dickerson, B. G. Doddridge, C. A. Piety and J. E. Johnson (2002), Latitudinal gradients in O₃ and CO during INDOEX 1999, *J. Geophys. Res.*, 107(D19), 8016, doi: 10.1029/2001JD000446.
- Subbaraya, B.H., A. Jayaraman, S. Lal, S. Venkatramni, T. John, K.S. Zalpuri, C.R. Sreedharan, S.K. Srivastava, S.P. Perov, G.A. Kouin, S.V. Tislin, S.A. Vyazambin, O.V. Shtirkov, A.F. Chizhov, V.M. Ignatov and V.N. Uvarov (1994), Variability in the vertical distribution of ozone measured over thumba during the 1990 DYANA campaign. *J. Atmosph. Terr. Phys.* 56, p. 1915.
- Subbaraya, B.H., Lal, S. (1998), Tropospheric chemistry. *PINSA*, 64, A. 3, 277–288.
- Suhre, K., Cammas, J.P., Nedelec, P., Rosset, R., Marenco, A. and Smit, H.G.A., (1997), Ozone-rich transients in the upper equatorial Atlantic troposphere. *Nature* 388, pp. 661–663.
- Syri, S., Karvosenoja N., Lehtila A., Laurila T., Lindfors V. & Tuovinen J. P. (2001), Modeling the impacts of the Finnish climate strategy on air pollution. *Atmospheric Environ.* 36: 3059-3069.
- Terao, Y., and J. A. Logan (2007), Consistency of time series and trends of stratospheric ozone as seen by ozonesonde, SAGE II, HALOE, and SBUV(2), *J. Geophys. Res.*, 112, D06310, doi:10.1029/2006JD007667.
- Talbot, R. W. et al. (1997), Chemical characteristics of continental outflow from Asia to the troposphere over the western Pacific Ocean, Results from PEM-West B, *J. Geophys. Res.*, 102, 28255-28274.
- Taupin, F. G., M. Bessaf, S. Baldy, and P. J. Bremaud (1999), Tropospheric ozone above the southwestern Indian Ocean is strongly linked to dynamical conditions prevailing in the tropics, *J. Geophys. Res.*, 104, 8057-8066.

- Tie, X., S. Madronich, S. Walters, D. P. Edwards, P. Ginoux, N. Mahowald, R. Zhang, C. Lou, and G. Brasseur, (2005), Assessment of the global impact of aerosols on tropospheric oxidants, *J. Geophys. Res.*, 110, D03204, doi:10.1029/2004JD005359.
- Thompson, A. M., R. W. Stewart, M. A. Owens and J. A. Herwehe. (1989), Sensitivity of tropospheric oxidants to global chemical and climate change, *Atmos. Environ.*, 23, 519-532.
- Thompson, A. M. (1992), The oxidizing capacity of the earth's atmosphere: Probably past and future changes, *Science*, 256, 1157-1165.
- Thompson, A. M., J. E. Johnson, A. L. Torres, T. S. Bates, K. C. Kelly, E. Atlas, J. P. Greenberg, N. M. Donahue, S. A. Yvon, E. S. Saltzman, B. G. Heikes, B. W. Mosher, A. A. Shaskov and V. I. Yegorov (1993), Ozone observations and a model of marine boundary layer photochemistry during SAGA-3, *J. Geophys. Res.*, 98, 16,955-16,968.
- Thompson, A. M., K. E. Pickering, D. P. McNamara, M. R. Schoeberl, R. D. Hudson, J. H. Kim, E.V. Browell, V. W. J. H. Kirchoff and D. Nganga (1996), Where did tropospheric ozone over southern Africa and the tropical Atlantic come from in October 1992 Insights from TOMS, GTE TRACE A and SAFARI 1992, *J. Geophys. Res.*, 101, 24,251-24,278.
- Thompson, A. M. and J.C. Witte (1999), A new data set for the Earth Science Community. *Earth Observer* 11, pp. 27-30.
- Thompson, A. M., B.G. Doddridge, J.C. Witte, R.D. Hudson, W.T. Luke, J.E. Johnston, B.J. Johnson, S.J. Oltmans and R. Weller (2000), A tropical Atlantic paradox: Shipboard and satellite views of a tropospheric ozone maximum and wave-one in January-February 1999. *Geophys. Res. Lett.*, 27, 3317-3320.
- Thompson, A. M., J. C. Witte, R. D. McPeters, S. J. Oltmans, F. G. Schmidlin, J. A. Logan, M. Fujiwara, V. W. J. H. Kirchoff, F. Posny, G. J. R. Coetzee, B. Hoegger, S. Kawakami, T. Ogawa, B. J. Johnson, H. Vomel and G. Labow (2003), Southern Hemisphere Additional Ozonesondes (SHADOZ) 1998-2000 tropical ozone climatology 1. Comparison with Total Ozone Mapping Spectrometer (TOMS) and ground-based measurements, *J. Geophys. Res.*, Vol.108 No. D2, 8238, doi: 10.1029/2001JD000967.
- Thompson, A. M., J. C. Witte, S. J. Oltmans, F. J. Schmidlin, J. A. Logan, M. Fujiwara, V. W. J. H. Kirchhoff, F. Posny, G. Co-etzee, B. Hoeger, S. Kawakami and T. Ogawa (2003), The 1998-2000 SHADOZ (Southern Hemisphere Additional Ozonesondes) tropical ozone climatology. 2. Tropospheric variability and the zonal wave-one, *J. Geophys. Res.*, 108(D2), 8241,10.1029/2002JD002241.

- Thornton, D. C. and N. Niazy (1982), Sources of background current in the ECC-ozone sonde: Implication for total ozone measurements, *J. Geophys. Res.*, 87, 8943-8950.
- Thornton, D. C. and N. Niazy (1983), Effects of solution mass transport on the ECC ozonesonde background current, *Geophys.Res.Lett.* 10, 148-151.
- Torres, A. L. (1981), ECC ozonesonde performance at high altitude: pump efficiency, NASA Technical Memorandum 73290, 10pp., NASA Wallops Flight Center, Wallops Island, V.A.
- Tripathi, S. N., et al. (2006), Measurements of atmospheric parameters during Indian Space Research Organization Geosphere Biosphere Programme Land Campaign II at a typical location in the Ganga basin: 1. Physical and optical properties. *J. Geophys. Res.* 111, D23209 doi:10.1029/2006JD007278.
- Tsunogai, S. and T. Kondo (1982), Sporadic transport and deposition of continental aerosols to the pacific ocean, *J. geophysical. Res.*, 87, 8870-8874.
- Ulanovsky, A. E. (2001), FOZAN-II, Fast - response Chemiluminescent Airborne Ozone Analyzer. *Instrument and Experimental Techniques*, 44, 2, pg 249-256.
- Varshney, C.K. and M. Aggrawal (1992), Ozone pollution in urban atmosphere of Delhi, *Atmospheric Environment* 26B (3), pp. 291–294.
- Vaisala (1985), Instruction manual for ground check set GC 22, Edition: GC22-TO199-1.3.
- Vaisala (1988), Instruction manual for radiosonde RS 80 and windsonde WS 80 operation, Edition: RS80 00036-2.2.
- Veefkind, J. P., de Haan, J. F., Brinksma, E. J., Kroon, M., and Levelt, P. F. (2006), Total Ozone from the Ozone Monitoring Instrument (OMI) using the DOAS technique, *IEEE Trans. Geo. Rem. 20 Sens.*, 44(5), 1239–1244, doi:10.1109/TGRS.2006871204, 2006. 2387.
- Von Kuhlmann, R., M. G. Lawrence, P. J. Crutzen, and P. J. Rasch (2003), A model for studies of tropospheric ozone and nonmethane hydrocarbons: Model description and ozone results, *J. Geophys. Res.*, 108(D9), 4294, doi:10.1029/2002JD002893.
- Volz, A. and D. Kley (1988), Evaluation of the Montsouris series of ozone measurements made in the nineteenth century", *Nature*, 332, 240-242.
- Warneck, P. (1988), *Chemistry of the natural atmosphere*, Academic Press, London.
- Waugh, D.W. and L.M. Polvani (2000), Climatology of intrusions into the tropical upper troposphere, *Geophys. Res. Lett.*, 27, 3857-3860.

- Weller, R., R. Lilischkis, O. Schrems, R. Neuber and S. Wessel. Vertical ozone (1996). Distribution in the marine atmosphere over the central Atlantic Ocean (56°S-50°N), *J. Geophys. Res.*, 101, 1387-1399.
- Wesely, M.L. (1989), Parameterisation of surface resistances to gaseous dry deposition in regional-scale numerical models. *Atmospheric Environment* 23, pp. 1293–1304.
- Wielicki, B.A. and R.N. Green (1989), Cloud identification for ERBE Radiative flux retrieval, *J. Appl. Meteorol.*, 28, 1131-1146.
- Wild, M., P. Calanca, S. C. Scherrer, and A. Ohmura (2003), Effects of polar ice sheets on global sea level in high-resolution greenhouse scenarios, *J. Geophys. Res.*, 108(D5), 4165, doi:10.1029/2002JD002451.
- Winkler, P. (1988), Surface Ozone over the Atlantic Ocean, *J. Atmos. Chem.*, 7, 73-91.
- World Meteorological Organization (WMO) (1995), Scientific Assessment of Ozone Depletion: 1994, Global Ozone Research and Monitoring Project – Report No. 37, World Meteorological Organization, Geneva.
- World Meteorological Organization (WMO) (1998), Scientific Assessment of Ozone Depletion: Global Ozone Research and Monitoring Project – Report No. 44, World Meteorological Organization, Geneva, 1999.
- Yamamori, M., Kagawa, A., Kasai, Y., Mizutani, K., Murayama, Y., Sugita, T., Irie, H., and Nakajima, H. (2006), Validation of ILAS-II version 1.4 O₃, HNO₃, and temperature data through comparison with ozonesonde, ground-based FTS, and lidar measurements in Alaska, *J. Geophys. Res.*, 111, D11S08, doi:10.1019/2005JD006438.
- Zachariasse, M., P. F. J. van Velthoven, H. G. J. Smit, J. Lelieveld, T. K. Mandal, and H. Kelder (2000), Influence of stratosphere-troposphere exchange on tropospheric ozone over the tropical Indian Ocean during the winter monsoon, *J. Geophys. Res.*, 105(D12), 15,403–15,416.
- Zhang, L., et al. (2006), Ozone-CO correlations determined by the TES satellite instrument in continental outflow regions, *Geophys. Res. Lett.*, 33, L18804, doi:10.1029/2006GL026399.
- Ziemke, J.R., Chandra, S. (1999). Seasonal and interannual variabilities in tropical tropospheric ozone. *Journal of Geophysical Research* 104, 21425–21442.

List of Acronyms and Abbreviations

AIRS	Atmospheric Infrared Sounder
AS	Arabian Sea
BOB	Bay of Bengal
ECC	Electro Chemical Cell
ECMWF	European Center for Medium Range Weather Forecast
GPS	Global positioning System
HYSPLIT	Hybrid Single Particle Lagrangian Integrated Trajectory Model
ICARB	Indian Campaign for aerosol and radiation Budget
IGP	Indo-Gangetic Plain
IPCC	Intergovernmental Panel on Climate Change
ITCZ	Inter Tropical Convergence Zone
MATCH-MPIC	Model of Atmospheric Transport and Chemistry - Max Planck Institute for Chemistry version
MBL	Marine Boundary Layer
MOPITT	Measurements of Pollution in the Troposphere
MOZAIC	Measurement of OZone by AIrbus in-service aircraft
NASA	National Aeronautics and Space Administration
NCEP	National Center for Environmental Prediction
NMHCs	Non Methane Hydro Carbon
NOAA	National Oceanic and Atmospheric Administration

ORV	Oceanic Research Vessel
PRL	Physical Research Laboratory
ppbv	parts per billion by volume
ppmv	parts per million by volume
PV	Potential Vorticity
SHADOZ	Southern Hemisphere Additional Ozonesonde
SPARC	Stratospheric Processes And their Role in Climate
STE	Stratosphere –Troposphere Exchange
TOMS	Total ozone mapping spectrometer
TTL	Tropical Tropopause Layer
TTO	Total Tropospheric Ozone
UTLS	Upper Troposphere Lower Stratosphere
WMO	World Meteorological Organization (UN)

Publications

1. Measurements of Atmospheric Parameters during ISRO-GBP Land Campaign II at a Typical Location in Ganga Basin: Part I- Physical and Optical Properties

S. N. Tripathi, Vinod Tare, N. Chinnam, A. K. Srivastava, Sagnik Dey, A. Agarwal, S. Kishore, R. B. Lal, Manish Manar, Vijay P. Kanwade, S. S. S. Chauhan, and M. Sharma R. R. Reddy, K. Rama Gopal, K. Narasimhulu and L. Siva Sankara Reddy and Shilpy Gupta, Shyam Lal. (JGR 2006).

2. Variability in the vertical distribution of ozone over a subtropical site in India during a winter month: Evidence of stratospheric intrusion into the troposphere.

Shilpy Gupta, S. Lal, S. Venkatramani, T. A. Rajesh and Y. B. Acharya, JASTP, 2007.

3. Emission characteristic of ozone related trace gases at a semi-urban site in the Indo-Gangetic plain using inter-correlations.

S. Lal, L. K. Sahu, S. Gupta, S. Srivastava, K. S. Modh, S. Venkataramani and T. A. Rajesh (accepted JAS).

4. Influence of convection on ozone distribution and related parameters observed over the Bay of Bengal,

Shilpy Gupta, Shyam Lal and S. Venkataramani (Under review GRL).

5. Variability in the anthropogenic pollutants and Stratosphere – Troposphere Exchange of ozone over the Arabian sea during the Pre - Monsoon season (April - May, 2006).

Shilpy Gupta, Shyam Lal, Y. B. Acharya and S. Venkataramani (Submitted JGR).

Papers presented at Conferences/Symposia/ Workshops : -

“Vertical distribution of ozone over Ahmedabad” First Prof. R. Ananthakrishnan Memorial conference on atmospheric science, climate change and Environmental studies, Indian Institute of Tropical Meteorology, Pune, India, 18-19 Jan. 2005

“Vertical distribution of ozone over Ahmedabad” International summer school on upper troposphere and lower stratosphere (UTLS), Cargese, France, October 3-15, 2005.

“Study of vertical distribution of ozone over Kanpur” in National Space Science Symposium (NSSS), Vishakhapatnam, India, February 11 – 14, 2006.

“Variability in the vertical distribution of ozone at Kanpur during a fog episode in December 2004: Stratosphere –Troposphere Exchange” in 7th International Symposium on Tropospheric Profiling (ISTP), Boulder, Colorado, U.S.A, June 11 – 17, 2006.

“Effect of Stratosphere - Troposphere Exchange (STE) on ozone distribution observed over Ahmedabad”, International Symposium on Aerosol-Chemistry-Climate Interactions, November 20-22 2007, Physical Research Laboratory, Ahmedabad, India.

”Effect of convection on ozone distribution observed over the Bay of Bengal” International Symposium on Aerosol-Chemistry-Climate Interactions, November 20-22 2007, Physical Research Laboratory, Ahmedabad, India.

“Effect of Long range transport on tropospheric ozone over Ahmedabad”, International Symposium on Aerosol-Chemistry-Climate Interactions, November 20-22, 2007, Physical Research Laboratory, Ahmedabad, India.

“Vertical distribution of ozone in the summer monsoon over Ahmedabad: effect of lightening” International Symposium on Aerosol-Chemistry-Climate Interactions, November 20-22 2007, Physical Research Laboratory, Ahmedabad, India.

Poster Presentation entitled “Seasonal variation of atmospheric boundary layer over Ahmedabad” International Symposium on Aerosol-Chemistry-Climate Interactions, November 20-22, 2007, Physical Research Laboratory, Ahmedabad, India.

Attended school of Physics and Chemistry of Air Pollution and their effects: Field course and data analysis, March 10 – March 22, 2008. held at Hyyutiala, Finland.

Award :-

Recipient of honorable mention in the **SOLAS student Poster Competition** (Runner up prize) for the presentation entitled” Variability in the vertical distribution of ozone and anthropogenic pollutants over the Bay of Bengal and the Arabian Sea during the pre – monsoon season.”



